Early-Age Mechanical Properties and Electrical Resistivity of Geopolymer Composites

A Thesis Submitted for the Degree of Master of Philosophy

by

Samira Safari

School of Engineering and Design, Brunel University London

April 2016

Abstract

Cement-less and/cement-like geopolymer mortars were made with pulverised fuel ash (PFA) or ground granulated blast furnace slag (GGBS) activated by alkali with different alkali moduli (AM) and alkali dosage (AD). Once synthesised the samples were cured at 20°C and 70°C up to 28 days. The flexural and compressive strengths of these samples at early ages up to 28 days were tested conforming to BS EN196-1:2005. The electrical resistivity of these materials was monitored using a set of non-contacting electrodes to the age up to 7 days to characterise the geopolymerisation process from a physical phenomenon point of view.

The effects of AD and AM on the early-age mechanical strengths and electrical resistivity of geopolymer materials were examined from the experimental results. The correlation between strength development and electrical resistivity was studied. The geopolymerisation process was characterised by a 5-stage model, based on electrical resistivity, analogue to hydration process of Portland cement. This research therefore proposes an alternative method for characterisation of geopolymerisation of geopolymers different from traditional methods based on chemistry. It is expected that such a physical phenomenon model will be better accepted by structural engineers for better promotion of usage of geopolymer composites, a type of low carbon and more sustainable binder-based materials, in construction.

Acknowledgement

First and foremost, I would like to express my sincere gratitude to my supervisor, Dr. Xiangming Zhou, for the continuous support of my MPhil study and related research, for his patience, motivation, and immense knowledge. His guidance helped me in all the time of research and writing of this thesis.

Besides my advisor, I would like to thank Neil Macfadyen and Simon Le Geyt for their help and patience working with me in the civil laboratory.

A special thanks to my family. I would not have been able to complete this research without the commitment, love, and support of them. I would like to dedicate this report to them and record my heartfelt gratitude for this trust and belief in me.

Table of Contents

List of Tables

List of Figures

Terms and Abbreviations

PC	Portland Cement
PFA	Pulverised Fly Ash
GGBS	Ground Granulated Blast-Furnace Slag
AD	Alkali Dosage
AM	Alkali Modulus
w/s	Water to Solid Ratio
w/b	Water to Binder Ratio
SSD	Saturated Surface Dry
SEM	Scanning Electron Microscopy
XRD	X-Ray Diffraction
GHG	Greenhouse Gas
C-S-H	Calcium Silicate Hydrate

1. Introduction

1.1 Research Backgrounds

Concrete is one of the main materials used in the construction industry. Currently, Portland Cement (PC) is the most important material for industrial use, as it is the main component for making concrete, which is in huge demand worldwide. The production of PC releases a significant amount of carbon dioxide (CO_2) to the atmosphere. For each tonne of PC produced, it is estimated that one tonne of CO_2 is released into the environment (Soura Kr.Das, 2014). As cement manufacturing is responsible for 5% of global greenhouse gas emissions (GHG) (Jos G.J. Olivier (PBL), 2014), this process has become a worrying issue due to its negative environmental impact. The effect of increasing carbon emissions on environmental protection has led to world-wide interest in the investigation of replacements of PC as a construction material.

In this concrete, one aim of the construction industry is to develop and identify sustainable materials by using by-products and recycled materials. The use of waste and recycled materials has beneficial effects on the environment by reducing energy consumption and saving valuable landfill space. The use of recycled materials in making concrete has been limited to recycled aggregates, admixtures reinforcement and fibre. However, the critical component of reversing harmful environmental impacts is to develop different cementitious materials to replace PC (Davidovits, 2011). Readily available recycled materials and by- products such as Pulverised Fly Ash (PFA) and Ground Granulated Blast furnace Slag (GGBS) have been approved to meet these demands.

PFA is a pozzolanic material produced world-wide in coal-burning power plants. To reduce the alkali-aggregate reactions and enhance the rheological properties of concrete, PFA was used as an admixture (Mindess, S., & Young, J.F., 1981) when making mortars and concrete. When PFA is combined with calcium hydroxide, it shows cementitious properties as a pozzolanic material. However, PFA from different sources may have different effects due to different chemical structures (Popovics, 1982). GGBS is a by-product of iron production, are generally used in geopolymer concrete. The problem of utilising GGBS is that the strength development at the early age under the 20℃ is noticeably slower than that of PC. Hence, GGBS is not used for fast track development, where high early-age strength is required. However, there are signs that

curing the GGBS at high temperature will significantly improve the early-age strength (Soutsos, et al., 2005).

Geopolymers are a range of reaction products synthesized from aluminosilicate activated by alkali. PFA can be mixed with an alkaline solution to produce original geopolymer binders due to its similarity to ordinary sources of aluminium and silicon oxides (Jing, W.,& Roy,D.M., 1992). Geopolymers are regarded as sustainable construction materials, due to the use of PFA and GGBS, which can have a huge impact on reducing CO_2 emission (LIVERPOOL, 2014).

1.2 Investigation

GGBS and PFA are commonly used with PC in construction. The use of such materials in concrete provides many technical benefits such as the long-term strength, durability and workability of the concrete mix. Geopolymers are not used in fast-track construction due to the fact that their strength development at an early age is remarkably slower than PC-based concrete. This is the main disadvantage of using geopolymers instead of PC. The modern construction industry needs fast-track concrete mixes with high early-age strength. Hence, issues like cementitious additions, curing temperature, and mix proportion that affect strength at an early age should be considered. The amount of PFA and GGBS that can be used as a PC substitute material in concrete depends on the essential strength at early ages. The input of PFA and GGBS into the hydration of total binder content in concrete must be studied.

The strength development of geopolymer concrete at early-age is tangled as its strength essentially depends on the mix balance of concrete and the environmental condition under which it is cured. Unfortunately, most of the available data and techniques for predicting the strength of geopolymer concrete were described on the PC information. Therefore, when the techniques are used to estimate the strength development of geopolymer, the results are not accurate enough and sometimes directed to incorrect outcomes. Furthermore, a specific method to estimate the strength development of geopolymer concrete is needed to assist contractors to recognise the exact early-age strength development of geopolymer concrete.

1.3 Project Aims and Objectives

The aim of this study is to investigate the early-age strength development of geopolymer concrete made using PFA and GGBS that are cured under different curing conditions. This will be required to investigate the effect of alkali dosage (AD) and alkali modulus (AM) on the strength of early age geopolymer concrete. AD is the mass ratio of alkali metal oxides in the activating solution to PFA and GGBS. AM is the mass ratio of alkali metal oxides to silica plus aluminate in the activating solution.

However, to better understand the structure of the geopolymer, in this project the Scanning Electron Microscopy (SEM) characterisation methods are employed to examine structure and morphology of geopolymerisation products to underpin the findings of macroscale properties of geopolymer particularly at early stages

The objectives of this project include:

- To determine the microstructure and chemistry of geopolymer synthesized from PFA and GGBS.
- To investigate the reactivity of PFA and GGBS to various alkaline solutions.
- To explore the behaviour of early-age hydration of geopolymer by using Electrical Cement and Concrete Resistivity Tests (CCR-2).

2. Literature Review

2.1 History of concrete

Various publications and studies refer to the application of concrete in the construction of many ancient structures. The history of concrete begins with the development of chemical reactions needed to bind materials which led to the development of cement. Assyrians and Babylonians used clay to bind structural materials together (Li, 2011). The ancient Egyptians used chalk and limestone as bonding substances, and the Greeks used siliceous volcanic Santorini earth in 500 BC (McArthur & Spalding, 2004). By heating limestone or chalk, Calcium Oxide (CaO)was produced. When reacting with water it results in the production of Calcium Hydroxide($Ca(OH)_2$), which was the basic chemical reaction of bonding mortar used then. During that period mortar could solidify as an effect of the formation of Calcium Carbonate($CaCo_3$). After half a millennium, Vitruvius found a material which improved the speed of the chemical reaction process and produced stronger and more durable concrete (Delatte, 2001). The material was then called "Pulvis Puteoolanis" as it was discovered in the town of Puteoli (now Pozzuoli) (McCann, 1988). Pulvis Puteoolanis was volcanic ash that included finely ground reactive silica that, mixed with Calcium Oxide (CaO), resulted in a quicker reaction and formed a calcium silicate hydrate binder. It is pointed to as Roman concrete and was applied widely in structures all over the Roman Empire.

Roman concrete has undergone many developments since then. In 1824, Joseph Aspdin invented Portland cement, which has made the most significant improvements to Roman concrete. He was granted the British Patent No_5022 for his invention of Portland cement (Ghosh, 1991). Portland cement is described in the British Standard BS EN 197-1:2000 as "clinker that is made by sintering a precisely specified mixture of raw materials including particles, usually signified as oxides, SiO_2, Fe_2O_3 , CaO, Al_2O_3 and small quantities of other substances. The raw mean, paste or slurry is finely broken, intimately mixed and, therefore, homogeneous."

2.2 Industrial use of Concrete

Concrete plays a role in essentially all construction projects because it is used extensively in structures such as dams, buildings, foundations and bridges. Lomborg

(2001) identifies concrete as the most commonly used man-made material in the world. Concrete, as with many other construction materials has advantages and disadvantages when used by alone. A summary of its main benefits and weaknesses, when used in structures can be seen in Table 2.1.

Table 2.1 Disadvantages and Advantages of concrete (Mindess S. and J.F. Yong, 1981)

Advantages	Disadvantages
Durable not in all environmental exposed conditions. Fire resistant Aesthetic properties Easy and on-site fabrication Easy to be formed into different Shapes	Low tensile strength Low ductility Low strength/ weight ratio High level of air pollution in manufacturing cement

2.3 Composition of concrete

Concrete is a composite material made of cement, water, aggregates (fine and coarse) and sometimes admixtures. In making concrete, a paste is produced by the mix and hence there is a chemical reaction between cement and water, the role of which is to bind all the materials and make a durable and strong composite (Gangarao, et al., 2006). Aggregate is composed of a combination of a coarse aggregate, which is made of gravel or crushed rocks and a fine aggregate similar to sand these could also be described as cheap fillers. The size, shape and quality of aggregates affect the properties of concrete in both its fresh and hardened stages (Parekh & Modhera, 2011). Admixtures could also be added to the mix on demand in both its fresh and hardened stages in order to alter the properties of the produced concrete (Khan, et al., 2013). Figure 2.1 displays a common concrete composition by volume.

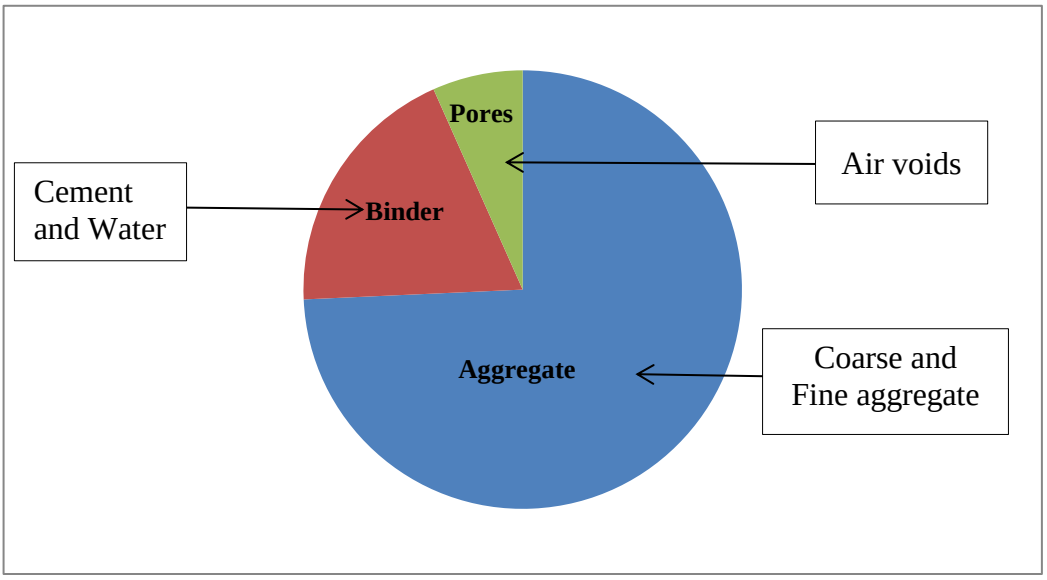

Figure 2.1 A Typical Concrete Composition by volume (Mulheron, 2012)

2.3.1 Cement

The main component of producing concrete is cement because cement reacts with water to form a binder that links aggregates together and, therefore, provides concrete with its integrity (Banfill, 2006). In the UK, there are three main cement types that are generally used Portland cement is the most typically used cement blend, and is described as CEM in BS EN197-1:2000. The other two popular blends use PFA and GGBS. There are also other cement classes such as CEM II and CEM III (R.K. Dhir and M.R. Jones, 1994).

2.3.1.1 Portland cement

The key material of concrete is cement. Nowadays the most well-known cement which is produced around the world is Portland cement. Manufacturing Portland cement first involves crushing and mixing raw components, then heating this material at an extraordinarily high temperature to get clinker, and at last crushing this clinker into powder. These are the main stages for producing Portland cement (Imbabi, et al., 2012).

The main compounds used in manufacturing Portland cement that are required for the clinkering development are Calcium Carbonate($CaCO_3$), Silica(SiO_2), Ferric Oxide (Fe_2O_3) and Alumina(Al_2O_3). Silica, ferric oxide and alumina are taken from shale or clay and calcium carbonate is obtained from limestone or chalk. These raw substances are combined and then heated to drive off water and Carbon Dioxide (CO_2) . Subsequently, they are burned at 1300 - 1450 °C in a rotating furnace until the substance softens slightly and fuses into balls up to 25 mm in diameter. This product is

known as clinker. Next, the clinker is ground and tempered into a light powder with the addition of approximately 3- 6 % of gypsum to control the setting time. The product is dried into a fine grey powder known as Portland cement, and it should be stored carefully to avoid contact with water (BS EN 197-1:2000, n.d.).

Portland cement comes in several varieties and each type is utilized for a different aim that is, specified to meet the demands of a particular job. Class I cement, known as "Ordinary Portland cement" is the most common cement type in the world and that is changed to Portland cement in BS EN standard. The table 2.2 displays various kinds of Portland cement and their compositions in BS EN 197-1.

Table 2.2 Various type of cement (BS EN 197-1:2000.)

Main types	Notation of the 27 products (types of common cement)		Composition [percentage by mass [a]]										
			Main constituents										Minor additional constituents
			Clinker	Blast-furnace slag	Silica fume	Pozzolana		Fly ash		Burnt shale	Limestone		
						natural	natural calcined	siliceous	calca-reous				
			K	S	D [b]	P	Q	V	W	T	L	LL	
CEM I	Portland cement	CEM I	95-100	–	–	–	–	–	–	–	–	–	0 to 5
CEM II	Portland-slag cement	CEM II/A-S	80 to 94	6 to 20	–	–	–	–	–	–	–	–	0 to 5
		CEM II/B-S	65 to 79	21 to 35	–	–	–	–	–	–	–	–	0 to 5
	Portland-silica fume cement	CEM II/A-D	90 to 94	–	6 to 10	–	–	–	–	–	–	–	0 to 5
	Portland-pozzolana cement	CEM II/A-P	80 to 94	–	–	6 to 20	–	–	–	–	–	–	0 to 5
		CEM II/B-P	65 to 79	–	–	21 to 35	–	–	–	–	–	–	0 to 5
		CEM II/A-Q	80 to 94	–	–	–	6 to 20	–	–	–	–	–	0 to 5
		CEM II/B-Q	65 to 79	–	–	–	21 to 35	–	–	–	–	–	0 to 5
	Portland-fly ash cement	CEM II/A-V	80 to 94	–	–	–	–	6 to 20	–	–	–	–	0 to 5
		CEM II/B-V	65 to 79	–	–	–	–	21 to 35	–	–	–	–	0 to 5
		CEM II/A-W	80 to 94	–	–	–	–	–	6 to 20	–	–	–	0 to 5
		CEM II/B-W	65 to 79	–	–	–	–	–	21 to 35	–	–	–	0 to 5
	Portland-burnt shale cement	CEM II/A-T	80 to 94	–	–	–	–	–	–	6 to 20	–	–	0 to 5
		CEM II/B-T	65 to 79	–	–	–	–	–	–	21 to 35	–	–	0 to 5
	Portland-limestone cement	CEM II/A-L	80 to 94	–	–	–	–	–	–	–	6 to 20	–	0 to 5
		CEM II/B-L	65 to 79	–	–	–	–	–	–	–	21 to 35	–	0 to 5
		CEM II/A-LL	80 to 94	–	–	–	–	–	–	–	–	6 to 20	0 to 5
		CEM II/B-LL	65 to 79	–	–	–	–	–	–	–	–	21 to 35	0 to 5
	Portland-composite cement [c]	CEM II/A-M	80 to 94	<---------- 6 to 20 ---------->									0 to 5
		CEM II/B-M	65 to 79	<---------- 21 to 35 ---------->									0 to 5
CEM III	Blastfurnace cement	CEM III/A	35 to 64	36 to 65	–	–	–	–	–	–	–	–	0 to 5
		CEM III/B	20 to 34	66 to 80	–	–	–	–	–	–	–	–	0 to 5
		CEM III/C	5 to 19	81 to 95	–	–	–	–	–	–	–	–	0 to 5
CEM IV	Pozzolanic cement [c]	CEM IV/A	65 to 89	–	<---------- 11 to 35 ---------->					–	–	–	0 to 5
		CEM IV/B	45 to 64	–	<---------- 36 to 55 ---------->					–	–	–	0 to 5
CEM V	Composite cement [c]	CEM V/A	40 to 64	18 to 30	–	<-------- 18 to 30 ----->			–	–	–	–	0 to 5
		CEM V/B	20 to 38	31 to 50	–	<-------- 31 to 50 ----->			–	–	–	–	0 to 5

[a] The values in the table refer to the sum of the main and minor additional constituents.
[b] The proportion of silica fume is limited to 10 %.
[c] In Portland-composite cements CEM II/A-M and CEM II/B-M, in Pozzolanic cements CEM IV/A and CEM IV/B and in composite cements CEM V/A and CEM V/B the main constituents other than clinker shall be declared by designation of the cement (for example see clause 8).

2.3.1.1.1 Hydration Process

Hydration is what we call the chemical reaction between water and cements that result in the development of a binder in the concrete mix. The reaction outcomes are the compound of calcium aluminate and calcium silicate and the main reaction takes place between the main and active components of cement (C_3S, C_2S, C_3A and C_4AF) and H_2O. The role of all of these elements in the hydration process is remarkable because they can modify the physical properties of concrete in various Portland cements (Steiger, 1995). Table 2.3 shows a list of the products produced by the reaction.

Table 2.3 Principle compounds in Portland cement with elements, symbols and hydration rate

Name of elements	Oxide elements	Chemical Symbol	Rate of reaction with water
Tricalcium Silicate	$3.Cao.SiO_2$	C_3S	Medium
Dicalcium Silicate	$2.CaO.SiO_2$	C_2S	Slow
Tricalcium Aluminate	$3.CaO.Al_2O_3$	C_3A	Fast
Tetracalcium Aluminoferrite	$4.CaO.Al_2O_3$	C_4AF	Slow

Three significant reactions happen when cement is mixed with water. The first reaction is between the clinker sulphates and gypsum that is dissolved producing a sulphur-rich alkaline solution. The second reaction is between Tricalcium Aluminate (C_3A) and water. The result of this reaction is calcium silicate hydrate gel, also known as C-S-H. The calcium silicate hydrate gel reacts with the sulphates that are presented in the solution and makes small bar-shaped crystals, which last only very shortly. Then, the initial setting phase starts, which is a term between 2 to 4 hours after hydration takes place. Cement begins binding by the water, so the paste loses its fluidity or workability (Maekawa, et al., 2008).

During the hydration of cement, the aluminates and silicate of the PC are developed to produce products of hydration that make the hardened mass found in cement paste after the initial setting process when the important stage of hydration starts. Calcium silicate and calcium hydroxide hydrate are produced from the hydration of C_2S and C_3S. The calcium silicate hydrates forms the “glue” that forms binding capacity within the cement’s hexagonal crystal of calcium hydroxide. Equations 2.1 and 2.2 explain the

major reactions in the hydration of OPC, increasing the strength after several weeks when the C_2S ultimately reacts (Winter, 2005).

$$2C_3S + 6H \rightarrow C_3S_2H_3 + 3CH \quad (2.1)$$

$$\text{Tricalcium silicate} + \text{Water} \rightarrow \text{C} - \text{S} - \text{H gel} + \text{Calcium Hydroxide}$$

$$2C_2S + 6H \rightarrow C_3S_2H_3 + CH \quad (2.2)$$

$$\text{Dicalcium silicate} + \text{Water} \rightarrow \text{C} - \text{S} - \text{H gel} + \text{Calcium Hydroxide}$$

The hydration reaction of Portland cement is an exothermic reaction and the temperature in mass concrete will exceed 60 ℃. This is because of the breaking and shaping of chemical bonds through the hydration process (Winter, 2012). The hydration development is displayed in Figure 2.2.

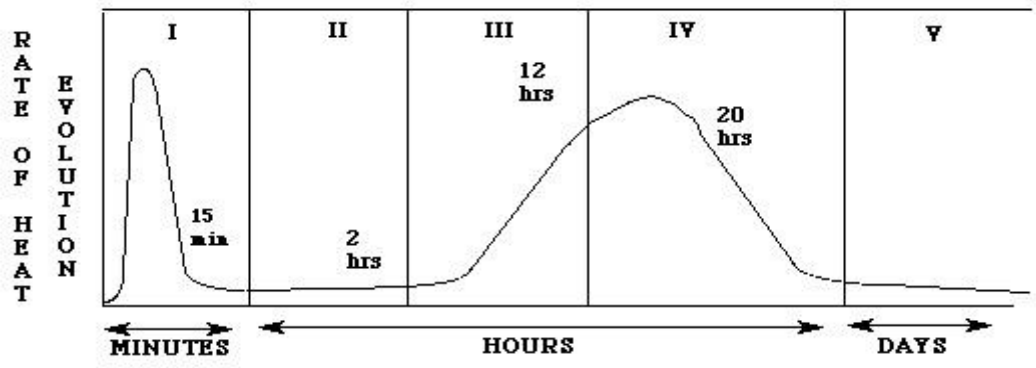

Figure 2.2 Rate of heat process while the hydration of Portland cements (Department of Materials Science and Engineering (UIUC), 2008)

The hydrolysis of the cement composites in phase I occurs with the accelerated changes in temperature. The dormancy period is identified as phase II, during which the temperature decreases strikingly. Throughout this period, the concrete is in a plastic state that enables it to be moved and settled without any major problems. In the next two phases (III&IV), the temperature starts to increase again due to the hydration of C_3S . Phase V is reached after a couple of days. The Portland cement with water in concrete will always be gaining strength; therefore, the hydration process is never chemically stable. The hydration process is for the most part caused by the heat of the concrete itself. Generally speaking the higher temperature implies rapid results, but it can have an adverse influence on the concrete's performance in the long term. This problem is

further explained in depth in this research (Department of Materials Science and Engineering (UIUC), 2008).

2.3.1.2 Pulverised Fuel Ash (PFA)

Pulverised Fuel Ash (PFA) also known as fly ash. Most of the commonly used fly ash is a low calcium waste product extracted mechanically or removed from flue fumes of ovens burning pulverized bituminous coal. Fly ash is a pozzolanic material and as such needs a source of calcium hydroxide before calcium silicate hydrates can be produced. Generally PFA is an acidic material containing acidic oxides such as Silicon(SiO_2), Iron(Fe_2O_3), Aluminium (Al_2O_3) and Calcium(CaO), which provide a potential for alkaline reaction (Williams, et al., 2002). Most PFA that comes from the burning of coal is produced from an inhomogeneous compound of aluminosilicate and silica glasses additional and small numbers of crystalline elements including quartz, hematite, mullite and magnetite. This degree of inhomogeneity means that extra care is needed to assure an optimum mix design and consistent final product (Song, et al., 2000).

The other characteristics of PFA that are frequently considered are fineness, uniformity and loss on ignition. The measurement of unburnt carbon known as loss on ignition (LOI) and also the regular fineness of PFA depend on the producing condition of coal crushers and the grinding method of the coal itself (Heidrich, 2002).

Particle fineness and particle size distribution are the physical characteristics of PFA that most actively change their reactivity although relevant silica content and this is important from a chemical perspective (Chen & Brouwers, 2007). The behaviour of highly reactive silica in the PFA enhances the formation potential of the aluminosilicate gel that provides mechanical strength to geopolymers materials. (Joshi & Kadu, 2012). In addition whether PFA is alkaline-activated is determined by several factors: the percentage of unburned elements in the PFA acting as inert particles, which causes an increase of the liquid: Solid ratio and the content at its different stage (Chen & Brouwers, 2007). Studies show that PFA with highly reactive Al_2O_3 and SiO_2 content and with $Si:Al$ ratios under 2.0 performs best under alkaline activation (Xie & Xi, 2001).

The alkali-activated PFA's final reaction result is an amorphous to semi-crystalline structure that is similar to a zeolite precursor. The degree of reaction and the activation

process in the geopolymer is directly linked to the glassy content of the ash material (Chen & Brouwers, 2007). Fernández-Jiménez and Palomo,(2003)found the optimum binding characteristics of PFA with the following properties: less than 5% pf unburned material; Fe_2O_3 not higher than 10%; the low content of CaO; reactive silica 40% to 50%; 80% to 90% of particles with a size below $45\mu m$; and also high content of vitreous state.

2.3.1.3 Ground Granulated Blast Slag (GGBS)

Ground Granulate Blast Furnace Slag consists of the clinkers built in a molten phase together with pig iron during the reduction of iron ore in a blast furnace and is formed mainly of alumina-silicates, magnesium and calcium. The slag is described by the way in which it is cooled. The best cementing properties are developed when it is doused iron to produce granules of an amorphous structure known as Granulate Blast Furnace Slag. GGBS is the fine powder produced from grinding and drying this material (Imbabi, et al., 2013).

GGBS is semi- cementitious and is capable of gradually setting on its own. Still, it is common to mix it with OPC between 10 to 90% of GGBS, which releases both sulphate and hydroxide ions that accelerate the strengthening gain of the GGBS (Bone, et al., 2004).

Both PFA and GGBS improve the workability of concrete with the same water content and increase the mobility for a given slump. These elements are also cheaper than OPC. With fly ash and GGBS, due to the lower density of the replacement, the volume of fine powder rises and leads to improved cohesiveness. There is less bleeding where PFA is used in concrete, but GGBS can increase bleeding for larger volume replacements. PFA and GGBS will raise settings times by 1 to 4 hours longer than OPC in the concrete blend. In the winter, more care is needed when using Fly Ash and GGBS, as the heat produced within the concrete is less enduring. The use of GGBS and PFA leads to a slower strengthening process, but higher final strengths are reached if the curing is maintained for long enough (King, 2012).

PFA and GGBS decreased alkali- silica attack, and increased sulphate resistance. Up to 70% cement replacement provides decreased heat of hydration and less restrained thermal stress. However, decreased creep may account for such results, and the tensile strain capacity could be lower (King, 2012).

Slag products can be used in various ways, and they are most commonly mixed with a 3.5/5.5% (by mass) sodium hydroxide or sodium silicate solution when being used as partial OPC replacements (Chen, 2006). This activation through an alkali forms a very low basic and highly amorphous calcium silicate hydrate gel (C-S-H). This mixture is sometimes termed alkali-activated slag, although the use of this mixture is increasingly uncommon (Pacheco-Torgal, et al., 2007).

The porosity and chemical shrinkage in saturated GGBS blend are notably higher than those in the OPC blend, and this is a logical concern during setting. Drying shrinkage has been found to be a direct outcome of the hydration process which increases with increased alkali modulus and dosages of sodium silicate based activators (Fernandez-Jimenez, et al., 2007). On the other hand, the rise in alkaline concentration in the blend increases the degree of hydration during the reaction, and while the pore volumes are decreased the microstructure properties of the C-S-H elements are improved (Fernandez-Jimenez, et al., 2007).

2.3.2 Water

Water acts a major role in the making concrete in two states, first in the mixing stage and then during the curing of concrete. The quality and quantity of water have an enormous influence over the quality of the concrete produced. Although water is the major factor that affects workability contaminants in water can change the setting of cement in the blend, decreasing the strength of produced concrete. It can also cause corrosion of steel reinforcement. Therefore it is important that the suitability of water for blending and curing of concrete is checked and addressed (Kucche, et al., 2015).

In many books and studies, the quality of water for mixing concrete is described as suitable for drinking. In levels of dissolved solids in the water-cement ratio of 0.5, the mass of solids will be 0.05% of the mass of cement, and, therefore, the impact of solids will be extremely small. In addition to dissolving solid in water, they are other properties that can affect the concrete mix such as degree of acidity and concentrations of minerals like potassium and sodium (Neville & Brooks, 1987).

2.3.3 Aggregate

Aggregate occupies approximately over 70% of the volume of concrete and, as a result, its quality is highly important and influential in concrete. The aggregate element

directly affects the strength, durability and structure of concrete. As mentioned earlier, aggregate is interlocked together by the cement mix. The strength is largely produced by the cement paste but it is dimensionally unstable and costly, so the use of aggregate in the concrete mix raises volume stability and decreases the price. It is important to note here that the advantages of using aggregate are balanced against the properties needed from concrete in its fresh and hardened state (Apebo, et al., 2013).

Aggregate is normally categorised according to its size and aggregate particles usually range in size from 0.15mm to 40mm. There are primarily two categories of aggregate in terms of size, coarse aggregate and fine aggregate with the distribution being at about 5mm (Jackson & Dhir, 1996).

To produce high-quality concrete, it is necessary to use both specified grades of aggregate. Coarse aggregate is generally applied as an idle, cheap material bound by the cement blend to produce a significant high amount of concrete. In spite of this, the impact that coarse aggregate physical, thermal and also chemical characteristics can have on the performance of concrete is remarkable. Use of coarse aggregate with an irregular surface develops higher final strength as it binds strongly with the cement blend. However, softer aggregate can affect the durability of concrete by reducing of cracks and stress caused by thermal development and shrinkage (Neville & Brooks, 1987).

Fine aggregate in the concrete blend helps coarse aggregate to bind more firmly together and it reduces the number of large voids within the concrete. This increases the bulk density, which develops the strength of the produced concrete. Fine aggregate also tends to keep the water within the blend after it is compacted, such that, increasing the quantity of fine aggregate decreases bleeding after compaction (Hu, 2005).

In making concrete, the mix of fine and coarse aggregates is considered to be a saturated surface dry (SSD) to stop either water absorption or addition to the mix. In fact, this may not be the point and additional water from the aggregate material can be unintentionally inserted. The bonding within the adhesive and aggregate blend is strongly dependent on the alkaline activator concentration. The interfacial bonding strength between the geopolymer mortars and rock will be low, while the activating was low in alkalis and dissolvable silicate (Feng, et al., 2004).

2.4 Geopolymer

Joseph Davidovits described geopolymers in the1970s, after which they were used in a range of solid materials manufactured by the reaction of an aluminosilicate powder with an alkaline solution, (Davidovits, 1982). The reaction from a polymeric material that created form rock, soil, or other related element that chemically mixes minerals is known as geopolymerisation (Khale & Chaudhary, 2007). The presentation of aluminosilicate elements such as GGBS, PFA, rice husk ash or thermally activated materials to high-alkaline conditions (Hydroxides (OH-), Silicates(SiO_4^{-4})) gives rise to the development of a geopolymer. Geopolymers are defined by a three-dimensional Si-O-Al structure (McDonald & Thompson, 2011).

2.4.1 Geopolymer Development

Geopolymers are a division of the group of inorganic polymers. The chemical structure of the geopolymer material is related to zeolite materials; but, the microstructure is amorphous rather than crystalline (Provis & Van Deventer, 2009). The polymerisation method includes an essentially quick chemical reaction below alkaline condition on Si-Al minerals, which creates a three-dimensional polymeric link and loop structure consisting of Si-O-Al-O bonds (Davidovits, 2011).

$$M_n[-(SiO_2)_z - AlO_2]_n . wH_2O \qquad (2.3)$$

Where:

M - Alkaline element / Cation (Sodium, Potassium or Calcium)

N - Degree of polymerisation ($z > n$)

z - Number between1-32

w - ≤ 3

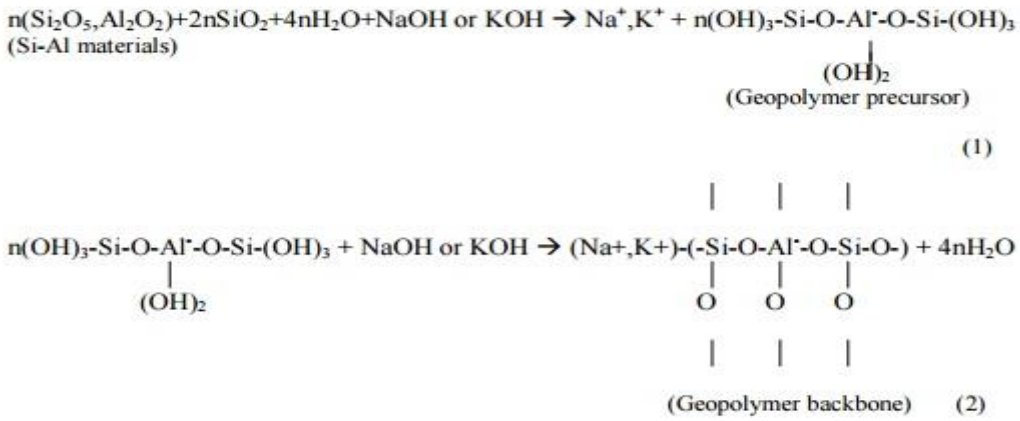

Figure 2.3: Formulation of geopolymer material as describe by equation A and B. (Van Jaarsveld, et al., 1997)

The last chemical term in Equation 2, Figure 2.3 explains that the development of geopolymer water is produced. During the curing and drying period of the geopolymer, this water will be expelled, the state behind nano-pores in the matrix that present advantages to the production of geopolymers. The water in geopolymer blend simply gives workability to the mix through handling. This is the difference to the chemical reaction of water in the OPC concrete blend during the hydration process (Rangan, 2010). The overall polymerization process in alkali-activated geopolymer is shown in Figure 2.4.

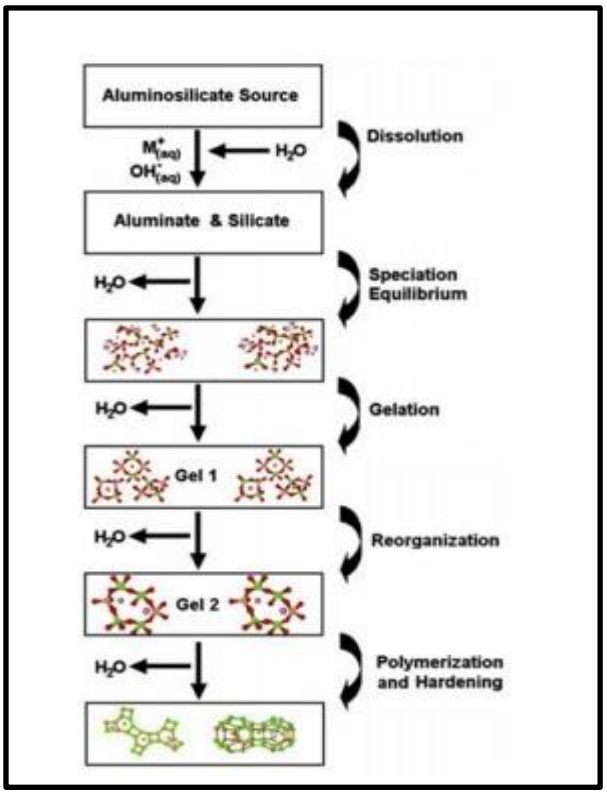

Figure 2.4 Conceptual Model for Geopolymerisation (Peterman & Saeed, 2012)

The chemical reaction may include the subsequent steps:

- Dissolution of Si and Al atoms from the source material into the action of hydroxide ions.
- Orientation, condensation, or transportation of precursor ions into monomers.
- Polycondensation or setting of monomers into a polymeric structure.

In addition, it is difficult to isolate and examine each of these steps due to the overlap of these steps with each other (Palomo & Fernandez-Jimenez, 2011).

2.4.1.1. Dissolution process

This stage occurs instantly when the aluminosilicate in the pozzolanic materials such as Fly Ash or GGBS is dissolved by the alkaline solution. Further, this stage provides for ionic interface within species and the breaking of covalent bonds in oxygen, aluminium and silicon atoms. The dissolution range is related to the volume of the PFA and GGBS and the pH of the activating solvent (Xie & Xi, 2001).

2.4.1.2. Polymerisation Process

This process is essentially a quick chemical reaction following alkaline conditions on Si-Al minerals, producing a three-dimensional polymeric of Si-O-Al-O bonds (Skvara, et al., 2005). The developed gel resulted includes alkaline cations that neutralize the deficit charges linked with the aluminium-for-silicon replacement (Xie & Xi, 2001).

These gels reveal the production of three-dimensional materials that develop the cementitious material that attaches unreacted fly ash spheres. In this aluminosilicate gel, the Si is discovered in a type of $Q^4(nAl)$, where n, ranging between 0 and 4 which is dependent on curing conditions and activators type (Fernández-Jiménez, et al., 2006). In silicate systems the Q-unit is used to indicate the different silicate atoms in a system. However, this notation is not sufficient to describe the basic building units in the zeolite or aluminosilicate frameworks. In the zeolite systems, the Q-units are always theQ^4, where each silicate is surrounded by four silicate or aluminate units (R. Szostak, 1989).

2.4.1.3. Growth

Through this method, the moderate growth of crystalline compositions becomes obvious as the centre of the polymerised gel approach significant size. Throughout the process from the initial step dissolution to the polymerisation stage in which the three-dimensional alluminosilicate are covered in Glukhovky's polymerisation model, the last phase of polymerisation and setting is the various essential of the microstructure of the final setting that geopolymer results. Eventually these factors create the physical characteristics of the resulting adhesive (Fernández-Jiménez, et al., 2006).

2.4.2 Advantages and Disadvantage of Using Geopolymer Concrete

2.4.2.1 Environmental

The production of geopolymers decreases the environmental effects of PC in two ways. By creating a commercially viable replacement for PC, the CO_2 emissions produced while making PC products would cease to exist. The production of one ton of PC concrete releases nearly one ton of CO_2 into the atmosphere (Skvara, et al., 2005). For this amount of PC, 2.8 tons of raw substances are needed, including fuel and extra materials, a process that produces 5% to 10% of all airborne dust (Khale & Chaudhary, 2007).

In addition, the use of cementitious products would limit the disposal of these substances into the environment in their dangerous, raw state. Currently, unclaimed PFA and GGBS are dumped into landfill facilities raising the hazard for leaking metals inside groundwater. Geopolymer cement production on a global system would reduce or eliminate this danger (Puertas & Fernández-Jiménez, 2003).

2.4.2.2 Economical

The production of geopolymers decreases the requirement for the expensive product of the clinker needed in PCs. The high cost of PC production is based on the huge quantity of energy demanded to provide the material. The especially high temperatures (1400-1500℃) required for PC production make this very expensive and energy-intensive process (Fernández-Jiménez & Palomo, 2005).

The pozzolanic materials used in geopolymer cement are easily accessible as waste products of manufacturing coal power plants, consequently making them a reasonable

alternative. Fernandez-Jimenez, et al. (2007), stated that only 30% to 40% of usable PFA actually used, leaving the remainder to be distributed in environmentally controlled methods to decrease the hazard of air polluting, leaching, and possible contamination of inland and marine waters. To relieve this developing difficulty by recycling the material of industrial production would not only be economically reasonable but also environmentally responsible (Sumajouw & Rangan, 2006).

2.4.2.3 Chemical Resistance

It has been pointed out that geopolymer paste shows great resistance to sulphates and many different acids. The degeneration of PC from sulphate attack is attributed to the development of broad gypsum and ettringite which cause cracking and spalling in the concrete. The higher production of geopolymeric elements in acidic situations is associated with the lower calcium content of the source material. Geopolymer cement provides no gypsum or ettringite structure, so no mechanism of sulphate charge in heat-cured, low-calcium fly ash based geopolymer cement is observed (Skvara, et al., 2005).

2.4.2.4 Pozzolanic Composition Analysis

The chemical structure and particle mass distribution of the PFA must be verified before use (Skvara, et al., 2005). The mechanics of hard geopolymers are directly linked to the mineralogical structure of the elected pozzolanic. Minor modifications in these substances have notable impacts on the resulting binder characteristics. The quantity and order of calcium in the raw materials plays an important role in limiting the reaction pathway and the physical characteristics of the ultimate result (Rangan, 2010).

Before activation, a micro-analysis of the pozzolanic must identify the present minerals and their size relevant to the overall mass. This will help determine the suitable activating agent and the concentration needed to perform the optimum reaction. The silica content of PFA is regularly observed to 40% to 60% of the ash substance, 20% to 30% alumina, and the presence of iron varies dramatically (Khale & Chaudhary, 2007).

2.4.2.5 Workability

The rheological characteristics of geopolymer paste are not similar to those observed in PC concretes. Pozzolanic-based geopolymers maintain more static and dynamic viscosities than PC products and vibration efforts can be expected to decrease air holes in the fresh paste (McDonald & Thompson, 2011).

2.4.3 Hydration Reaction

Within these process intervals, thermodynamic and kinetic parameters are developed to gel formation and reaction degree. Various issues immediately affect the degree of reaction (α) examined in a mixed geopolymer paste. These issues can either improve or harm the polymerization process and the following states explain the formed cementitious properties of the hardened cement. The element size division and mineral structure of the PFA or GGBS affect the rate of activation reaction and the chemical structure of the reaction output (Fernández-Jiménez, et al., 2006).

2.5 Alkaline Activators

The most commonly used activators are Sodium Hydroxide $(NaOH)$, Sodium Sulphate (Na_2SO_4), Sodium Carbonate (Na_2CO_3) and Sodium Silicate (Na_2SiO_3). Commonly, alkaline salts or caustic alkalis are used as alkaline activators of alkali-activated concrete and cement (Glukhovsky, 1980). These are arranged into six groups according to their chemical structures as follows, where M is an alkali ion: (Pacheco-Torgal, et al., 2007).

1) Caustic Alkalis (MOH)
2) Non-Silicate weak acid salts $(M_2CO_3, M_2SO_3, M_3PO_4, MF)$
3) Silicates$(M_2O * nSiO_3)$
4) Aluminates$(M_2O * nAlO_3)$
5) Aluminosilicate $(M_2O * nAl_2SO_3 * (2-6)SiO_2)$
6) Non-Silicate strong acid salts (M_2SO_4)

The most frequently used cost-effective, and easily accessible chemicals are $NaOH, Na_2CO_3, nSiO_2Na_2O$,and Na_2SO_4. However, potassium hydroxide has been used in a few studies, but its use is difficult due to price and availability. In addition, the properties of the potassium and sodium are similar, so it is not worth the cost to use potassium as an alkali activator when making geopolymer (Kong, et al., 2008).

2.5.1 Sodium Hydroxide (NaOH)

Sodium Hydroxide (NaOH) is commonly used as an alkali activator in geopolymer production, because sodium cations are smaller than potassium (K^+) ions which allows the cations to move everywhere in the paste network with much less energy. Moreover,

NaOH produces a large charge density that promotes extra zeolitic formation power (Rangan, 2010).

The mass and molarity of this specific activating solution cause the resulting paste characteristics. A high volume of NaOH can accelerate dissolution, reducing ettringite and CH formation during the binder development process, (Khale & Chaudhary, 2007). Furthermore, higher concentrations of NaOH increase higher strength at early ages of reaction. This is but superseded by settling the strength of aged materials. This is due to the excessive OH^- in the solution, which affects undesirable morphology and non-uniformity of the last mixture product, (Rangan, 2010). Other advantages associated with the use of NaOH activators included improved durability in aggressive conditions where acids and sulphate are present, owing to improve crystallinity, (García-Lodeiro, et al., 2007).

Furthermore, the use of sodium hydroxide (NaOH) as an activator preserves the pH of pore solutions, controls hydration activity, and directly changes the formulation of the C-S-H product in the geopolymer cement. There is a linear relationship between the concentration of sodium hydroxide and the quantity of heat generation when the concentration of the acid is raised there will be more number of acid in the same volume, so more heat energy will be required for the reaction of these acid particles. And although there is an inverse relationship between the concentration of sodium hydroxide and the time at which is at a maximum of the hydration heat (Damilola, 2013).

2.5.2 Sodium Silicate (Na_2SO_3)

Sodium Silicates (Na_2SO_3) are produced when sand fuses, (SiO_2) by sodium carbonate or sodium-potassium (Na_2CO_3 or K_2CO_3) at the extreme high temperature of 1100℃, dissolving through high-pressure fumes in to a semi-viscous fluid as called, *waterglass* (Fernández-Jiménez, et al., 2006). Waterglass is infrequently applied as an independent activating element because it does not have the sufficient activation potential to start the pozzolanic reaction by itself. It is generally combined with sodium hydroxide (NaOH) as a fortifying factor to improve alkalinity and develop general sample strength. In polymerization, the most general alkaline liquid used is a compound of potassium hydroxide (KOH) or sodium hydroxide (NaOH) and sodium silicate(Na_2SO_3) (McDonald & Thompson, 2011).

A sodium silicate solution is commercially available in several grades and types. However, when comparing powdered and liquid form of waterglass, it should be noted that the powdered waterglass form leads to lower performance (Kong, et al., 2008). Furthermore, for best results the activation solution should be prepared 24 hours prior to use (Skvara, et al., 2005). The main significant characteristic of this product is its mass ratio of $SiO_2 : Na_2O$ which is commercially feasible in the scale of 1.5 to 3.2 (Fernández-Jiménez, et al., 2006).

The solubility of silicate decreases the alkali saturation in pore solutions and can support better the inter particle bonding by pozzolanic and aggregate elements. Testing has shown that activating solutions applied for activations that contain small or no soluble silicate are notably weaker compressive strengths of mortars and concrete than those with greater doses of solvent silicates. The present of mentioned silicate material can also enhance the bonding within coarse aggregate and geopolymer mortar at an interfacial level. Various studies have noted that in some experiments under rising temperatures, samples that contain waterglass decrease strength during those containing just a base activator; through it normally produces higher strength. However, additional studies are required to precisely define the specific effects produced by the addition of waterglass in samples (Fernández-Jiménez, et al., 2006).

2.6 Binder Constituent Proportioning

Geopolymer binder characteristics are very dependent on the kind of, rates and concentrations of blend components. Individual constituents and the variables linked with that constituent, act as an important role in limiting the properties of the ultimate result.

2.6.1 Activator Concentration

The alkaline activator is an important part for strong geopolymer formation and the development of high compressive strength. Despite activator classification, an improvement of concentration raises the reaction speed and degree to a few acceptable and stronger cement materials. The increasing of activators and rise in concentration lead to a rise in the volume of smaller pores and lowers the entire porosity for the PFA based methods, therefore rising the initial strength of the mortar samples (Chareerat, et al., 2006). The impact of activator concentration develops with time. The minimum

molarity PFA and GGBFS mixtures are 2 to 10 molar Furthermore, better strength is achieved when the concentration approaches the highest range (Song, 2007).

Higher strength capabilities potentially will be the result of higher concentration; there is a maximum limit for all activators. Therefore, the outcome will be affected by passing the limit. Polymer formation can be delayed by increasing alkaline concentration because it increases setting time. One must consider the extreme ion boundary, the fluidity, and the potential to mix by possible reactive varieties. Therefore, the concentration has to be clearly addressed in a geopolymer mix (Khale & Chaudhary, 2007).

2.6.2 Pozzolanic / Activator Ratio

The rate of PFA, GGBS, and calcined clays to the chosen activator affects some important characteristics of the geopolymer basis. Strength is very affected by this variable. The recommended ratio of an alkaline liquid to a PFA (by mass) uses the scale of 0.3 to 0.45 (Skvara, et al., 2005). The PFA to activator ratio seemed to be the most important parameter for overall strength and fire resistance of the geopolymer (Fernández-Jiménez, et al., 1999).

2.6.3 Sodium Silicate and Hydroxide Activator Ratio

The addition of sodium silicates to the process raises mechanical characteristics beyond the capacity of a hydroxide activator individual. However, the rate within every element must be carefully applied and set. Some books suggest that the ratio of sodium silicate to sodium hydroxide solution (by mass) be fixed to 2.5 (Fernández-Jiménez, et al., 1999).

2.7 Geopolymer Production

This section explains the recommended method for designing, processing, and curing a geopolymer mortar mix. Each feature of the design must be completely reviewed and engineered in order to avoid undesired outcomes.

2.7.1 Aggregates

In geopolymer mortars, a concrete aggregate worked the same way as PC-based materials. However avoiding any possible attack from aluminosilicate reactivity by the alkaline activating needs priority care. Mineral structures containing cryptocrystalline

silica, opaline, and quartz are sensitive to an aluminosilicate reactivity charge that could eventually begin to aggregate dissolution (Khale & Chaudhary, 2007).

Furthermore, between 70- 80% mass of the geopolymer concrete is from the aggregate. The recommended size for fineness aggregate in a geopolymer mix is 4.5 to 5, which allows the most interaction and bonding with the geopolymer paste. (Skvara, et al., 2005). The aggregate material is applied fundamentally for filler material to decrease the quantity of the binder needed for production. The geochemical characteristics of the coarse aggregates seem to have limited impact on the compressive strength of geopolymer concretes (Feng, et al., 2004).

The aggregates (fine and coarse) in geopolymer mixes are considered to be saturated surface dry (SSD) to prevent water addition or absorption to the mix. In fact, this will not be the problem and additional water from the aggregate will accidentally be added to the mix. For this purpose, providing slight compensation in the w/s ratio in the geopolymer design is suggested. The alkaline activator concentration can affect the interfacial bonding between the binder paste and aggregate mix. When silicates or alkalis amount are low in the activating solution it could result in interfacial bonding between geopolymer mortars and rocks which are also low (Feng, et al., 2004).

The study indicates that when the interfacial bonding is weak, the alkalinity thermal charging of geopolymers, including aggregate, can be harmful to the concrete. The strength of the geopolymer failed with the addition of aggregate, probably due to the differential in thermal development between the aggregate and paste masses. It is understood that the geopolymer matrix experiences the thermally caused shrinkage during the aggregate growth in extreme loading (Fernández-Jiménez, et al., 1999).

2.7.2 Mixture Proportioning

Geopolymer elements play a major part in determining the final outcome of features. The mechanics of hardened concrete and geopolymer mortar are directly linked to factors like aggregate size, pozzolanic structure, activator and concentration, and ratios of water. (Palomo & Fernandez-Jimenez, 2011). Based on zeolite chemistry, in order to reach great strength and durability the applications of the specific molar ratio for the alkaline activator are: $\frac{SiO_2}{Al_2O_3}$ (3.5-4.5), $\frac{Na_2O}{Al_2O_3}$ (0.8-1.6), $\frac{Na_2O}{SiO_2}$ (0.2-0.48); between metakaolin and activator: $\frac{H_2O}{Na_2O}$ (10-25) (Wallah & Rangan, 2006).

During each component, which was applied to form the geopolymer, which demonstrates significance in the final result, it has been concluded that the best composition resulted in the following chemical ratios: $\frac{Na_2O}{SiO_2}$ =0.25, $\frac{SiO_2}{Al_2O_3}$ = 3.3, $\frac{H_2O}{Na_2O}$ = 10. Moreover, water content was identified as an influential reason to the benefit of the geopolymer, as testing by H2O/Na2O molar ratios equal to 25 produced very low mechanical effects. (Silva & Thaumaturgo, 2002).

2.7.3 Curing Geopolymer Method

Puertas and Fernández-Jiménez observed that in synthesizing PFA- based geopolymers; they did not set at 23℃. A challenge for strong geopolymer mortar is reaching suitable mechanics at ambient heats. The geopolymers reaction is more simply achieved by an exterior heat source to increase the alkaline activity of the pozzolanic materials.

A study has been performed to analyse geopolymer designs, including the possibility to strongly harden under room temperature conditions. However, limited knowledge has been obtained about techniques of a large-scale ambient geopolymer cure (Skvara, et al., 2005).

2.8 Electrodeless and Real-time Cement and Concrete Resistivity Analyser-CCR2

Cement-based materials are generally applied during construction because they are very economical materials. In a concrete or cement-based materials study, it is important to realise an understanding in the deformation characteristics of stated materials. There are several limitations to consider. One of the most relevant limitations is the sensitivity of early-age cracking. In various uses, it is important or useful to measure the electrical resistivity of cement-based materials (Li & Li, 2003). These include the technique of the ring constraint or uniaxial, which are applied to determine the cracking time of materials. However, this method is difficult and in accurate because of the long observation period (Wei & Li, 2005).

”Electrodeless and Real-time Cement and Concrete Resistivity Analyzer-CCR2” is a recently designed piece of equipment for monitoring the hydration process of freshly mixed cement-based materials (Li & Li, 2003). In the CCR-2 measurement, there is no electrode used. This completely erases the problems that linked with this technology

due to the electrodes in the form of polarisation and cracking. CCR-2 can also measure the temperature variations of the hydration materials while the measurement (Li, et al., 2003). CCR-2 includes three parts: a mainframe, a specimen platform and a computer (Figure 2.5).

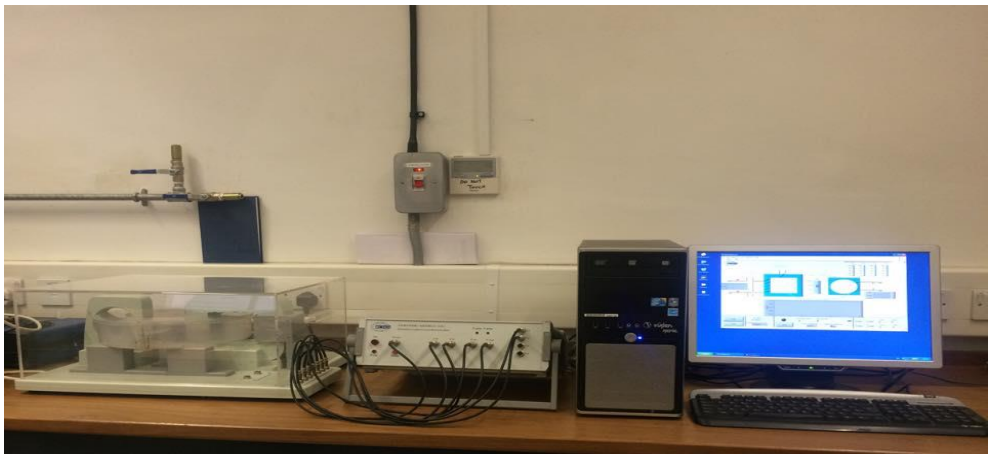

Figure 2.5 CCR-2 testing equipment (Brunel University London)

The resistivity of fresh cementitious- based substances is known to change through the hydration process. That can be applied to explain the hydration process of fresh cementitious- materials, and the effect of changes to the mix (chemical admixtures, minerals and etc.). While measuring the resistivity of fresh mortar/cement paste and plotting the consequent characteristic curves of resistivity over time, the effects of water-cement ratio and the hardening and setting characters of cementitious- materials can be determined. A real- time automatic analysis technique for the study on the hydration of cement-base materials, a major development to the traditional ways, such as hydration heat release and ultrasonic technique has been developed by Li, et al.(2003).

2.8.1 Determination on Water/ Cement ratio

The resistivity-time curves of materials (Figure 2.6) by different w/c ratios are very different. Numerous changes occur with minimum resistivity. However, the resistivity-time curve for cementitious- materials with a standard w/c ratio can outcome the amount of added water in other mixes in comparing minimum resistivity. Therefore, a test can be used to determine that the water added is beyond a standard level if the time of minimum resistivity is observed longer than the standard one, and the minimum resistivity value is lower than the standard one (Wei & Li, 2005).

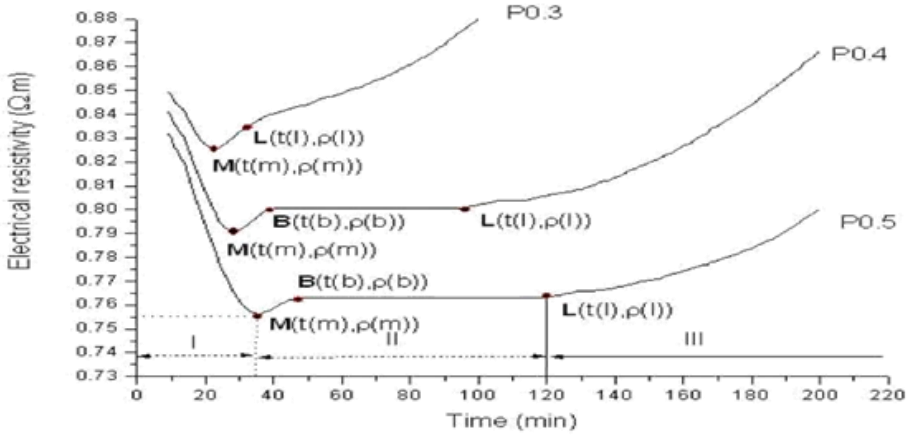

Figure 2.6 Resistivity-time curves of cement-based materials (Wei & Li, 2005)

2.8.2 Stages of Hydration Process

Given particular characteristic points on resistivity curves, the hydration process of the material can be separated into three periods; the dissolving period, the induction period, and the setting and hardening period. Once the hydration process enters the induction period, an ettringite product layer forms around material at the cement base. Later, as hydration enters the setting and hardening period, the ettringite product layer, breaks down. A reduced resistivity value during the dissolution is attributable to the increased concentration of the cementitious material paste. By contrast, increased resistivity during the setting and hardening period is because of a reduction in the liquid term, as the porosity of the cement paste diminishes. As the water/cement (w/c) ratio for induction increases, the briefer dissolution and the induction period become. As a result, resistivity during the setting and hardening period develops more quickly and the resistivity value ultimately becomes greater than it would be otherwise (Xiao & Li, 2008).

2.9 Strength Development

2.9.1 Strength Development of Concrete at Early Ages

The early development of strength and mechanical properties is crucial for concrete Carino, et al.(1989), indicated two factors for such development. The long-term strength of concrete is greatly affected by its early history and, for instance the impact of extreme loading at early ages.

As Bergström and Byfors.(1980), posited, through that the term *early ages* for concrete has no definitive meaning the characteristics of concrete while the first two days after casting are crucial. In attempting to define *early ages*, these authors emphasised that, oddly enough, time is not the chief parameter. For various cement materials, curing temperature and admixtures emerge at different degrees of hydration, which in turn establish diverse properties for the concretes at an early age, even if the mix proportions are identical.

Carino, et al. (1989) defined *early ages* as the period during which the characteristics of concrete change rapidly, which occurs regularly until the degree of hydration exceeds 50%. It is nevertheless challenging to specify any particular quantities of that characterize early ages, since the degree of hydration is highly contingent upon the physical and chemical characteristics of the cement, the particle size combination of the cement or adhesive, the w/c ratio, the supplementary cement base materials, the synthetic admixtures, and the curing heat. (Wang, et al., 2006). More or less, 50% of cement type I in PC concrete kept at a standard curing temperature of 20℃ hydrates in three days. By some contrast, concrete substituted substantially with GGBS required more time to attain the hydration degree of 50%. (Bergström & Byfors, 1980).

Among other definitions of *early ages,* Glišić and Simon. (2000), recognised the period as the time that begins during running and ends when the thermal methods in the concrete have completed. Reinhardt. (1990), called concrete at early ages "young" that is, aged from one to seven days, during which, the concrete surface needs to develop toward, becoming strong enough to survive weathering, corrosion, and other attacks. At early ages concrete already begins to exhibit durability.

2.9.2 Long- Term Strength Development of Concrete

Though the strength of concrete is normally assessed at the age of 28 days, strength continuously improves after this point. Concrete’s strength during later periods is significant, especially if the structure is exposed to a specific kind of loading later on (Neville, 2011)&(Al-Khaiat & Fattuhi, 2001).

Several researchers have discovered that using additional cementitious materials such as silica fume, GGBS and PFA, and their combinations, as replacement for cement, can improve the production of both fresh and hardened time, in terms of, the strength, durability, and workability of concrete. Concrete should proceed to perform its

functions throughout the service period of the construction which demands that the concrete's strength and serviceability should be maintained. Concert's action against all charges is known as durability (Al-Khaiat & Fattuhi, 2001) & (Toutanji, et al., 2004).

Wood (1992), assessed the long-term characteristics of concrete with PC in terms of compressive strength, flexural strength, and elastic modulus during 5 and 20 years periods in open-air and moist curing situations. Results revealed a slight difference in the strength of the samples kept in a moist room from those kept outdoors. In another study, the rate of the strength of samples kept outdoors to the that of samples kept in the moist room ranged from 0.8 to 1.0 (Neville, 2011). Meanwhile, the strength of concrete cured in conditions of low comparative humidity did not rise considerably after 28 days.

However, the outcome of a flexural strength experiment showed that the characteristic is remarkably dependent upon moist curing, as the strength of samples kept in moist situations was greater than that of those kept in dry situations by 20- 30% (Aitcin, et al., 1994). Dynamic analyses of the elastic modulus were too sensitive to the amount of moisture in specimens. For moist cured specimens the elastic modulus increased with time, yet became relatively constant after the drying process commenced (Neville, 2011).

2.9.3 Strength Development of Alkaline-Activated Concrete

Having, studied the impact of clinker chemistry on the early progress of strength in a GGBS mix. Gee (1979) reported that the method in which the clinker delivers calcium and alkalis changed the hydration speed at the early ages of the cement-based mix. GGBS reacts with water in alkali settings and later reacts with calcium hydroxide delivered by cement hydration in pozzolanic material to further improve C-S-H gel in the adhesive. (Siddique, 2007).

The hydration outcome $Ca(OH)_2$ initiates the GGBS mix's hydration of a low CaO/SiO_2 ratio of C-S-H. The pozzolanic effect can enhance the C/S ratio to a rate of approximately 1.7 in a GGBS mix due to low amounts of $Ca(OH)_2$ and C-S-H (Siddique, 2007) & (Siddique & Iqbal Khan, 2011).

Hogan and Meusel (1981) reported that in mixes of 40- 60% GGBS concrete, compressive strength developed slower than that of PC concrete given the same water-binder ratio for the first three days. They nevertheless added that the improved strength

of GGBS concrete after three days was greater than that of concrete with PC only, particularly for concrete of 40% GGBS. Roy and Idorn (1982), also found that the improvement in strength of concrete of 20- 60% GGBS was not reached until 28 days, whereas with an equal or long duration, strength become balanced with that of concrete using only PC.

Analyses of compressive strength have been applied in various studies as instrument to measure the progress of geopolymerisation. The low-purity of compressive strength measurement have also been examined, given that determining strength's progress is a fundamental method of measuring the efficiency of materials at different stages of construction (Provis, et al., 2005).

The compressive strength of geopolymers dependents upon several circumstances, including gel state strength, the rate of the gel state and undissolved Al-Si particles order, the hardness of the undissolved Al-Si particle quantities, the amorphous kind of geopolymer or number of crystallinity, and the external reaction in the gel state and the undissolved Al-Si particles (Jaarsveld, et al., 2003)& (Xu & Deventer, 2000).

Following geopolymerisation, the undissolved particles stay bonded in the matrix, meaning that the hardness of the minerals is positively affected by the ultimate compressive strength (Xu & Deventer, 2000). With the geopolymerisation of common minerals, after introducing aggregate, for example, or granular sand to the geopolymer mix, the compressive strength increases (Xu & Deventer, 2002).

The amount of metakaolin in the geopolymer matrix, along with the concentration of potassium hydroxide (KOH) and addition of sodium silicate (Na_2SO_3), plays a crucial role in the material's ultimate compressive strength. Swanepoel, et al.(1999) reported that strength rises by rising the amount of metakaolinite, largely because it can affect the amount of Al gel, which forms more in systems with higher levels of polymerisation. Some studies have shown that compressive strength, by the density and the amorphous state of metakaolinite-based geopolymer, develops by the rise of sodium hydroxide(NaOH) concentration in the range 4 to12 mol/L, largely due to the enhanced dissolution of the metakaolinite particulates and, the accelerated concentration of the monomer in the presence of more highly concentrated NaOH. (Wang, et al., 2005).

Luz Granizo,et al, (2007) investigated the effects of the alkaline activation of cementitious materials containing sodium silicate and NaOH solutions. Among their

results, the materials displayed higher mechanical strength than those activated with NaOH only.

2.10 Analytical methods

Many methods, both advanced and simple can be used to elucidate geopolymerisation mechanisms. The ability of Al–Si crystals to support geopolymerisation might be predetermined by particular surface area measurements, which imply the amount of surface area that participates in different reactions in a solid–fluid system. (van Jaarsveld, et al., 2002).

Microscopy can reveal notable characteristics of microstructures since it displays results according to the physical quantity and design of various features of geopolymers. X-ray fluorescence (XRF) spectrometry works remarkably well for the elemental analysis of Al–Si crystals. X-ray diffraction (XRD) might be also a useful method, through the amount of information that may be collected is limited as a result of the large amorphous kind of geopolymer. This method will present information concerning the extent to which crystalline origin materials have reacted (van Jaarsveld, et al., 2002). Figure 2.7 displays the XRD model of a geopolymer for which PFA is used as the raw material and initiated with an NaOH (8M) solution and cured at 85℃ for 20 hours. (Fernández-Jiménez, et al., 2004).

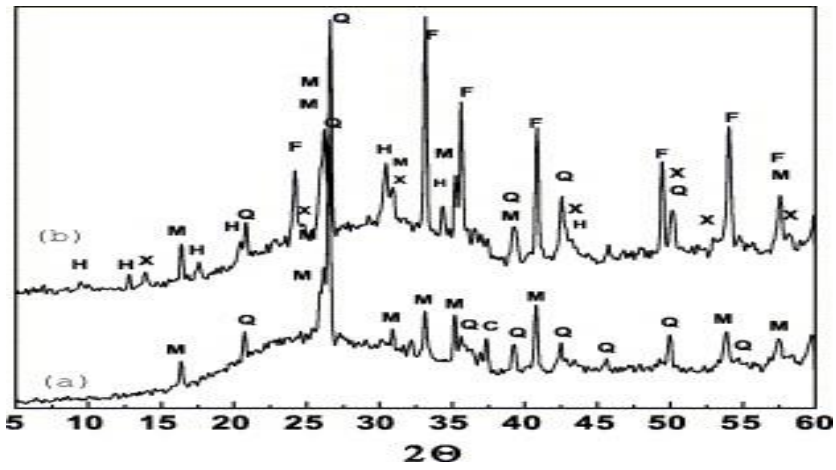

Figure 2.7: XRD spectra (a) un-reacted fly ash; (b) alkali-activated fly ash 20 h at 85 °C.

At the same time, scanning electron microscopy (SEM) enables the optical analysis of results in millimetres to micrometres, thereby yielding an absolute topographical

report on the physical and mechanical specification of the microstructures of crystalline and amorphous substances, which cannot be identified by other methods (Duxson, et al., 2012).

Fernandez Jiminez, et al. (2004) reported that geopolymer microstructures (Figures 2.8- 2.11) can be described distributing characteristic morphologies in a large amount of predominantly featureless hydration results (i.e., alumina-silica gel). Rarely is, cracking in these objects is recognised, largely due to the thermal method performed during activation, mechanical destruction during the specimens preparation or shrinkage due to drying in electron microscope's vacuum. The low magnification images shown in Figures 2.8 and 2.9 reveal the number of various component stages while Figures. 2.10 and 2.11 show the increase in local items.

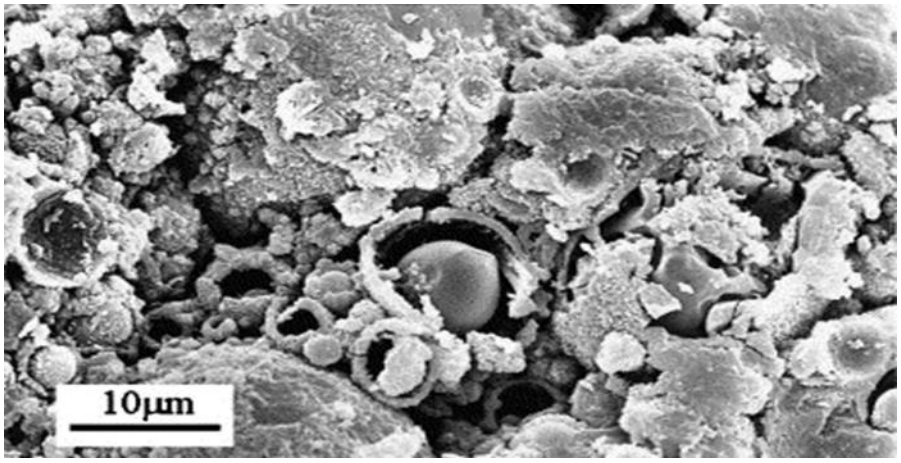

Figure 2.8: SEM micrograph of fracture surface of alkali-activated PFA geopolymer. Fe2O3 is arrowed (Fernández-Jiménez, et al., 2004).

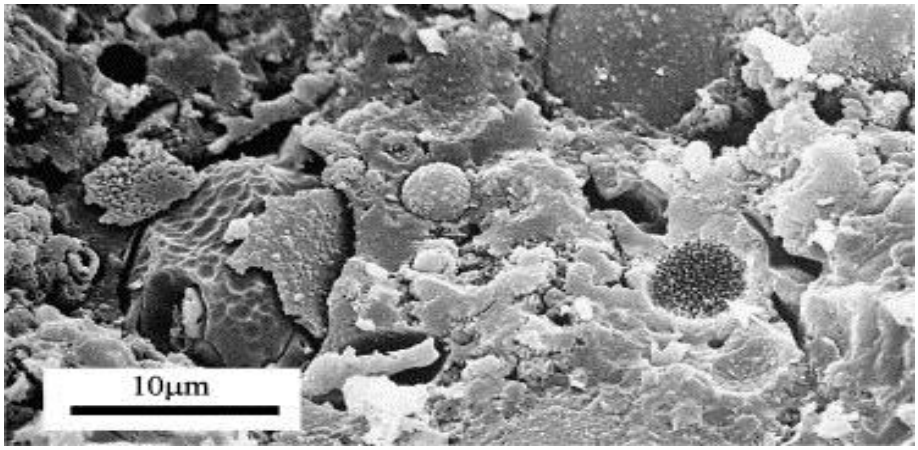

Figure 2.9: SEM micrograph of fracture surface of alkali-activated PFA geopolymer. (Fernández-Jiménez, et al., 2004)

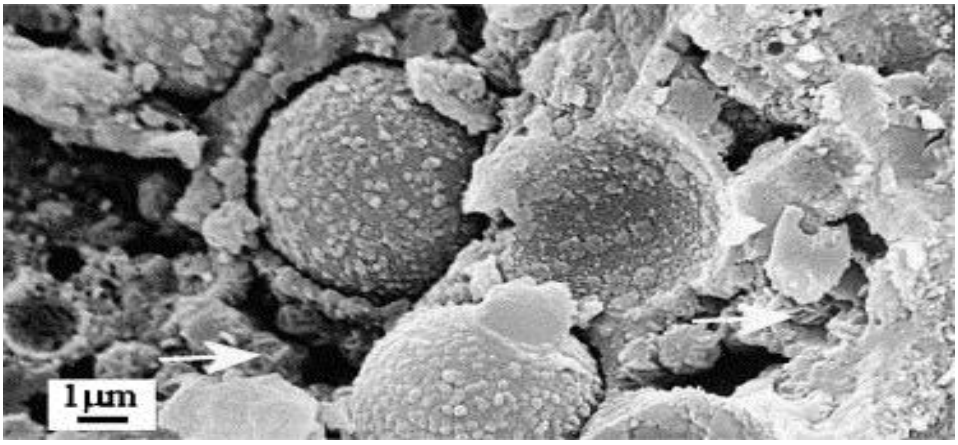

Figure 2.10: SEM micrograph of fracture surface of alkali-activated PFA geopolymer showing PFA particle with reaction shells and also unidentified spherical assemblages (arrowed). (Fernández-Jiménez, et al., 2004).

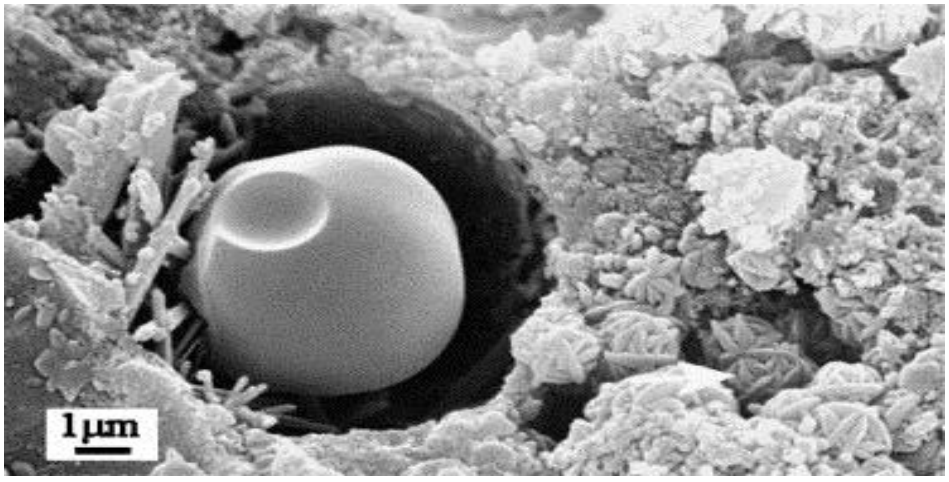

Figure 2.11: SEM micrograph of fracture surface of alkali-activated.

3. Experimental Methodology

This chapter outlines the materials which used, the mixing, casting and curing methods of geopolymer concrete investigated in this study. The techniques of measuring flexural and the compressive strength of geopolymer mortar samples and those of SEM are also explained. Electrical resistivity test also was carried out to monitor the properties of geopolymer concrete.

3.1 Raw Materials

All raw materials utilised in this investigation were the same. They were all in accordance with the relevant BS EN standards and were validated to be acceptable for the scope of this investigation.

3.1.1 Pulverise Fuel Ash (PFA)

The PFA which used in the geopolymeric mix was produced by CEMEX Co. and was sufficient for categorisation conforming to BS EN450-1, with a fineness Classification of S. The mix was in the formation of a fine grey powder consisting typically of round particles formed of aluminosilicate glass. This special grading was almost 50% silica (SiO_2) and 26% alumina(Al_2O_3) (Appendix B).

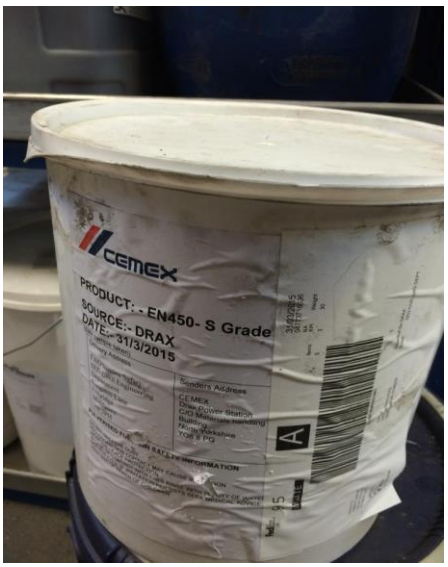

Figure 3.1: PFA

3.1.2 Ground Granulate Blast Furnace Slag (GGBS)

The GGBS which utilised in the blends was provided by Hanson (Heidelberg Cement Group) from their Scunthorpe works and was the category to BS EN15167-1. The GGBS was a fine powder. The chemical components of the substance were comparatively standard by a smaller amount of CaO to PC and higher Al_2O_3 than PC. The special gravity of the GGBS was 2.9.

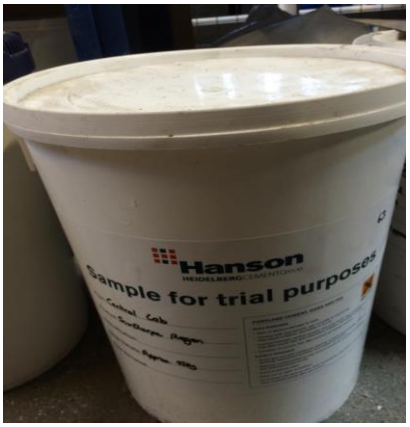

Figure 3.2: GGBS

3.1.3 Sand

The sand which was used in the blend was produced by Howie & Howie Limited. The sand conformed to BS EN196-1 and was standard sand for the strength measurement of cement to EN196-1:2005. It was natural sand, with good fractions of silica ate least 98% content and considering mostly of isometric and round particles. Being both cleansed and dried from its producer, sand was ready to use. Table 3.1 displays the particle sizing of standard sand.

Table 3-1: Particle Sizing of standard sand (Howie & Howie limited, 2015)

Square Mesh Size (mm)	Cumulative (%) Retained
0.08	99± 1
0.16	87± 5
0.50	67± 5
1.00	33± 5
1.60	7± 5
2.00	0

3.1.4 Chemical Admixture

Sodium silicate(Na_2SiO_3) and Sodium Hydroxide (NaOH) both were produced by Fischer Scientific UK. They both have high PH value which for sodium silicate is 12.6 and for sodium hydroxide is 14. Sodium hydroxide which have been used was fully soluble and with the molecular weight of 40. The molecular weight of sodium silicate was 122.06 and it is also soluble in water.

Figure 3.3: Sodium hydroxide and Sodium Silicate

3.2 Experimental Procedures

3.2.1 Alkaline Activators

Research explains that mortars and concretes based on Fly Ash activated with mixtures of sodium hydroxide and sodium silicate provide the excellent material qualities. The balances of these two types of alkalis and concentration were described with two values of AM and AD.

- *Alkali Modulus* (AM) is the mass ratio of sodium oxide to silica in the activate or solution and is a substitute for the amount of adding silica in the activator solution.

$$\text{Alkali Modulus} = \frac{Na_2O}{SiO_2} \qquad (3.1)$$

- *Alkali Dosage* (AD),$\%Na_2O$, represented as the mass ratio of sodium oxide (Na_2o) or equivalent sodium oxide in the activate or solution to fly Ash and is a substitute for the concentration of the alkali activator solution.

$$\%Na_2O = \frac{Na_2O}{PFA} \tag{3.2}$$

- *Water Solid ratio*, describes the ratio of Pozzolanic feedstock to fine sand by mass.

$$W/S = \frac{\text{Total Water Mass}}{\text{Alkali Solids} + \text{Total mass of PFA}} \tag{3.3}$$

- *Total Water to Solid ratio*, as per previous Water-Solid ratio with the inclusion of the mass of all fine aggregate.

$$W_t/S_t = \frac{\text{Total Water Mass}}{\text{Alkali solids} + \text{Fine aggregates} + \text{Total mass of PFA}} \tag{3.4}$$

- *Na_2O available in NaOH*, describes the amount of Sodium Oxide within Sodium Hydroxide solids.

$$Na_2O \text{ available in NaOH} = \frac{NaOH_{\text{Solid mass}} \times Na_2O_{\text{molar mass}}}{NaOH_{\text{molarmass}} \times 2} \tag{3.5}$$

- *H_2O available* represents the amount of water within sodium hydroxide solids. The available sodium hydroxide is made in pellet shape and consequently it is important to determine H_2O in order to be capable of defining alkaline dosage and alkaline modulus. The method is:

$$H_2O \text{ available in NaOH} = \frac{NaOH_{\text{solid mass}} \times H_2O_{\text{molar mass}}}{NaOH_{\text{molar mass}} \times 2} \tag{3.6}$$

Composition of Water Glass:

Sodium silicate solid, with the mass ratio of Na_2O: SiO_2 equal to 2:1 as supplied by Fisher Scientific Ltd. was firstly mixed with distilled water in a beaker to make a

solution with the mass ratio of 25.5 % Si_2O , 12.7% Na_2O and 61.8%H_2O at 24 hours before it was used for making geopolymer mortar.

- H_2O present in Water Glass = $0.618 \times \text{Water Glass}_{\text{mass}}$
- Na_2O present in Water Glass = $0.127 \times \text{Water Glass}_{\text{mass}}$
- Si_2O present in Water Glass= $0.255 \times \text{Water Glass}_{\text{mass}}$

3.2.2 Mix Description

Different mixes were considered in test programme that presented as below:

1) Mix series 1: 100 % PFA

	A1 (AD:7.61/AM:1.26)	**B1** (AD:9.51/AM:0.95)	**C1** (AD:9.51/AM:0.95)
PFA (Kg)	5	5	5
GGBS(Kg)	0	0	0
Sand (kg)	13.75	13.75	13.75
NOH (ml)	153.8	92.8	185.6
Water Glass (ml)	725.2	436.6	869.5
Added Water (ml)	1100	1400	950

2) Mix series 2: 50% PFA and 50% GGBS

	A2 (AD:7.61/AM:1.26)	**B2** (AD:9.51/AM:0.95)	**C2** (AD:9.51/AM:0.95)
PFA (Kg)	2.5	2.5	2.5
GGBS(Kg)	2.5	2.5	2.5
Sand (kg)	13.75	13.75	13.75
NOH (ml)	153.8	92.8	185.6
Water Glass (ml)	725.2	436.6	869.5
Added Water (ml)	1100	1400	950

3) Mix series 3 : 30% PFA and 70% GGBS

	A3 (AD:7.61/AM:1.26)	**B3** (AD:9.51/AM:0.95)	**C3** (AD:9.51/AM:0.95)
PFA (Kg)	1.5	1.5	1.5
GGBS(Kg)	3.5	3.5	3.5
Sand (kg)	13.75	13.75	13.75
NOH (ml)	153.8	92.8	185.6
Water Glass (ml)	725.2	436.6	869.5
Added Water (ml)	1100	1400	950

4) Mix series 4: 70% PFA and 30% GGBS

	A4 (AD:7.61/AM:1.26)	**B4** (AD:9.51/AM:0.95)	**C4** (AD:9.51/AM:0.95)
PFA (Kg)	3.5	3.5	3.5
GGBS(Kg)	1.5	1.5	1.5
Sand (kg)	13.75	13.75	13.75
NOH (ml)	153.8	92.8	185.6
Water Glass (ml)	725.2	436.6	869.5
Added Water (ml)	1100	1400	950

3.3 Mixing and setting

The first step was preparing alkaline solutions. Water glass and water scaled after blending in a beaker. The sodium hydroxide was measured and put into a different beaker. Then the sodium hydroxide pellets were poured into the beaker with water and the solution was stirred till the NaOH pellets had disappeared and the solution became visible. The operation of preparing alkali solution was placed in the fume cupboard because this process is exothermic therefore the significant volume of heat can be released. To secure that the heat did not act in the geopolymer process, the solution was left to cool down for a 24 hours before it was used in preparing geopolymer materials.

A Hobart Planetary mixer with the capacity of 30 litters was used for preparing various geopolymer mixtures in this study. The solids were combined in the following procedure: initially about half of the sand, then Pozzolanic binder and the remainder of the sand. The mixer was started for 3 minutes at a low speed of gear 1. The activator solution was composed of waterglass, water and sodium hydroxide. Activator solutions

were first mixed into a beaker and then added to the mixture. Then the mixing programme was continued after adding all ingredients for 2.5 minutes at the speed of gear 1. The mixer was stopped for one minute and the paddle and sides were scraped. After that, the mixing programme was continued at speed 2 for another 2.5 minutes.

Figure 3.4: Hobart Planetary mixers

3.3.1. Casting

To measure the strength of the geopolymer, specimens were cast into 160mm × 40mm × 40 mm mortar moulds. The mould was set on a vibrating table. The moulds was half filled and vibrated for 60 seconds. After that, it was filled up to the top and vibrated for another one minute to have a sufficient level of compaction.

3.4 Curing

All samples were placed in the room temperature (20 ℃ $\pm$ 2) for 24 hour with exposed surfaces sealed by plastic sheet to prevent moisture loss. After that, the samples were demoulds. Half of the samples were wrapped with cling film immediately after

demoulding and then cured at 20℃ $\pm$ 2 to simulate a curing environment of 20 ℃ and 100 % RH.

The remaining samples were placed in an oven which was preheated at 70℃ for half an hour before samples were moved in. The preheating is to ensure that the temperature within the oven reached 70 ℃ when samples were moved in designed curing environment. All specimens were placed into oven bags to secure that moisture was maintained inside the specimen. Then they were put into an aluminium tray in order to prevent any possible damage during leaching. Then the specimens were cured in the oven at 70℃ for 2 hours. After 2 hours, the specimens were taken out of the oven and stored into another curing room with temperature of 20℃. They were afterwards tested at 3, 5, 7 and 28 days.

Figure 3.5: ELE prismatic moulds 40x40x160 mm3

Figure 3.6: Sample preparation for curing at 20 °C

Figure 3.7: Sample preparation for curing at 70 °C

Figure 3.8: Strength testing INSTRON jig for compression and flexural test

3.5 Testing

3.5.1 Flexural Strength Testing

The three-point bending test was performed on the 160mm × 40mm × 40 mm mortar specimens with a loading rate of 300 N/min, as required by BN EN196-1:2005. The flexural strength is worked out as:

$$R_f = \frac{1.5 \times F_f \times l}{b^3} \tag{3.7}$$

Where:

R_f - Flexural strength, in megapascal

F_f - The load applied to the middle of the prism at fracture, in newtons.

b - Side of the square section of the prism, in millimeters

l - Distance between the supports, in millimetres.

Firstly any sharp edges of samples were removed with a sandpaper so there was less friction with platens. Then specimens were mounted into test rig with smooth surfaces contacting the load in apparatus. All specimens were adjusted to be symmetrical, to ensure reliable results. The test was then started and the failure of samples was observed during test procedure. The flexure strength of the geopolymer prism was then recorded.

Figure 3.9: INSTRON 5584 System used for sample three-point Flexure test

3.5.2 Compressive strength testing

The compressive strength test was performed on 40mm × 40mm × 40 mm samples at the loading rate of 144 KN/min according to BN EN196-1:2005. The results of this test and also flexure test were used as one of the primary benchmarks to the resistivity which was determined with CCR-2. The specimens which were broken in two pieces in the flexural testing were used for compressive strength testing. Next, the compression test rig was adjusted and fit into the main frame of the loading machine see Figure 3-6. The mortar sample was placed onto the compression test rig. Then the load applied to the samples and when they failed, their compressive strength was then recorded. Fragmented pieces from the compression test were saved for microscopic (SEM) characterisation.

The Compressive strength is worked out as:

$$R_c = \frac{F_c}{1600} \tag{3.8}$$

Where:

R_c- Compressive strength, in mega Pascal

F_c - Maximum load at fracture, in newton

1600 - Area of the platens (40mm×40mm), in square millimetres

Figure 3.10: INSTRON 5584 System used for sample Compressive test

3.5.3 Electrical Resistivity Measurement

The electrical resistivity of geopolymer at early ages was monitored by an electrodeless and real-time fresh cement and concrete resistivity analyser (CCRR-2). To conduct such test, the freshly blended geopolymers was cast into the mould to a specific height. Then the mould was gently compacted by hand for expelling air from the geopolymer mixture in the mould. Then the mould was sealed by plastic covers. Then the geopolymerisation process was monitored sample at each 15 minutes for the next 7 days to collect data of electrical resistivity. After seven days, the monitoring process terminates, and the specimens were removed from the CCR-2 apparatus and the test facility was cleaned for next test.

3.5.4 Scanning Electron Microscopy (SEM)

A supra 35VP SEM was used in order to analyse the geopolymer microstructure. All samples were coated with gold before using for SEM analysis. Then all samples placed into the supra SEM.

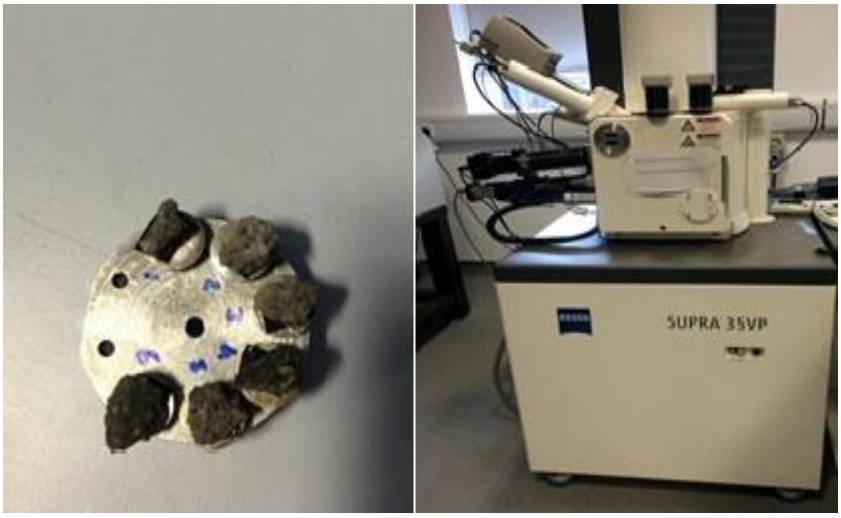

Figure 3.11: Samples prepared on plates (Left), SEM equipment (Right)

4. Experimental Results and Discussion

4.1 Introduction

In this chapter, experimental results are presented and discussed. Flexure and compressive strength and electrical resistivity data are presented in tables and/or plotted in figures. All specimens prepared in the laboratory were tested for their physical and chemical properties.

One of the main points of this research is to investigate the effects of AM and AD on the strength of geopolymer mortars at early ages which is an understudied area. PFA and GGBS-based geopolymer specimens were synthesised and cured at room temperature or at elevated temperature in oven which the level. AM and/or AD, of alkaline activator and the mixture was varied. Specimens were then tested for flexural strength at early ages of 3, 5, 7 and 28 days. All Figures from 4.1 to 4.14 illustrates the effect of curing condition on the flexural and compressive strength for all investigated mixtures in this study. High curing temperature resulted in higher compressive strength, although an increase in the curing temperature at 70 ℃ did not increase the compressive strength largely.

Furthermore a test was utilized to measure the resistivity of the mix over time to characterise the geopolymerisation process of the mixtures. The CCR-2 test was applied in order to obtain the data which has been compared and joined to the quantitative data from flexure and compressive strength. The method was developed as per the manufacturer's instructions in a room with a constant temperature of 20℃. All different mixes were considered in experimental work are given in Appendix A.

4.1.1. Engineering Properties Mix Series 1

Figure 4.1 shows the values of flexure strength for mix series one over the first 28 days of maturity. Figure 4.1 shows that there are a broad number of factors that can be attributed to a number of variables, including mixture specification as well as age. One finding is worthy to note here is that the decrease in flexural strength as age grows up to 7days for some mixtures, most notably mix design C1. This goes against the findings of many other authors and what has been pre-established in the literature review. This may be due that strength development for Mixture C1 is very slow at earlier ages and a few days different in age will not increase strength of the material. Rather the natural of experimental data variation dominates so that there is actually no strength increment observed from 3 days to 7 days. But eventually its 28-days strength is much higher than that at earlier ages as expected.

Figures 4.3 and 4.4 present the rates of compressive strength for mix series one. By looking at the data we can observe the compressive strength developed over time in general which is assumed, this followed for all mixes excluding mix C1.

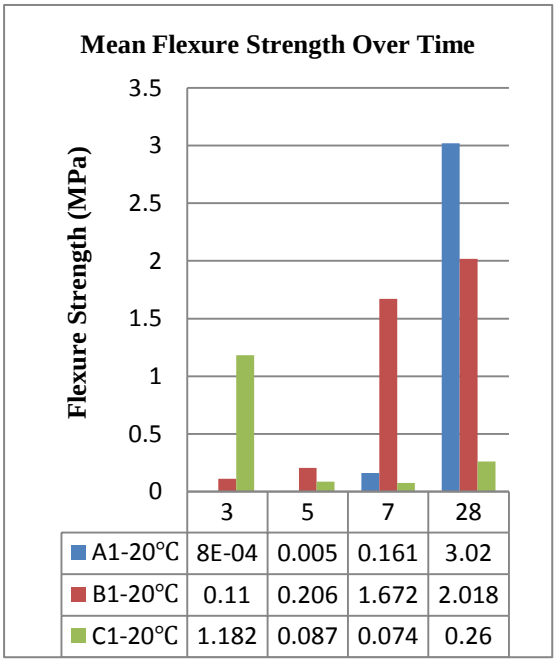

Figure 4.1 Average Flexural Strength of Design Mixture 1 Cured At 20°C

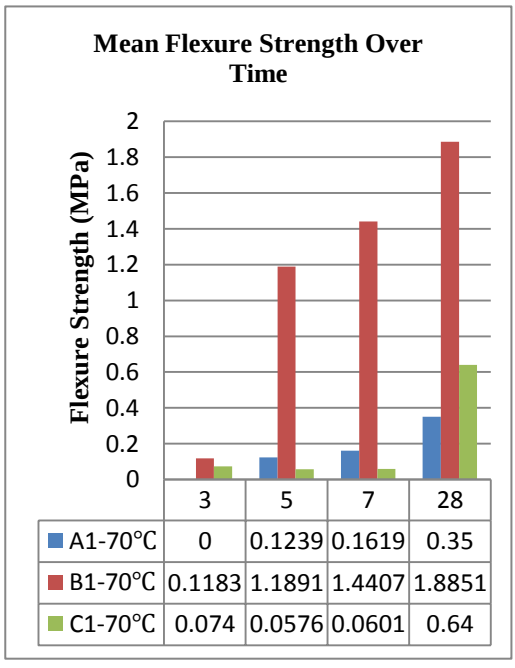

Figure 4.2 Average Flexural Strength of Design Mixture 1 Cured At 70°C

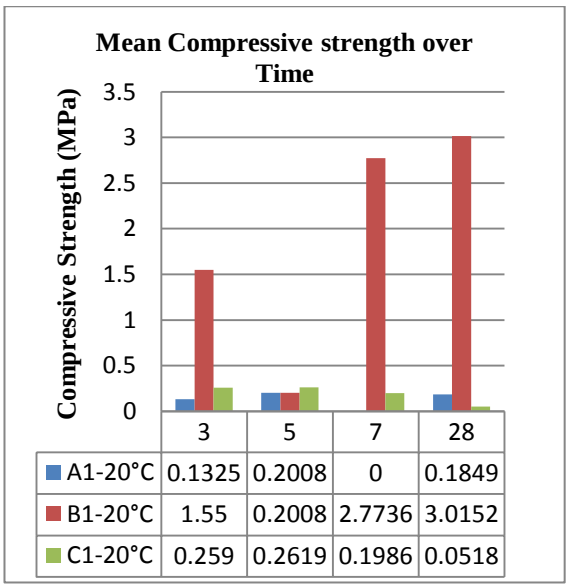

	3	5	7	28
A1-20°C	0.1325	0.2008	0	0.1849
B1-20°C	1.55	0.2008	2.7736	3.0152
C1-20°C	0.259	0.2619	0.1986	0.0518

Figure 4.3 Average Compressive Strength of Design Mixture 1 Cured At 20°C

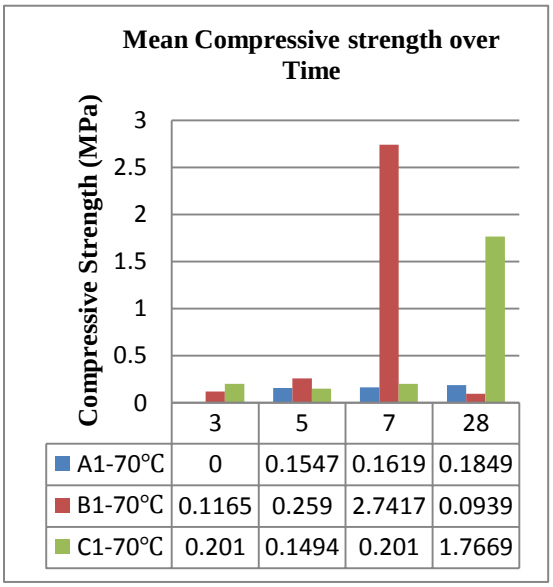

	3	5	7	28
A1-70°C	0	0.1547	0.1619	0.1849
B1-70°C	0.1165	0.259	2.7417	0.0939
C1-70°C	0.201	0.1494	0.201	1.7669

Figure 4.4 Average Compressive Strength of Design Mixture 1 Cured At 70°C

4.1.2. Engineering Properties Mix Series 2

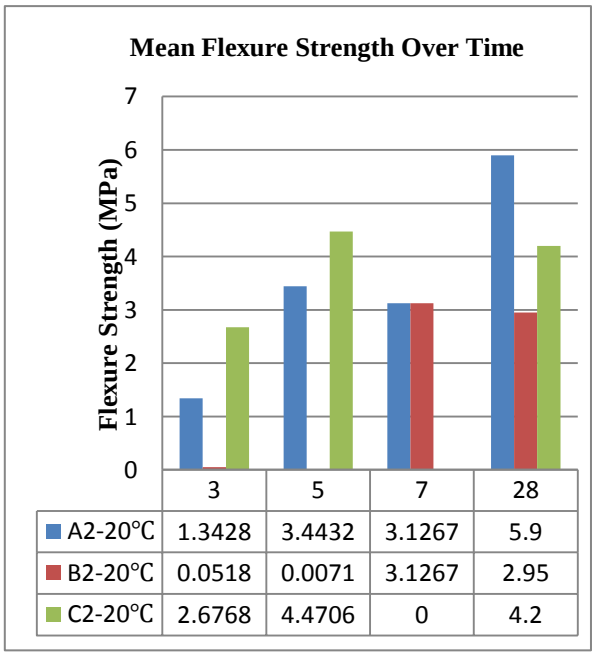

	3	5	7	28
A2-20°C	1.3428	3.4432	3.1267	5.9
B2-20°C	0.0518	0.0071	3.1267	2.95
C2-20°C	2.6768	4.4706	0	4.2

Figure 4.5 Average Flexural Strength of Design Mixture 2 Cured At 20°C

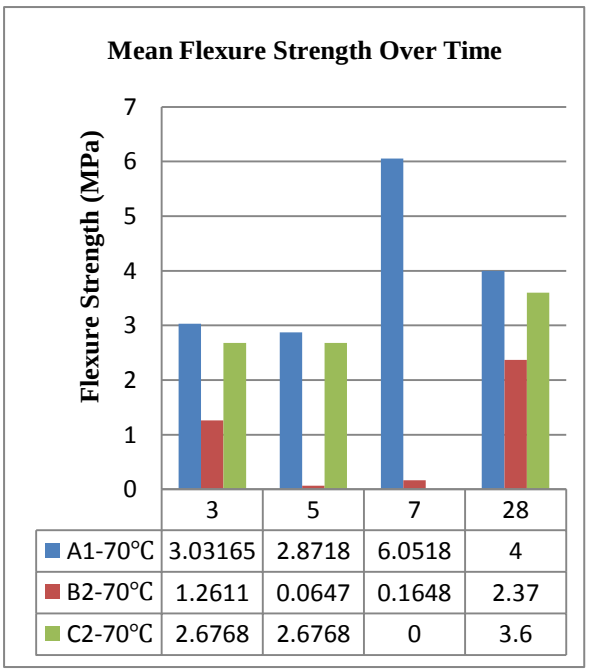

	3	5	7	28
A1-70°C	3.03165	2.8718	6.0518	4
B2-70°C	1.2611	0.0647	0.1648	2.37
C2-70°C	2.6768	2.6768	0	3.6

Figure 4.6 Average Flexural Strength of Design Mixture 2 Cured At 70°C

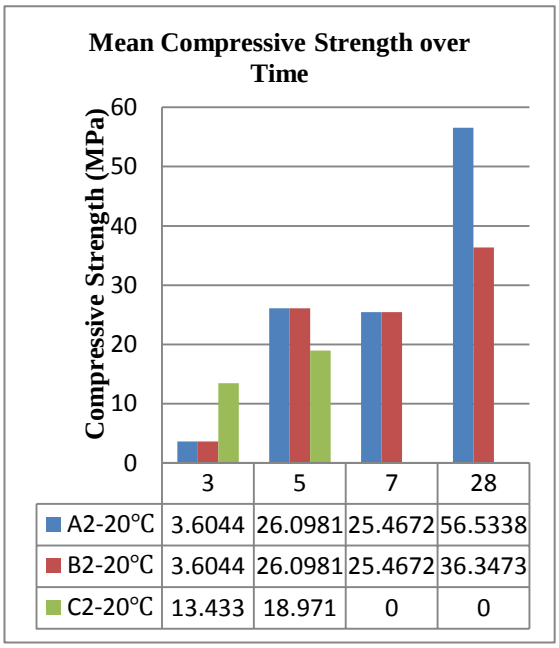

Figure 4.7 Average Compressive Strength of Design Mixture 2 Cured At 20°C

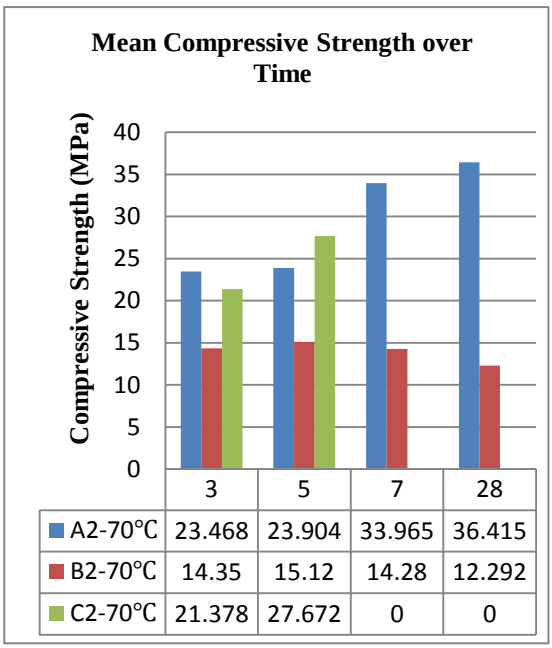

Figure 4.8 Average Compressive Strength of Design Mixture 2 Cured At 70°C

Figures 4.7 and 4.8 illustrate the variations in compressive strength for the design mixture two over the first 28 days of maturity. It can be seen from the different peaks that there is a wide distribution of strengths which can be attributed to the same variables such as; age, materials and curing system are affecting the flexural strength properties. The graph simply points out that the strength gain properties confirm previous work in the sense that grown specimen maturity leads to developed compressive strength. A point to note is the decrease in flexural strength as age increases for mixture B2 cured at oven. Reasons for these differences will be further explored and explained in Chapter 5.

4.1.3. Engineering properties Mix Series 3

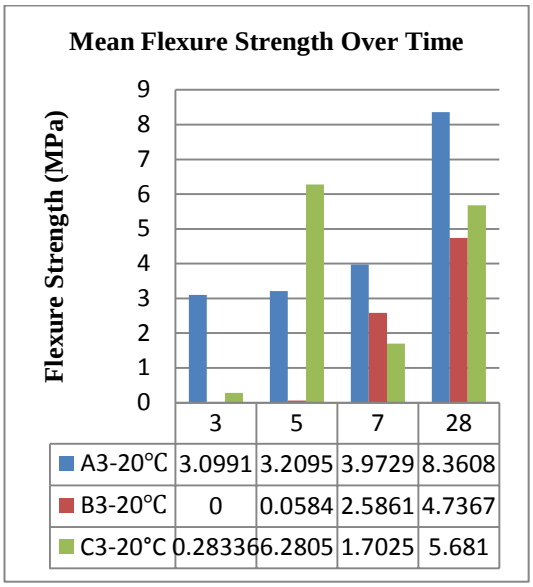

Figure 4.9 Average Flexural Strength of Design Mixture 3 Cured At 20°C

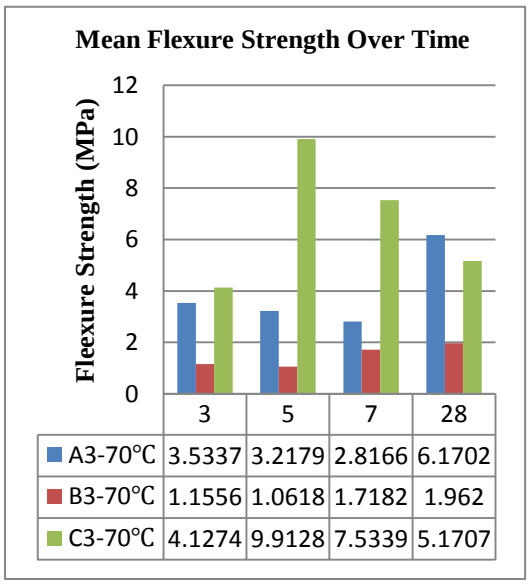

Figure 4.10 Average Flexural Strength of Design Mixture 3 Cured At 70°C

Figures 4.9 and 4.10 demonstrate the variations in Flexure strength for the design mixture 3 series over the first 28 days of maturity. It can be seen mix C3 which cured at 20 ℃ has the distribution shows glimpses of following the expected trend**.**

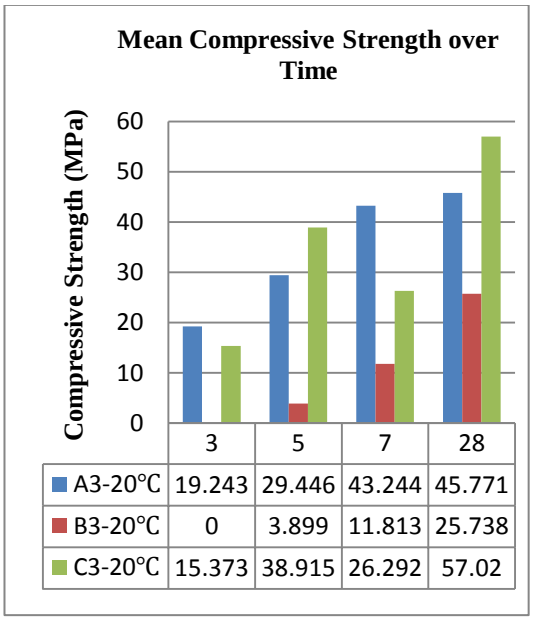

Figure 4.11 Average Compressive Strength of Design Mixture 3 Cured At 20°C

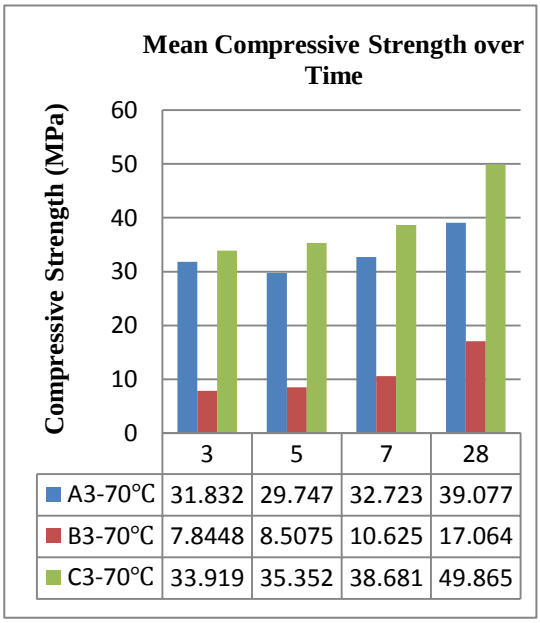

Figure 4.12 Average Compressive Strength of Design Mixture 3 Cured At 70°C

Figures 4.11 and 4.12 illustrate the distribution in compressive strength for the design mixture 3. It can be seen that the distribution shows glimpses of following the expected trend.

4.1.4. Engineering Properties Mix Series 4

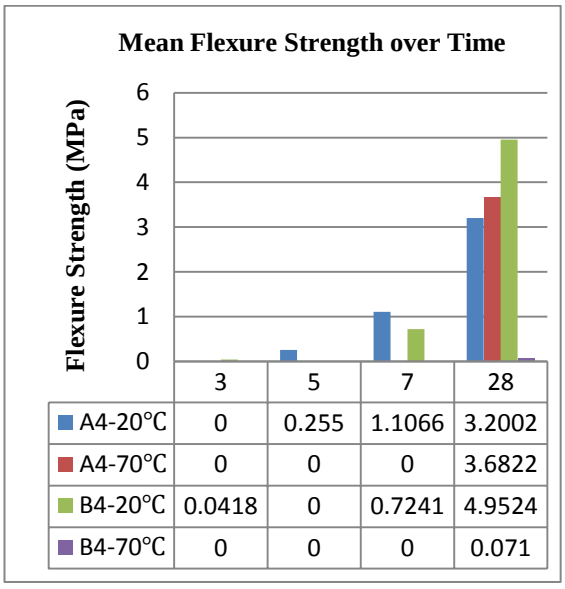

	3	5	7	28
A4-20°C	0	0.255	1.1066	3.2002
A4-70°C	0	0	0	3.6822
B4-20°C	0.0418	0	0.7241	4.9524
B4-70°C	0	0	0	0.071

Figure 4.13 Averages Flexural Strength of Design Mixture 4

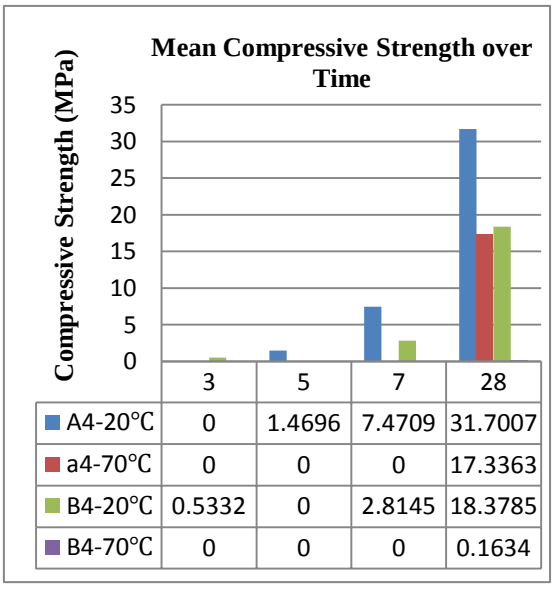

	3	5	7	28
A4-20°C	0	1.4696	7.4709	31.7007
a4-70°C	0	0	0	17.3363
B4-20°C	0.5332	0	2.8145	18.3785
B4-70°C	0	0	0	0.1634

Figure 4.14 Averages Compressive Strength of Design Mixture 4

Figures 4.13 and 4.12 illustrate the distribution in flexural and compressive strength for the design mixture series 4. It can be seen that the distribution shows glimpses of following the expected trend.

4.1.5. Engineering Properties Mix Series A

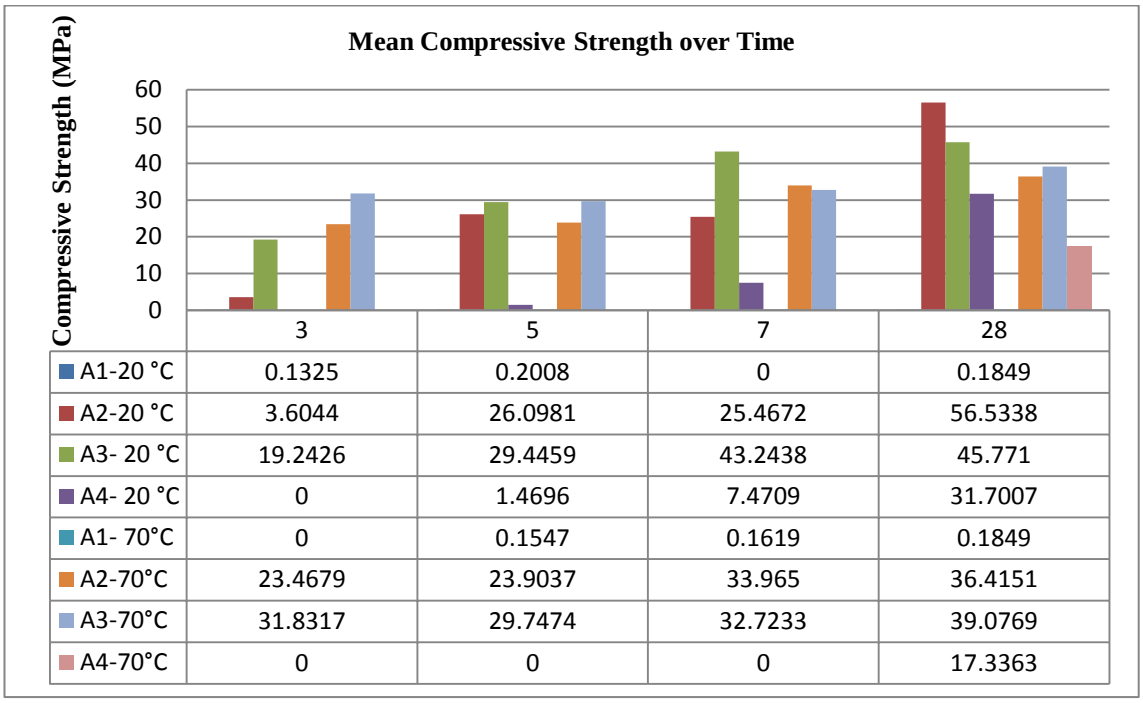

	3	5	7	28
A1-20 °C	0.1325	0.2008	0	0.1849
A2-20 °C	3.6044	26.0981	25.4672	56.5338
A3- 20 °C	19.2426	29.4459	43.2438	45.771
A4- 20 °C	0	1.4696	7.4709	31.7007
A1- 70°C	0	0.1547	0.1619	0.1849
A2-70°C	23.4679	23.9037	33.965	36.4151
A3-70°C	31.8317	29.7474	32.7233	39.0769
A4-70°C	0	0	0	17.3363

Figure 4.15 Averages Compressive Strength of Design Mixture Series A

Figure 4.15 demonstrates the variations in compressive strength for the design mixture A series over the first 28 days of maturity. It can be seen mix A2 which cured at 20 ℃ has highest compressive strength over the time. It can be seen that the rate of strength gaining for blends with the higher amount of GGBS is higher than others and it can be assumed that eventually it will produce the higher value of mean compressive strength.

4.1.6. Engineering Properties Mix Series B

The Figure 4.16 compares the mean compressive strength of all mix design of series B. The Figure shows the compressive strength developed over time which is expected, this results for all mixes except mix B1 which cured at 70 ℃. Mixes B2 and B3 samples which cured at 20 ℃ shows the highest strengths of 36.34 MPa and 25.73 MPa.

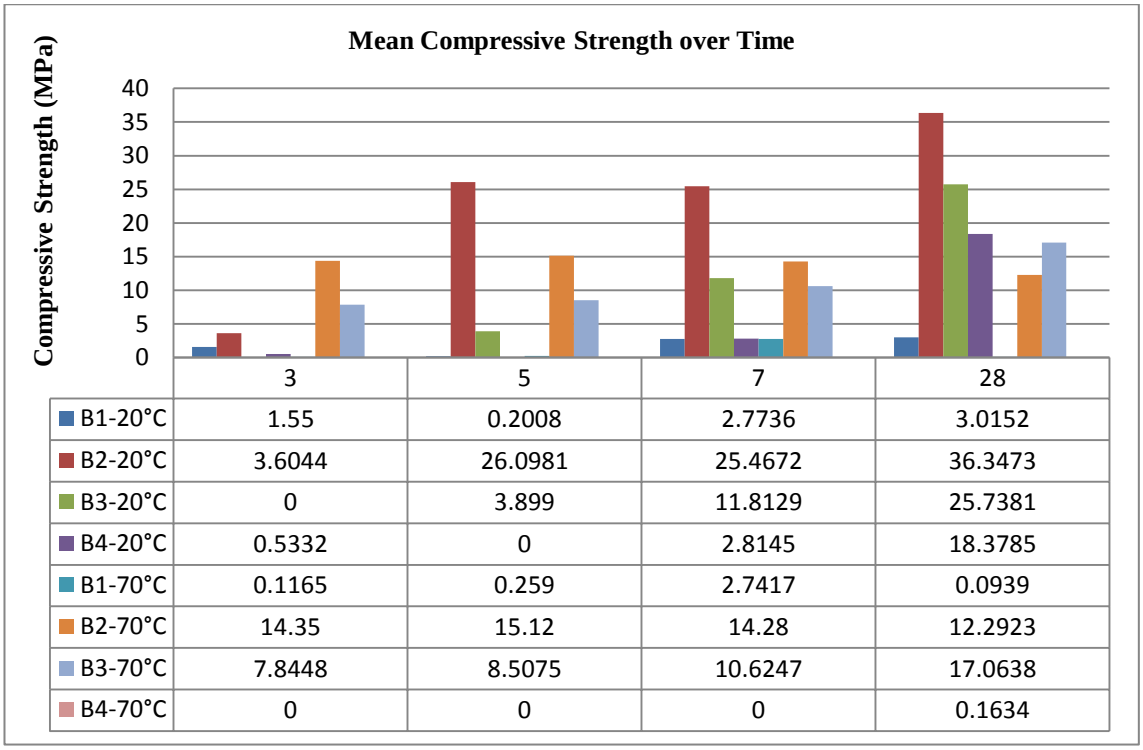

	3	5	7	28
B1-20°C	1.55	0.2008	2.7736	3.0152
B2-20°C	3.6044	26.0981	25.4672	36.3473
B3-20°C	0	3.899	11.8129	25.7381
B4-20°C	0.5332	0	2.8145	18.3785
B1-70°C	0.1165	0.259	2.7417	0.0939
B2-70°C	14.35	15.12	14.28	12.2923
B3-70°C	7.8448	8.5075	10.6247	17.0638
B4-70°C	0	0	0	0.1634

Figure 4.16 Averages Compressive Strength of Design Mixture Series B

4.1.7. Engineering Mix Series C

Figure 4.17 illustrate the distribution in compressive strength for the design mix series C. It can be seen C2 blend has the greatest rebound strength over 28 days. All samples from C4 they were so weak and they breakdown before testing.

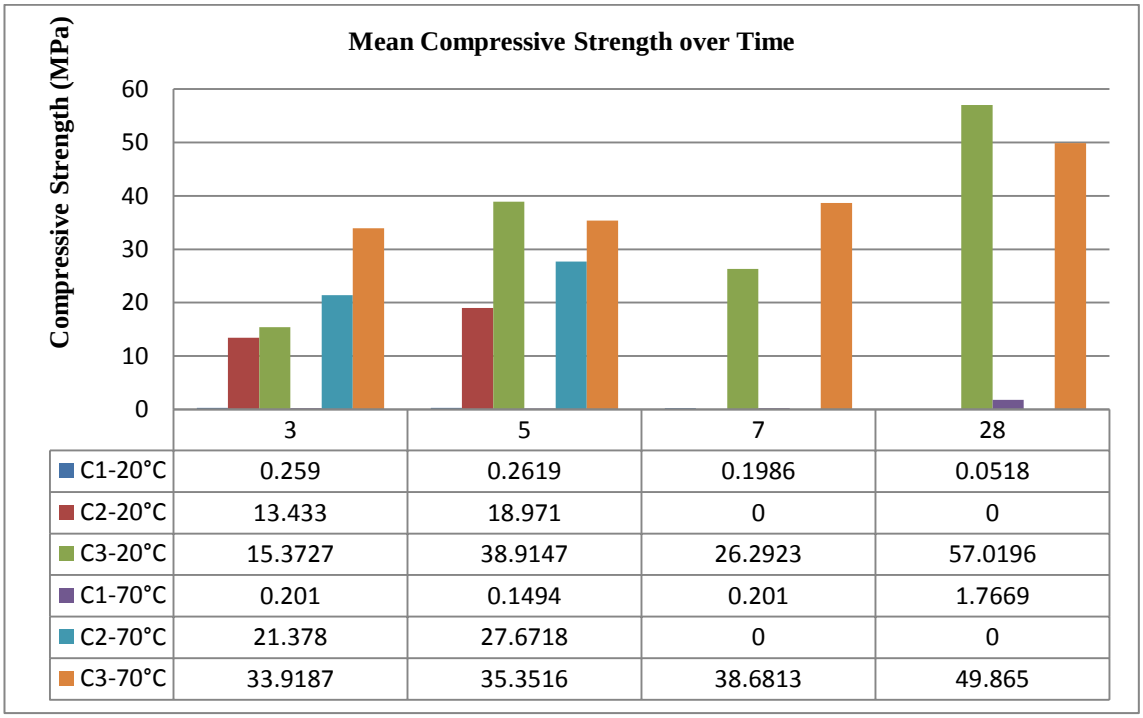

	3	5	7	28
C1-20°C	0.259	0.2619	0.1986	0.0518
C2-20°C	13.433	18.971	0	0
C3-20°C	15.3727	38.9147	26.2923	57.0196
C1-70°C	0.201	0.1494	0.201	1.7669
C2-70°C	21.378	27.6718	0	0
C3-70°C	33.9187	35.3516	38.6813	49.865

Figure 4.17 Averages Compressive Strength of Design Mixture Series C

4.1.8. CCR-2 Resistivity

Figure 4.18 shows the resistivity curves for all mixes against time for 7 day period. It can clearly be seen that the resistivity curves all begin to show a similar trend in that as time is increasing resistivity also rises. Mixtures A3, B3 and C3 curves are showing higher resistivity over the time this can be attributed to the inclusion of GGBS. The rest of mixtures are exhibiting almost constant resistivity with a quite small fluctuation. These results will be further explained in chapter 5.

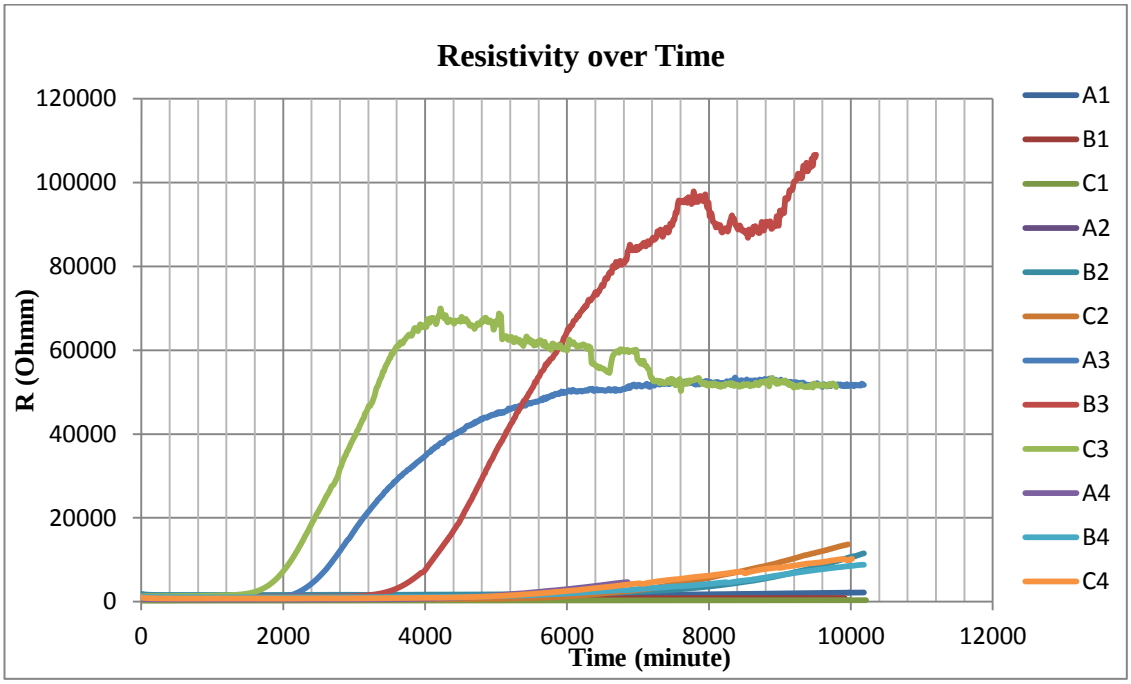

Figure 4.18 Resistivity of all Design Mixtures over Time

5. Analysis and Discussions

5.1Strength Development

The tests for flexural and compressive strength were conducted at 3, 5, 7 and 28 days for specimens made of PFF and GGBS. There were 3 specimens for flexure strength tasted under 3-point bending and 6 samples for compressive strength for each mixture which results in a huge amount of raw data. Displaying of them is not useful, so the mean values were determined to describe the data.

5.1.1 Strength Developments at Curing Temperatures of 20℃ and 70℃

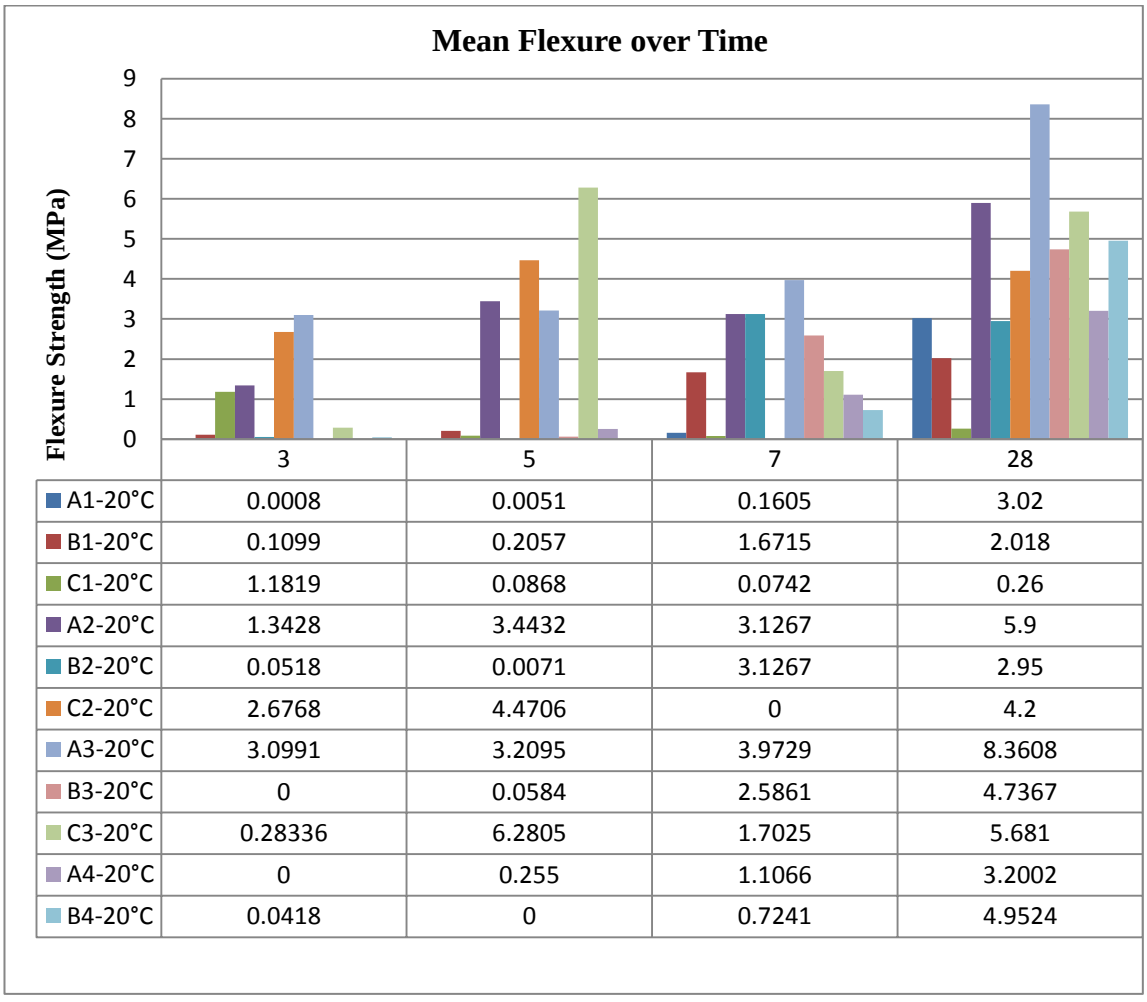

	3	5	7	28
A1-20°C	0.0008	0.0051	0.1605	3.02
B1-20°C	0.1099	0.2057	1.6715	2.018
C1-20°C	1.1819	0.0868	0.0742	0.26
A2-20°C	1.3428	3.4432	3.1267	5.9
B2-20°C	0.0518	0.0071	3.1267	2.95
C2-20°C	2.6768	4.4706	0	4.2
A3-20°C	3.0991	3.2095	3.9729	8.3608
B3-20°C	0	0.0584	2.5861	4.7367
C3-20°C	0.28336	6.2805	1.7025	5.681
A4-20°C	0	0.255	1.1066	3.2002
B4-20°C	0.0418	0	0.7241	4.9524

Figure 5.1 Average Flexural Strength of all Design Mixture at 20 ℃

A summary of flexure strength for all mixes cured at 20±2 ℃ temperatures is presented in Figure 5.1 which shows the development of strength over time. The outcomes exhibited a similar trend as occurred with the early strength, which increase

when GGBS percentage increased. From data available in Figure 5.1, it can be seen that flexural strength of mixture C1 decreased form 1.182 MPa at 3 days to 0.26 MPa at 28 days. For the same mix which cured at 70 ℃, the flexural test was good because as the mixture got mature, the strength increased. It can be seen from the data in Figure 5.2 that the design mixes of A3, B3 and C3 present higher compressive strength. However samples which cured for 70℃ for two hours and then kept at 20 ℃ have lower flexure strength than the one cured on 20℃. The chart shows abrupt changes in strength between ages as expected and therefore reinforces the work of previous authors as mentioned in literature review (2.9).

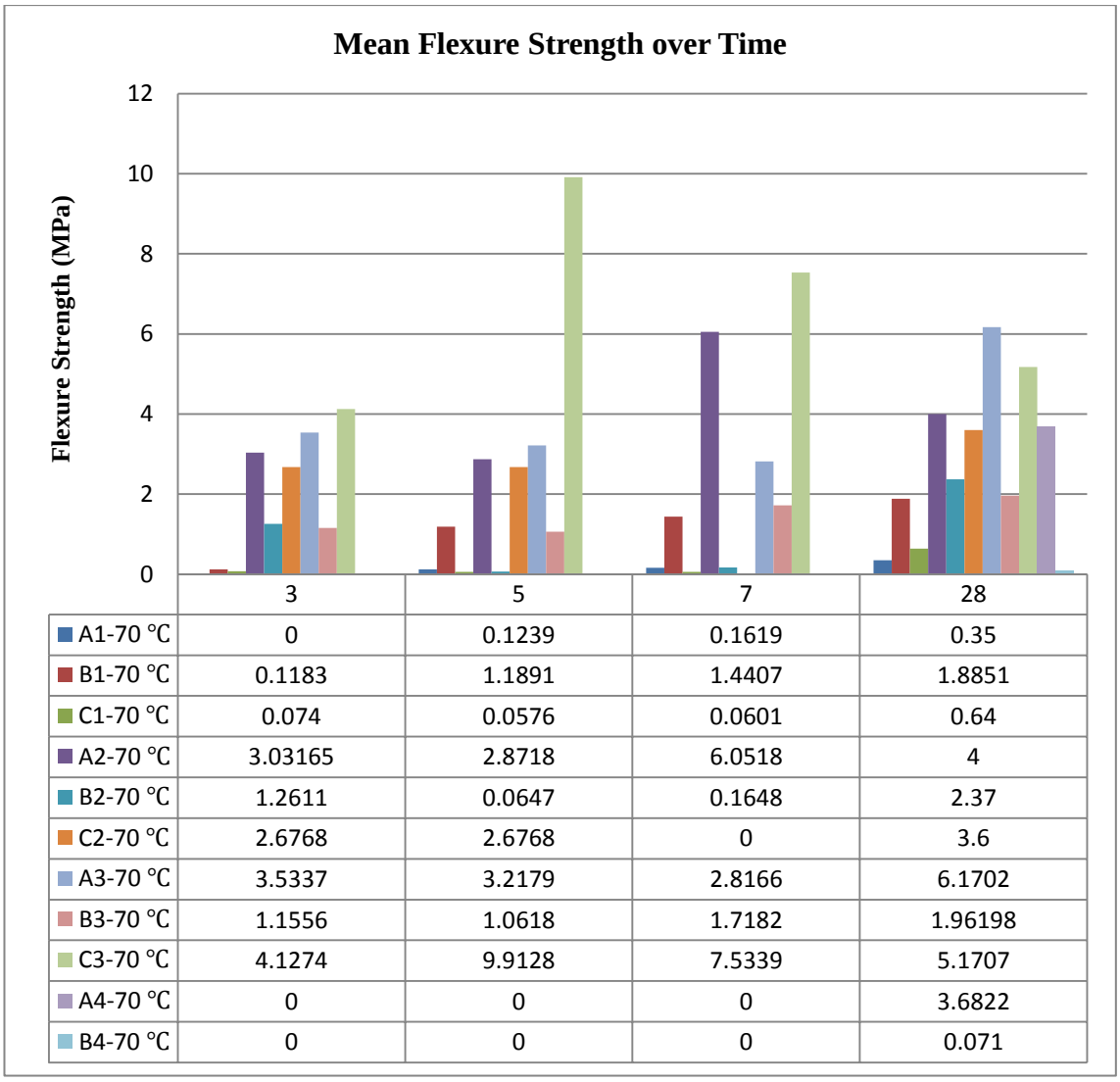

	3	5	7	28
A1-70 ℃	0	0.1239	0.1619	0.35
B1-70 ℃	0.1183	1.1891	1.4407	1.8851
C1-70 ℃	0.074	0.0576	0.0601	0.64
A2-70 ℃	3.03165	2.8718	6.0518	4
B2-70 ℃	1.2611	0.0647	0.1648	2.37
C2-70 ℃	2.6768	2.6768	0	3.6
A3-70 ℃	3.5337	3.2179	2.8166	6.1702
B3-70 ℃	1.1556	1.0618	1.7182	1.96198
C3-70 ℃	4.1274	9.9128	7.5339	5.1707
A4-70 ℃	0	0	0	3.6822
B4-70 ℃	0	0	0	0.071

Figure 5.2 Average Flexural Strength of all Design Mixture at 70 ℃

The Figure 5.3 compares the compressive strengths of all design mixes which cured at 20℃ over a 28 day period. It can be concluded that there was once again a wide distribution amongst the compressive strength of mixes. This distribution did not however yield any stand out results and instead followed the required model of rising

compressive strength over time. There is a significant point to note however mixture C1 yet again produced the weakest sample with strength of 0.0518 MPa at 28 days. This is not surprising and proportional given the poor flexural properties displayed. Mixtures A2 and C3 show the highest strengths of 56.53 MPa and 57.019 MPa.

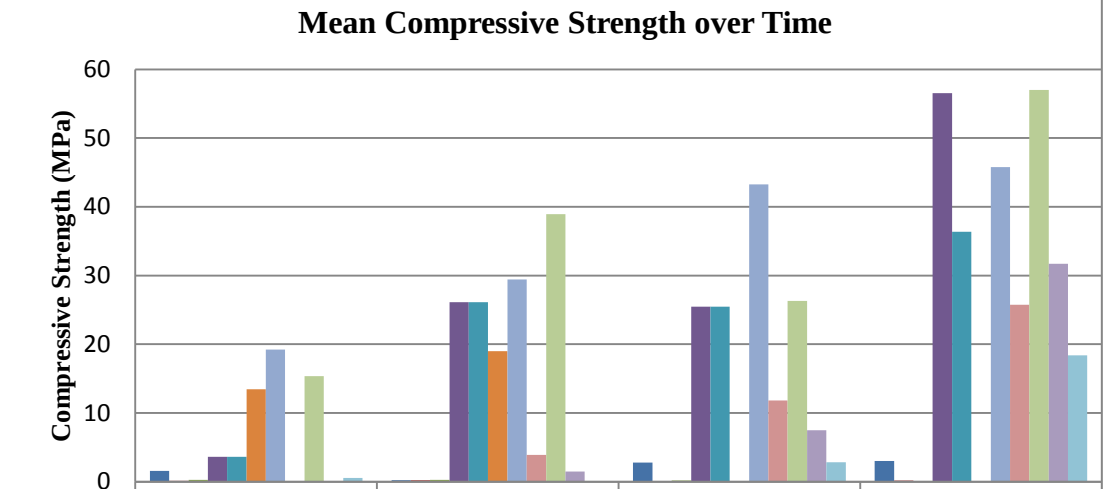

	3	5	7	28
A1-20 °C	1.55	0.2008	2.7736	3.0152
B1-20 °C	0.1325	0.2008	0	0.1849
C1-20 °C	0.259	0.2619	0.1986	0.0518
A2-20 °C	3.6044	26.0981	25.4672	56.5338
B2- 20°C	3.6044	26.0981	25.4672	36.3473
C2-20°C	13.433	18.971	0	0
A3-20°C	19.2426	29.4459	43.2438	45.771
B3-20 °C	0	3.899	11.8129	25.7381
C3-20°C	15.3727	38.9147	26.2923	57.0196
A4-20°C	0	1.4696	7.4709	31.7007
B4-20°C	0.5332	0	2.8145	18.3785

Figure 5.3 Average Compressive Strength of all Design Mixture at 20 ℃

Figure 5.4 illustrates the mean value of compressive strength for all the mixtures which cured at 70°C. By looking at the data, we can observe the compressive strength developed over the time which is expected. This happens for all mixes except mix A1. The compressive strength of mix A1 shows minimal change and a limited reduction in strength over the 28 days. It can be seen that the degree of strength for blends with GGBS are greater than others and it can be assumed that it will produce a greater rate of mean compressive strength.

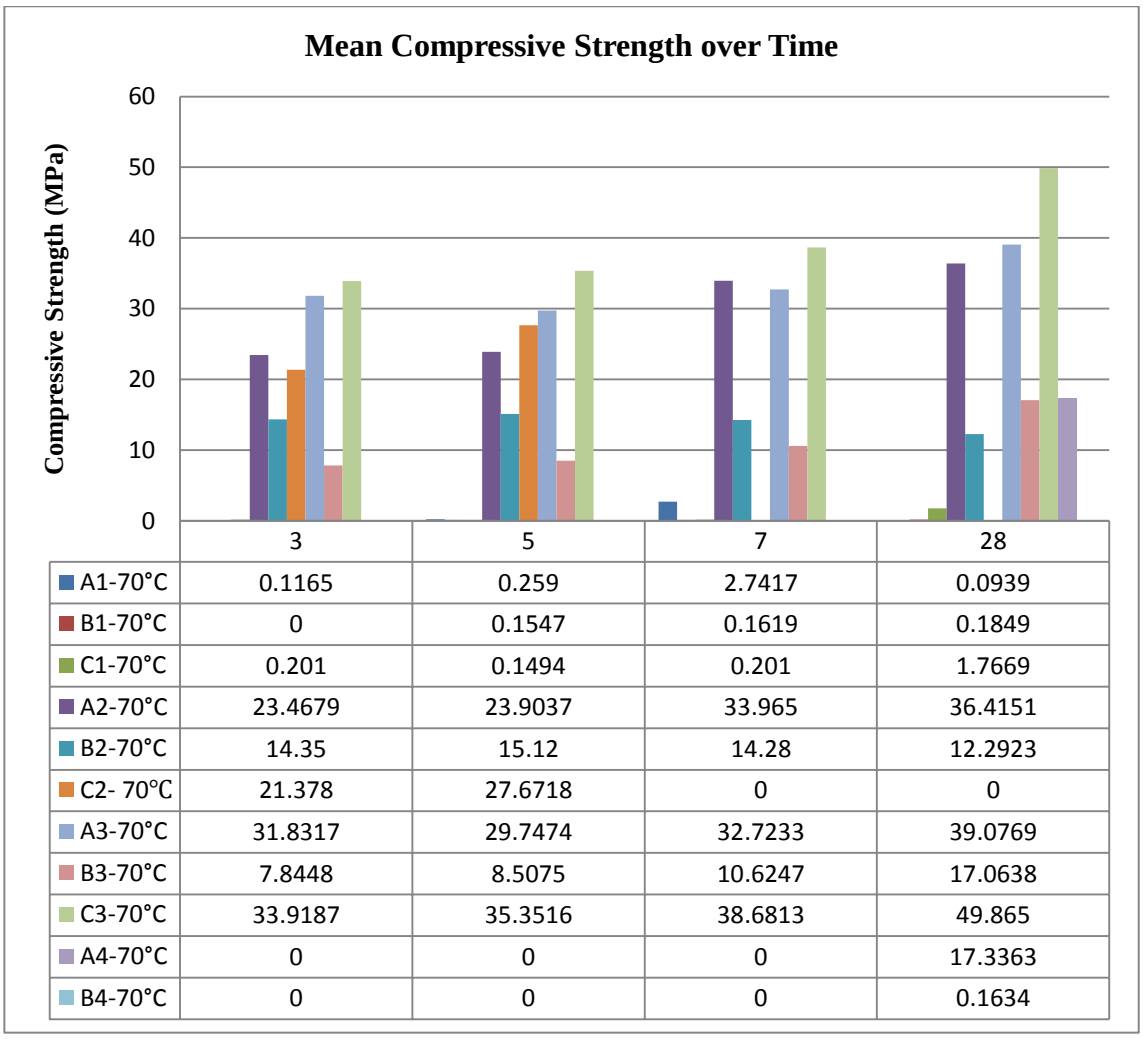

	3	5	7	28
A1-70°C	0.1165	0.259	2.7417	0.0939
B1-70°C	0	0.1547	0.1619	0.1849
C1-70°C	0.201	0.1494	0.201	1.7669
A2-70°C	23.4679	23.9037	33.965	36.4151
B2-70°C	14.35	15.12	14.28	12.2923
C2- 70°C	21.378	27.6718	0	0
A3-70°C	31.8317	29.7474	32.7233	39.0769
B3-70°C	7.8448	8.5075	10.6247	17.0638
C3-70°C	33.9187	35.3516	38.6813	49.865
A4-70°C	0	0	0	17.3363
B4-70°C	0	0	0	0.1634

Figure 5.4 Average Compressive Strength of all Design Mixture at 70 ℃

Figure 5.5 and 5.6 compare compressive strength of all series A design mixes which cured at 70℃ and 20℃ over the 28-day period. It can be concluded that there was once again a wide distribution amongst the compressive strength of mixes. Longer curing period improved the geopolymerisation process which resulting in higher compressive strength. As can be seen from both figures the mix A3 with 70% GGBS has higher strength over time. The results show that mix A2 gains strength over time. Figure 5.6 shows at 28 days mix A2 had the highest strength over time.

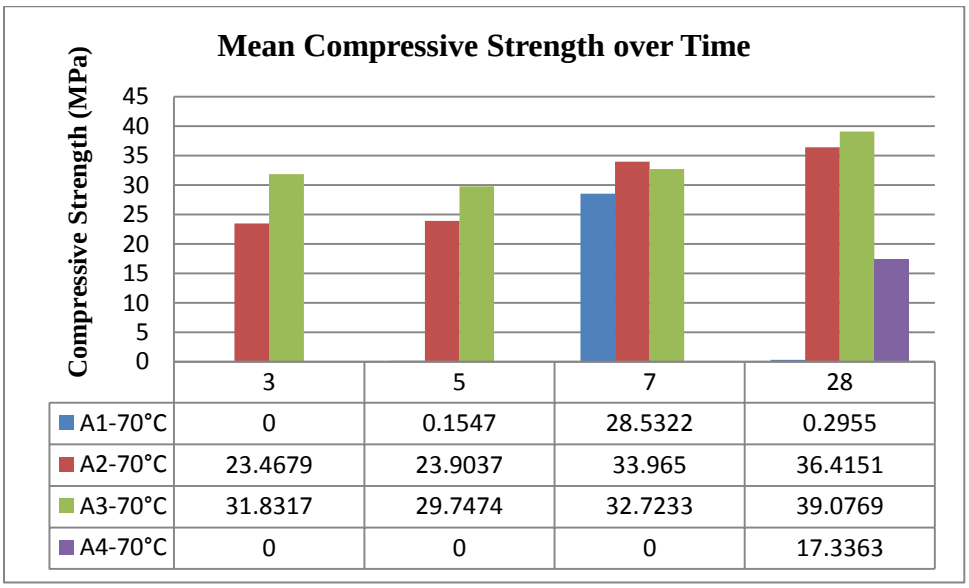

	3	5	7	28
A1-70°C	0	0.1547	28.5322	0.2955
A2-70°C	23.4679	23.9037	33.965	36.4151
A3-70°C	31.8317	29.7474	32.7233	39.0769
A4-70°C	0	0	0	17.3363

Figure 5.5 Average Compressive Strength of series A, Design Mixture at 70 ℃

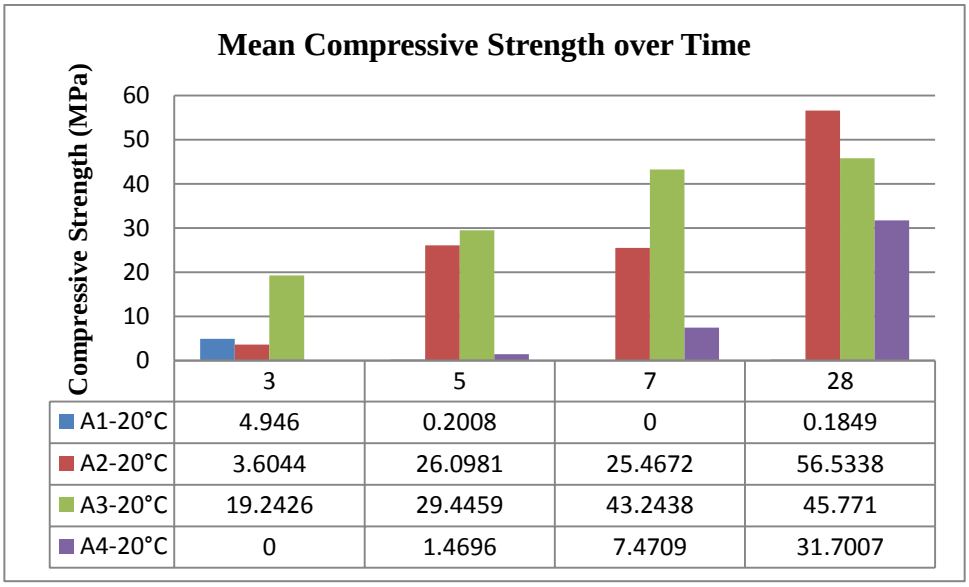

	3	5	7	28
A1-20°C	4.946	0.2008	0	0.1849
A2-20°C	3.6044	26.0981	25.4672	56.5338
A3-20°C	19.2426	29.4459	43.2438	45.771
A4-20°C	0	1.4696	7.4709	31.7007

Figure 5.6 Average Compressive Strength of series A Design Mixture at 20 ℃

The compressive strength data on Figure 5.7 presents the expected general trend for mixes with 50% PFA and 50% GGBS and cured at 70℃. Mix B2 has the highest strength over time due to the amount of alkaline dosage. Curing temperature rise promotes a raise in pozzolanic reaction. Hence, ambient temperature (20℃) curing results in a remarkably slow reaction. Figure 5.8 explains this point of enhanced performance from PFA/ GGBS mixtures.

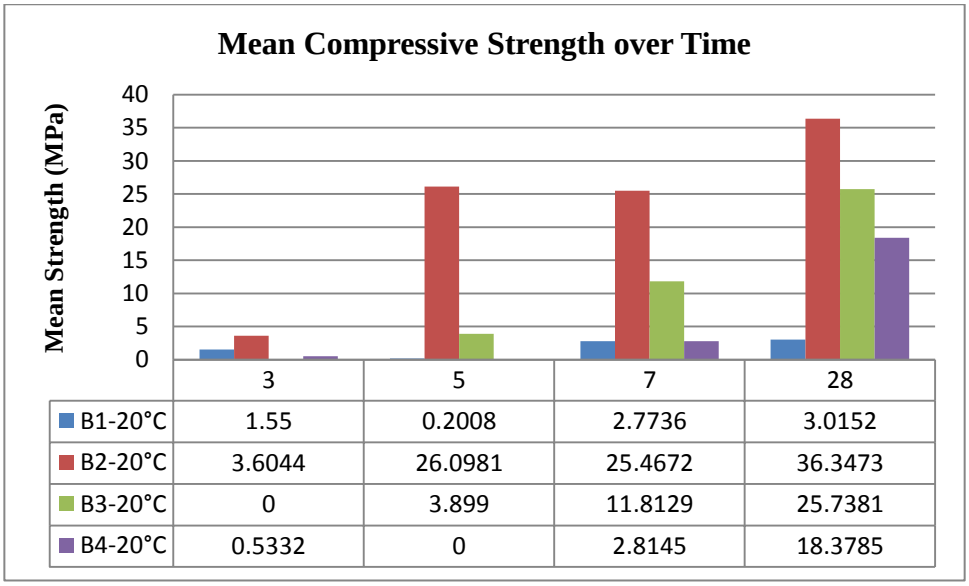

	3	5	7	28
B1-20°C	1.55	0.2008	2.7736	3.0152
B2-20°C	3.6044	26.0981	25.4672	36.3473
B3-20°C	0	3.899	11.8129	25.7381
B4-20°C	0.5332	0	2.8145	18.3785

Figure 5.7 Average Compressive Strength of series B Design Mixture at 70 ℃

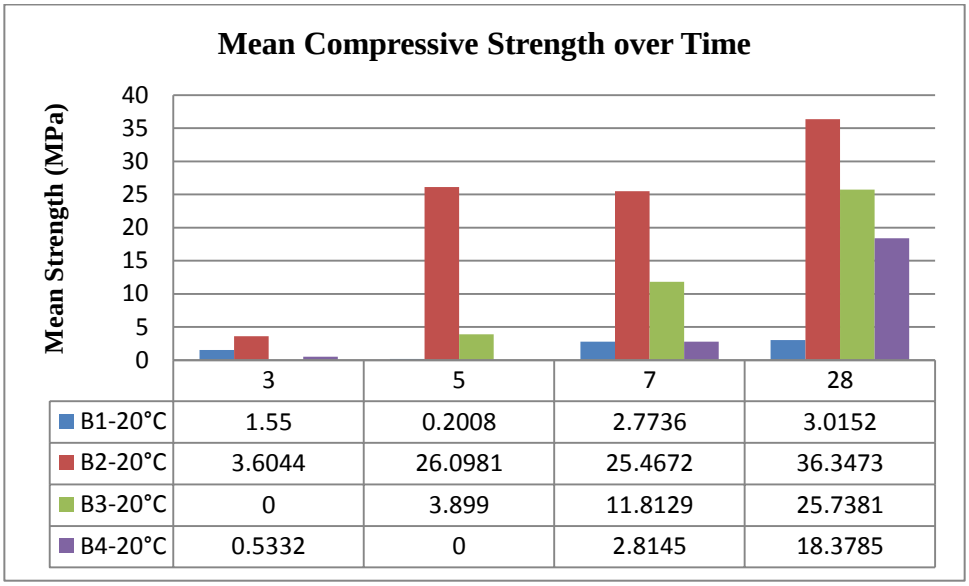

	3	5	7	28
B1-20°C	1.55	0.2008	2.7736	3.0152
B2-20°C	3.6044	26.0981	25.4672	36.3473
B3-20°C	0	3.899	11.8129	25.7381
B4-20°C	0.5332	0	2.8145	18.3785

Figure 5.8 Average Compressive Strength of series B Design Mixture at 20 ℃

The data of compressive strength for mix design C are presented in Figures 5.9 and 5.10. The results indicate that this mix design had the lowest compressive strength over time. Compressive strength of mix C2 which cured at 20℃ increased over time.

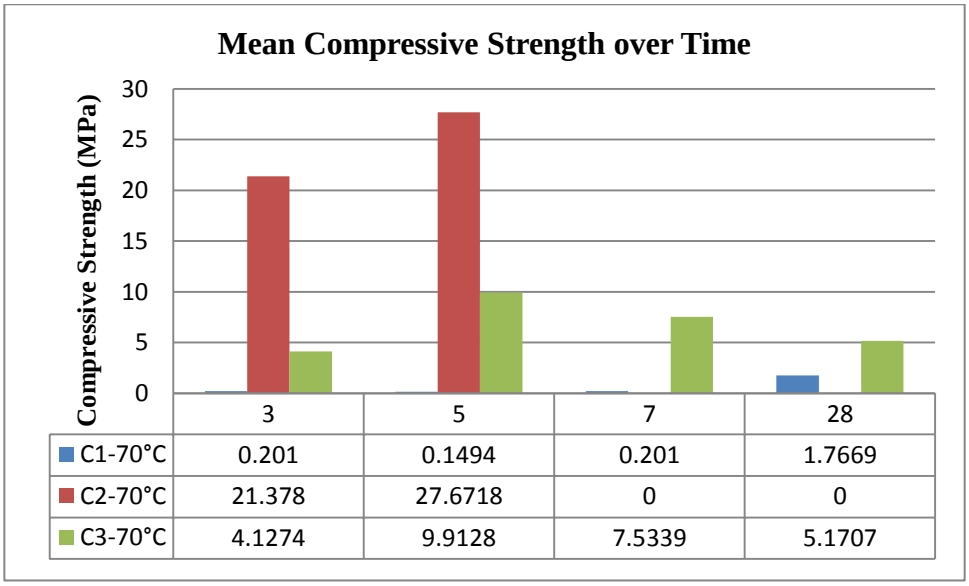

	3	5	7	28
C1-70°C	0.201	0.1494	0.201	1.7669
C2-70°C	21.378	27.6718	0	0
C3-70°C	4.1274	9.9128	7.5339	5.1707

Figure 5.9 Average Compressive Strength of series C Design Mixture at 70 ℃

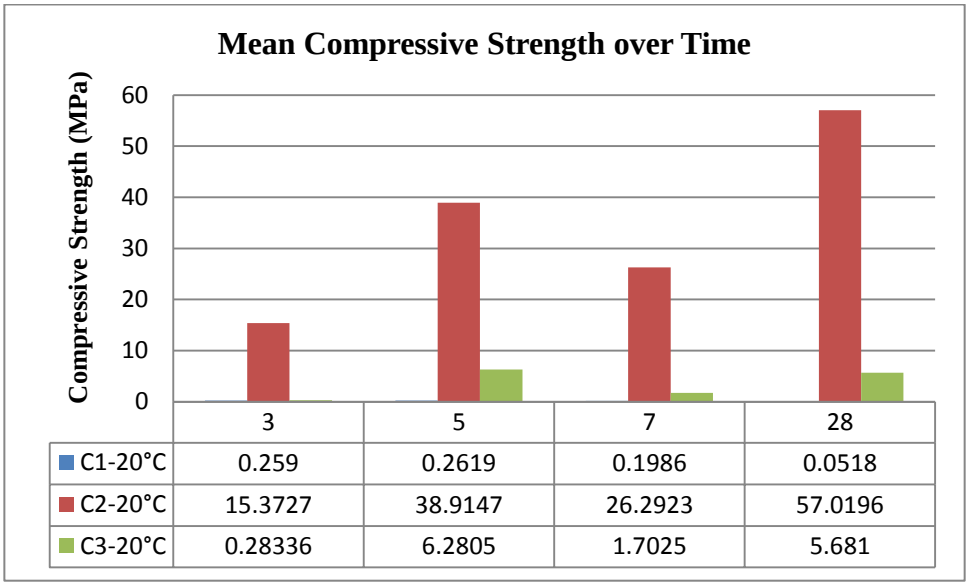

	3	5	7	28
C1-20°C	0.259	0.2619	0.1986	0.0518
C2-20°C	15.3727	38.9147	26.2923	57.0196
C3-20°C	0.28336	6.2805	1.7025	5.681

Figure 5.10 Average Compressive Strength of series C Design Mixture at 20 ℃

5.1.2 Effects of AD and AM on Engineering Properties

5.1.2.1. Surface Carbonation and Loss of Cohesion

A possible explanation into the leaching of alkali solution can be attributed to the curing environment in which the mortar sample is left. Research shows that the environment in which a geopolymer is left to synthesise is important to the overall performance of the material. This has been confirmed various times by various authors and the experimental results from this project agree with the conclusions in that, an elevated curing temperature yields material of greater engineering benefit.

Leaching was not found on any mortar samples which had been oven cured (Figure 5.11 a) but was very common in the 100% PFA mixtures left to cure in 20℃, (Figure 5.11 b). After the initial 3 day period, surface carbonation was becoming visible and disintegration amongst the specimen was showing. Minor surface cracks were forming from which alkali was leaking. This can be related to an unexpected, premature loss in reactivity.

Figure 5.11a Sample with surface carbonation

Figure 5.11b Sample without surface carbonation

Approximately 4 out of 10 specimens that were cured at 20 ℃ displayed evidence of alkali leaching. Unsurprisingly the vast majority of these specimens came from mix C1. This presents an analysis into the beyond below average engineering properties demonstrated. On the basis of the findings of this experimental method, it can be recommended that surface carbonation and the leaching of alkali solution is possible to happen within specimens which are 100% PFA and cured under variable ambient environment. The current study found that heat is indeed an accelerator of the Geopolymerisation process. It can be advised that the rate of Geopolymeric bond creation and the process of dihydroxylation are rapid and extremely efficient. Therefore the possibility of surface carbonation and alkali leaching is vastly decreased. From a chemical point of view, this can be related to the essential ions that required to produce the atmospheric reaction is not being available to the sequence, (Figure 5.11).

In contrast to earlier findings, however, the above method can also be used to support the conclusions of oven cured specimens presenting relatively rapid strength gain and synthesis. Alkali expulsion was not observed on oven cured specimens and it can be assumed that this is due to the unavailability of the required cations.

The surface carbonation and leaching can be relevant factors to the mechanical behaviour of the specimens. This can actually be used as a reason for the significant decrease in material strength which is apparent from the results gained as a result of this

laboratory method, in which it can be seen that the ambient cured specimens demonstrated significantly decreased flexural and compressive strengths than those of the samples which have been oven cured.

It was however reported at the 34th Annual Cement and Concrete Science Conference, 2014, that expulsion of an activating solution and surface carbonation was recognised in a number of specimens produced as part of an experimental method based within the UK. This reinforces the assumption that PFA may be the differentiating factor in the sense that the coal from which the PFA originates changes from area to area based on the geological characteristics of the area from which it is developed. Much of this PFA is also unregulated, although some standards exist they are simply guidelines and adhering to them is near on incredible based on the incredibly differing properties of the material. This unregulated PFA will almost certainly always yield geopolymeric materials of unpredictable quality; a seriously high risk of defects and different characteristic behaviour under engineering applications in which it is being used as a 100% cement replacement.

From a scientific chemical point of view, the phenomenon can be attributed to an atmospheric chemical reaction between the sodium hydroxide with CO_2. This produces Sodium Carbonate and water. This is an amphoteric product basically meaning that the product can either take the character of a base and an acid. Although, these can be assumed that an acidic character will delay the process of synthesis on the basis of basic principles in which an acid will neutralise an alkali leading to a significant decrease in PH. Together with the added water in the mix using the form of fine water, these high levels of H_2O can further amplify the effects of the atmospheric reaction providing a higher strength acid. This is describe by Equation (5.1)

$$2NaOH + CO_2 \rightarrow Na_2CO_3 + H_2O \qquad (5.1)$$

5.1.2.2. Effects of AD and AM on Engineering Properties

The highest flexural strength of samples which cured at 70℃ (Figure 5.2), was given by mix A3, which had an AD of 7.61 and an AM of 1.26. The weakest flexural strength was displayed by mix C1, which had an AD of 9.51 and an AM of 0.95. The highest compressive strength AT 70 ℃ was given by mix C3 and A3 (Figure 5.4). Blend C3 has an AD of 9.51 and an AM of 0.95. The lowest compressive strength was demonstrated

by mix B2. However, composition 2 yielded the highest compressive strength too. It can be seen that the rate of the strength of the mortar in both compressive and flexure increased for blends with GGBS. In mixtures with GGBS, the laboratory method has proved that a lower AD and higher AM is the key to gaining maximum strength.

In addition, an increase in AM results in an increased availability of soluble silicates. This development in soluble silicates eventually results in an increased degree of reaction. However, these results can also be used to describe why blends with a higher AM gain strength faster relevant to those with a lower AM. Only increasing in value of AM and not changing the AD value, also leads to a decrease in the quantity of hydroxide available. Hydroxides are necessary to the dissolution of silicate and aluminate monomers, a key stage in the synthesis process as identified in section 2.3.1.1.1. It is therefore imperative to ensure that the correct ratio between AD and AM is used.

5.1.3 Resistivity Response to Mortar Maturity

The CCR-2 measuring equipment was based in a temperature controlled room in which the temperature was constantly kept at 20°C. Relative humidity was also maintained constant. This was necessary to have an uninfluenced environment on the synthesis reactions inside the mix. Figure 5.12 presents curves of the resistivity over age have been plotted for design mixtures of 1, 2 and 4.

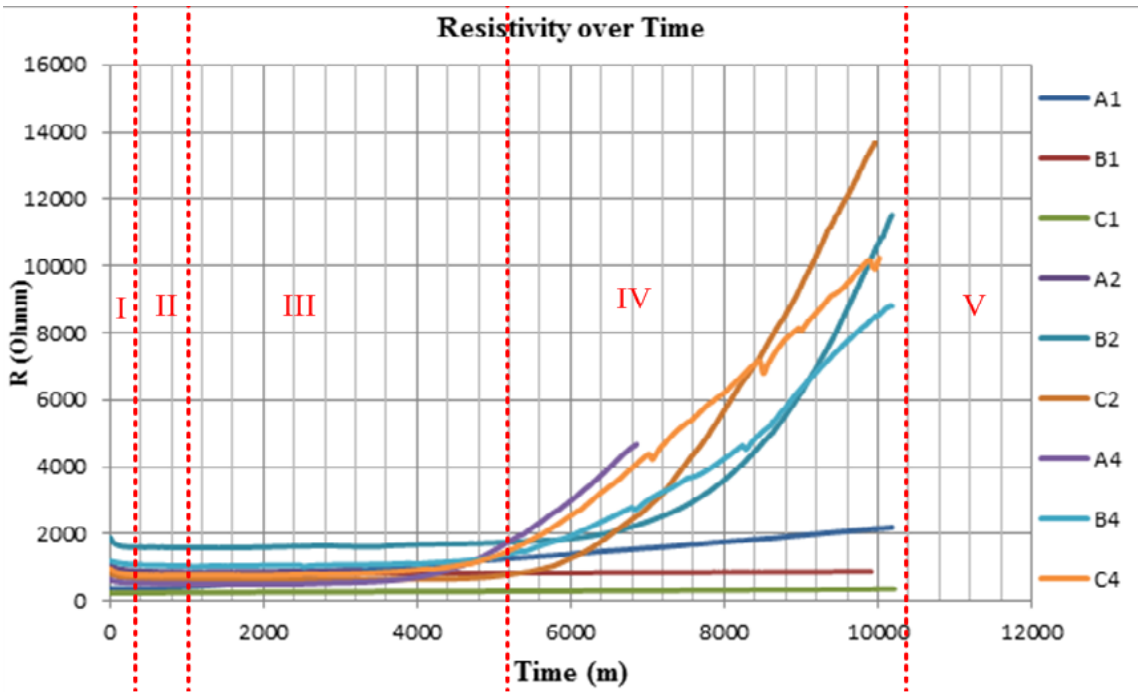

Figure 5.12 Curves of Resistivity over Time, with zone identified

The Figure 5.12 shows that all the mixes are following the same general pattern. The following very basic model can be suggested. This model is by no means right and/or perfect however a small suggestion as to what could be proceeding, on the basis of the idealistic reaction process recognized in section 2.3.1.1.1.

- Zone I: 0-200 mins shows that the higher beginning resistivity reading drops into a lower linear level. At this point it is visualized that the chemical reaction is in the degree of dissolution and monomer bonds are beginning to break.

- Zone II: 200-600 mins determines the timescale in which the resistivity is approximately constant and this can be related to the "Speciation Equilibrium" stage in the Geopolymeric theory model.

- Zone III: 600-4600 mins is the zone in that most blends are developing a relatively linear pattern with a moderately constant resistivity. This can be compared to the gelation stage of the synthesis model.

- Zone IV: 4600-10080 mins is the range in which the near exponential spike in resistivity takes place. This zone can be identified as the period in that reorganisation takes place. This is the common active part of the synthesis process.

- Zone V: 10080 + mins is the zone in which the model can be compared to the polymerisation and hardening stage. (Resistive behaviour unknown due to CCR-2 test only being run for 7 days).

Figure 5.13 presents the resistivity over age for design mixtures series A From the graph it can be seen that mix 3 is not following the same general pattern same as other blends. As can be seen from the Figure (below), all mixes follow by the model which was explained before, but the hydration of mix series A3 is different due to the amount of GGBS.

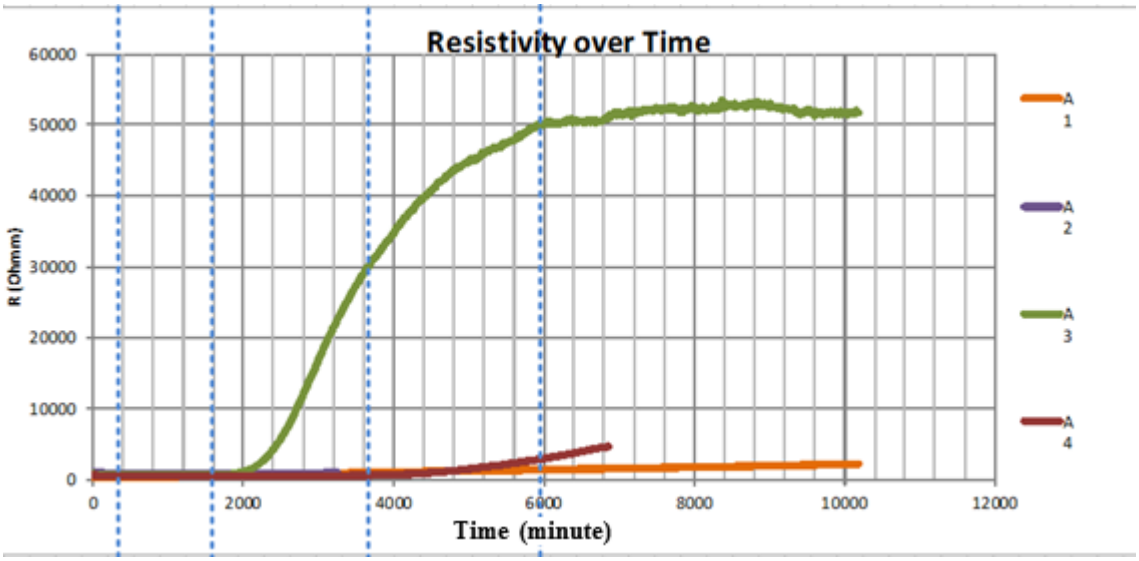

Figure 5.13 Curves of Resistivity over Time, With Zone Identified For Mixture Series A

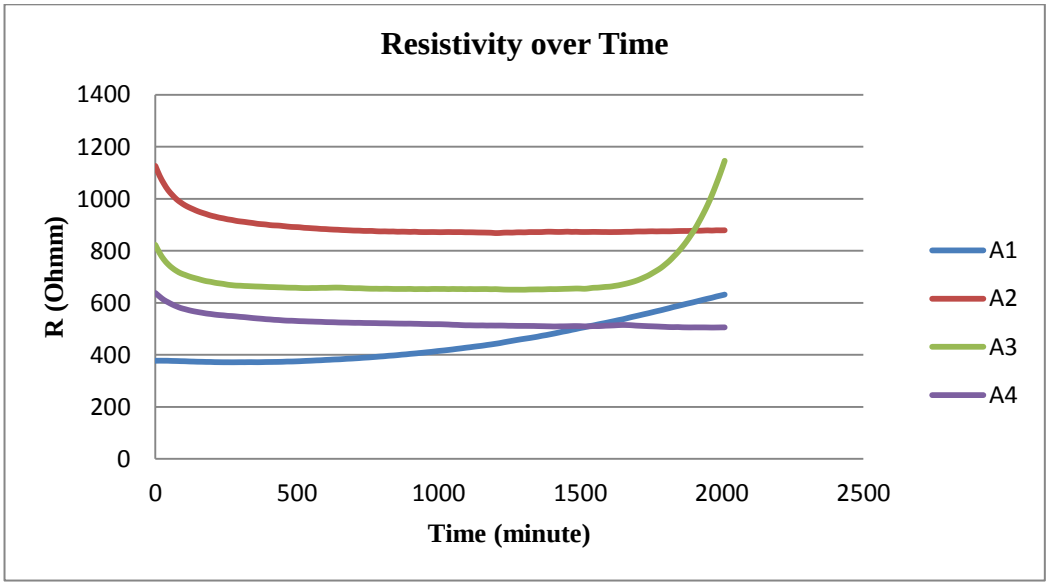

Figure 5.14 Resistivity over Time (0-2010 m), for mixes series A

5.1.3.1. Relationship between Resistivity and Compressive strength

In order to keep accuracy and to determine the nearest relationship, it is important to compare the resistivity with strengths developed for mortar in comparable curing conditions. The resistivity increases the compressive strength is also required to increase. This connection is shown for all mixes for 7days at 20°C. From the data in Figure 5.15, it is apparent that many different patterns are displayed. Some mixtures show a rise in strength together with an increase in resistivity, a factor which would give some substance to the aforementioned model. However, there is a different relation between blends which are as a result of faulty equipment and human error. In order for any sensible analysis to take place, it is needed to repeat the experiment ensuring a true 20°C curing environment.

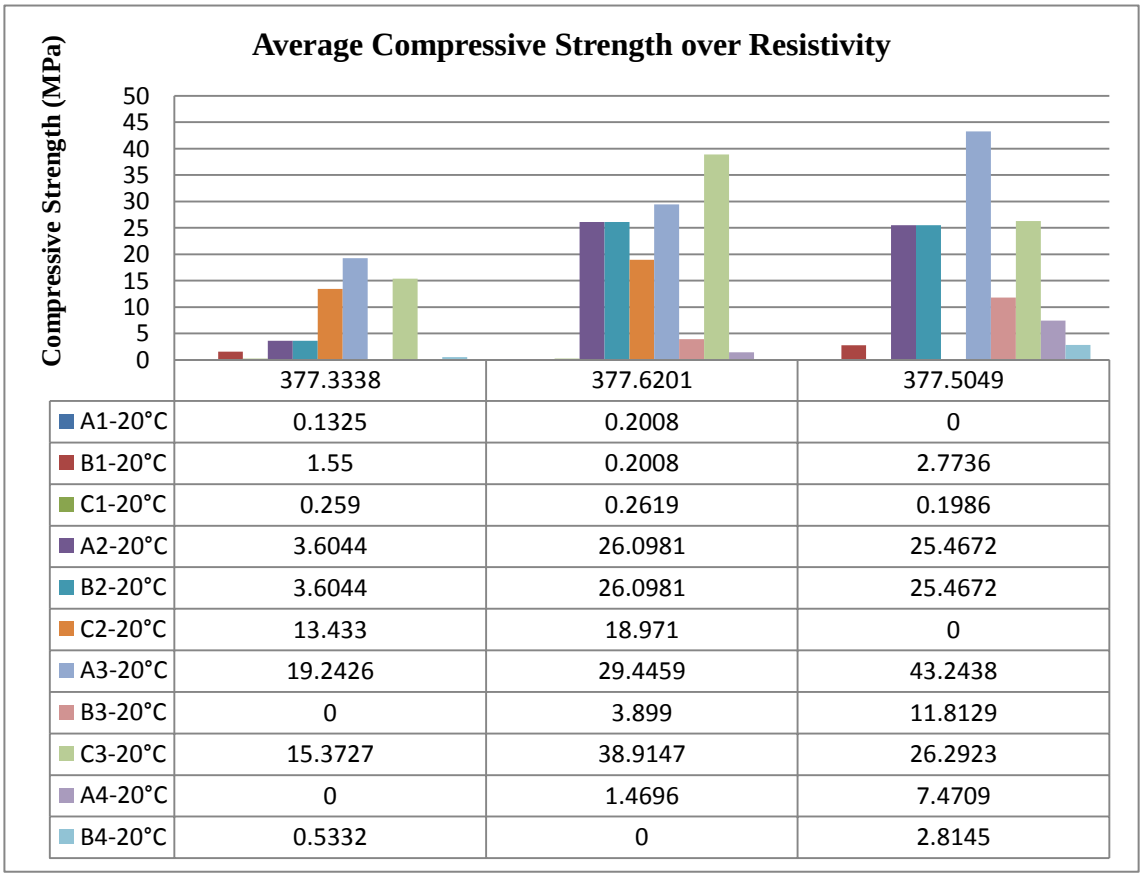

	377.3338	377.6201	377.5049
A1-20°C	0.1325	0.2008	0
B1-20°C	1.55	0.2008	2.7736
C1-20°C	0.259	0.2619	0.1986
A2-20°C	3.6044	26.0981	25.4672
B2-20°C	3.6044	26.0981	25.4672
C2-20°C	13.433	18.971	0
A3-20°C	19.2426	29.4459	43.2438
B3-20°C	0	3.899	11.8129
C3-20°C	15.3727	38.9147	26.2923
A4-20°C	0	1.4696	7.4709
B4-20°C	0.5332	0	2.8145

Figure 5.15 Average Compressive Strength for different Resistivity for all Design Mixtures

5.1.4 Qualitative Imaging

Scanning Electron microscope (SEM) was utilized to analyse the microstructure of various mortars which cured for 28 days. The morphology of samples from all designed mixes is shown in Appendix B.

5.1.4.1 Unreacted Material

As mentioned in the literature review, most of the geopolymer process models are good and determine the existence of precise reactions. However in reality the nature of PFA and GGBS geopolymer have different stages of unreacted materials. Unreacted materials effects in the reduction of both compressive and flexure strengths as they cause distortions within the large 3-dimensional material bonds network. However, this unreacted material can also act as a "micro-aggregate" in the geopolymer microstructure, actually positively adding to the overall strength of the system. There is a multiple of reasons as to why the mixtures can include the unreacted material including a loss in Al or Na particulates, needed to form the foundations of the oligomeric chains as part of the 3-dimensional crystal networks as shown in Figure 2.2. Compromised dissolution networks period in which not enough reactions were made. This weak dissolution stage can be linked to many factors; however, the most likely reason is due to be either the alkali solution or environmental conditions.

Another factor to consider which can firmly affect the strength of the mortar samples is the quantity of contact of the raw feedstock makes with the whole liquid solution of the blend (activator + water). When there is a comparatively lower w/s ratio the solution is immediately consumed by the raw feedstock which comes quickly in contact including the solution. There is then the insufficient connection within the remaining dry material and solution irrespective of the mixing time and/ or speed.

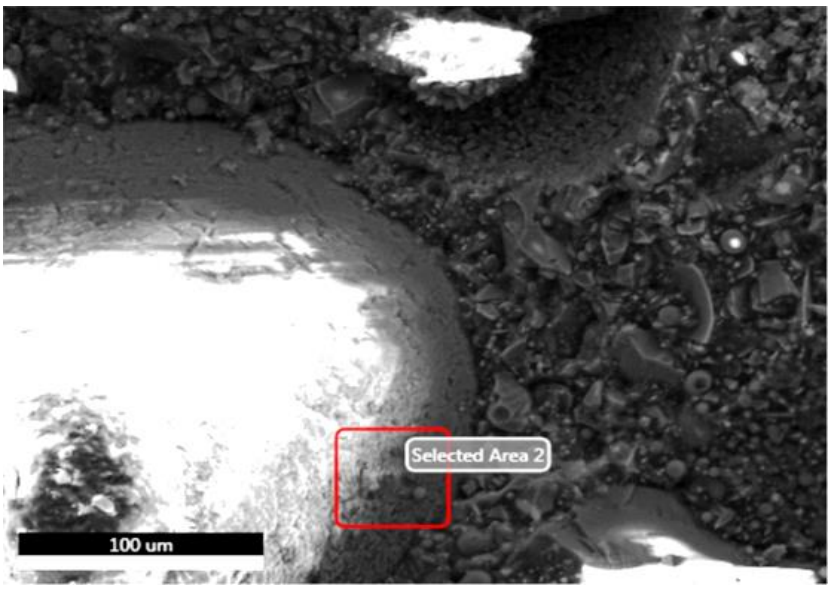

Figure 5.16 Large amount of PFA within geopolymer matrix

6. Conclusions and Recommendations

6.1 Conclusions

Based on the analysis of both literature on the subject and the experimental work reported in this research, the following conclusions are drawn:

- Higher concentration of alkaline activators results in higher compressive strength of geopolymer.
- Samples with higher percentage of GGBS tend to have an overall higher flexural and compressive strength.
- The resistivity increases with the age of geopolymer mortar, which shows the quality of the geopolymer mortar is growing with time.
- There is a strong correlation between resistivity and compressive strength. By increasing resistivity, the compressive strength increased for all mixes.
- The PFA blends give lower resistivity which because they gain strength more gradually than the mix with GGBS.
- Higher temperature results in faster geopolymerisation.
- Compressive strength of geopolymer increased over the time for both different curing conditions.
- The resistivity of samples with higher amount of GGBS is higher which is because that GGBS mixes gain strength more faster than PFA mixes.

6.2 Recommendation for future works:

- This research only used GGBS and PFA as the precursor for synthesizing geopolymer. Other materials can be considered for further studies such as rice husk, silica fume, and metakaolin.
- An investigation into the micro-cracks in geopolymers mortars and also investigating the relationship of strength and nano-crystallisation particles of geopolymer mortars.
- Study of the flexure strength development of geopolymer mortars cured at temperatures other than those applied in this research.
- Further study required regarding to the relationship between flexure strength development of geopolymer mortars and geopolymerisation process of them.

- Additional study is required to examine the effect of ambient conditions, type of formwork and structural elements on the temperature increase in the mix.

Reference

1. Delatte, N. J., 2001. Lessons from Roman Cement and Concrete. *Professional Issues in Engineering Education and Practice,* 127(3), pp. 109-115.

2. Duxson, P., Lukey, G. C. & van Deventer, J., 2012. *Nanostructural Design of Multifunctional Geopolymeric Materials.* Melbourne, Australia: The University of Melbourne .

3. Fernández-Jiménez, A., Palomo, A., Sobrados, I. & Sanz, J., 2006. The role played by the reactive alumina content in the alkaline activation of fly ashes. *Microporous and Mesoporous Materials,* 91(1-3), pp. 111-119.

4. García-Lodeiro, I., Paloma, A. & Fernández-Jiménez, A., 2007. Alkali-Aggregate Reaction in Activated Fly Ash Systems. *Cement and Concrete Research,* 37(2), pp. 175-183.

5. Jaarsveld, J. v., Deventer, J. v. & Lukey, G., 2003. The characterisation of source materials in fly ash-based geopolymers. *Materials Letters,* 57(7), pp. 1272-1280.

6. McDonald , M. & Thompson, J. L., 2011. *Sodium Silicate a Binder for the 21st Century,* Philadelphia-USA: Industrial Chemicals Division- The PQ Corporation.

7. Mindess S. and J.F. Yong, 1981. *Concrete.* NewJersey: Prentice-Hall Inc.

8. Petermann , J. C. & Saeed, A., 2012. *Alkali-Activated Geopolymers: A Literature Review,* Panama: Defense Technical Information Center.

9. Puertas, F. & Fernández-Jiménez, A., 2003. Mineralogical and microstructural characterisation of alkali-activated fly ash/slag pastes. *Cement and Concrete Composites,* 25(3), pp. 287-292.

10. Sumajouw, M. D. & Rangan, B. V., 2006. *low-calcium fly ash-based geopolymer concrete: reinforced beams and columns,* Perth, Australia: Curtin University of Technology.

11. Toutanji, H. et al., 2004. Effect of supplementary cementitious materials on the compressive strength and durability of short-term cured concrete. *Cement and Concrete Research,* 34(2), pp. 311-319.

12. van Jaarsveld, J., van Deventer, J. & Lukey, G., 2002. The effect of composition and temperature on the properties of fly ash- and kaolinite-based geopolymers. *Chemical Engineering Journal,* 89(1-3), pp. 63-73.

13. Aitcin, P.-C., Miao, B., Cook, W. D. & Mitchell, D., 1994. Effects of Size and Curing on Cylinder Compressive Strength of Normal and High-Strength Concrete. *Materials,* 91(4), pp. 349-355.

14. Al-Khaiat, H. & Fattuhi, N., 2001. Long-term strength development of concrete in arid conditions. *Cement and Concrete Composites,* 23(4-5), pp. 363-373.

15. Apebo, N., Lorwua, M. & Agunwamba, J., 2013. Comparativeanalysisofthecompressive Strengthofconcretewithgravelandcrushed Overburntbricksascoarseaggregates. *Nigerian Journal of Technolog,* 32(1), pp. 7-12.

16. Banfill, P., 2006. *Rheology of fresh cement and concrete,* Edinburgh: School of the built Environment, Heritot-Watt University.

17. Bergström , S. & Byfors, J., 1980. Properties of concrete at early ages. *Materials and Structers,* 13(3), pp. 265-274.

18. BN EN196-1:2005, n.d. *Method of Testing cement- Part1: Determination of strength,* s.l.: s.n.

19. Bone, B. et al., 2004. *Review of scientific literature on the use of stabilisation/solidification for the treatment of contaminated soil,solid waste and sludges,* Bristol: Environment Agency, Rio House, Waterside Drive, Aztec.

20. BS EN 197-1:2000, n.d. *Cement- Prt 1: Composition, specifications and conformity criteria for common cements,* s.l.: s.n.

21. Chareerat, T., Lee-Anansaksiri, A. & Chindaprasirt, P., 2006. *Synthesis of High Calcium Fly Ash and Calcined Kaoline Geopolymer Mortar.* Thailand, International Conference on Pozzolan, Concrete and Geopolymer.

22. Chen, W., 2006. *Hydration of Slag Cement Theory, Modeling and Application,* Netherland: University of Twent.

23. Chen, W. & Brouwers, H., 2007. The hydration of slag,part 1: reaction models for alkali-activated slag. *J Mater Sci,* Volume 42, pp. 428-443.

24. Davidovits, J., 1982. *Mineral Polymers and Methods of Making Them.* s.l.:United State Patent.

25. Davidovits, J., 2011. *Geopolymer chemistry & applications(3rd ed).* s.l.:Saint-Quentin : Institut Geopolymer.

26. Davidovits, J., 2011. *Geopolymer Chemistry and Applications.* 3rd ed. Frence: Institut Géopolymère.

27. Department of Materials Science and Engineering (UIUC), 2008. *Concrete: Scientific Principle,* s.l.: University of Illinois.

28. Feng, D., Tan, H. & Van Deventer, J., 2004. Ultrasound Enhanced Geopolymerisation. *Journal of Materials Science,* Volume 39, pp. 571-580.

29. Fernandez-Jimenez, A., Gracia-Loderio, I. & Palomo, A., 2007. Durability of alkali-activated fly ash cementitious materials. *J Mater Sci,* Volume 42, pp. 3055-3065.

30. Fernández-Jiménez, et al., 2004. Microstructural characterisation of alkali-activated PFA matrices for waste immobilisation. *Cement and Concrete Composites,* 26(8), pp. 1001-1006.

31. Fernández-Jiménez, A. & Palomo, A., 2005. Mid-infrared spectroscopic studies of alkali-activated fly ash structure. *Microporous and Mesoporous Materials,* 86(1-3), pp. 207-214.

32. Fernández-Jiménez, A., Palomo, J. & Puertas, F., 1999. Alkali-activated slag mortars: Mechanical strength behaviour. *Cement and Concrete Research,* 29(8), pp. 1313-1321.

33. Gangarao, Taly & Vijay, 2006. *Reinforced Concrete Design with FRP Composites.* New York: Taylor & Francis Group.

34. Gee, K., 1979. *The potential for slag in blended cements.* s.l.:s.n.

35. Ghosh, S., 1991. *Cement and Concrete Science and Technology,First Edition.* New Delhi: ABI Books Privte Limited.

36. Glukhovsky, V., 1980. *High Strength Slag Alkaline Cements.* 7th ed. Paris: Congress on the Chemistry of Cement.

37. Heidrich, C., 2002. *Ash Utilisation-An Australia Perspective.* Melbourne, Australia, Siloxo, Geopolymers International Conference.

38. Howie & Howie limited, 2015. [Online]
Available at: http://www.s-n-l.fr/Produits_en_0_S196-1-_standard-sand-iso-CEN-196-1-ISO-679.html

39. Hu, J., 2005. *A study of effects of aggregate on concrete rheology* , Ames: Iowa State University .

40. Imbabi, M. S., Carrigan, C. & Mc Kenna, S., 2012. Trends and developments in green cement and concrete technology. *International Journal of Sustainable Built Environment,* 1(2), pp. 194-216.

41. Jackson, N. & Dhir, R. K., 1996. *Civil engineering materials.* 4th ed. s.l.:Macmillan Education.

42. Jing, W.,& Roy,D.M., 1992. Hydrothermal processing of new fly ash cement. *American Ceramic Society Bulletin,* pp. 642-647.

43. Jos G.J. Olivier (PBL), G. J.-M. (.-J., 2014. *Trends in global CO2 emissions: 2014 Report,* s.l.: © PBL Netherlands Environmental Assessment Agency.

44. Joshi, S. & Kadu, M., 2012. Role of Alkaline Activator in Development of Eco-friendly Fly Ash Based Geo Polymer Concrete. *International Journal of Environmental Science and Development,* 3(5), pp. 417-421.

45. Khale, D. & Chaudhary, R., 2007. Mechanism of Geopolymerization and Factors Influencing Its Development: AReview. *J Mater Sci,* Volume 42, pp. 729-749.

46. Khan, S. U., Nuruddin, M. F., Ayub, T. & Shafiq, N., 2013. Effects of Different Mineral Admixtures on the Properties of Fresh Concrete. *The Scientific World Journal*, pp. 1-11.

47. King, D., 2012. *The Effect of Silica Fume on the Properties of Concrete as Defined in Concrete Society Report 74, Cement Materials.* Singapore, 37th Conference on Our World in Concrete & Structures.

48. King, D., 2012. *THE EFFECT OF SILICA FUME ON THE PROPERTIES OF CONCRETE AS DEFINED IN CONCRETE SOCIETY REPORT 74, CEMENTITIOUS MATERIALS.* Singapore, 37th Conference on Our World in Concrete & Structures, pp. 29-31.

49. Kong, L., G, J., Daniel & Sanjayan, 2008. Damage Behavior of Geopolymer Composites exposed to elevated temperatures. *Cement and Concrete Composites,* 30(10), pp. 986-991.

50. Kucche, K., Jamkar, S. & Sadgir, P., 2015. Quality of Water for Making Concrete:A Review of literature. *International Journal of Scientific and Research,* 5(1).

51. LIVERPOOL, U., 2014. *Geopolymer Concretes-Presentation*, s.l.: Liverpool University.

52. Li, Z., 2011. *Advance Concrete Technology.* Canada: John Wiley & Sons, Inc., Hoboken.

53. Li, Z. & Li, W., 2003. Contactless, transformer-based measurement of the resistivity of materials. *US Patent, 6639401,* 28 10.

54. Li, Z., Wei, X. & Li, W., 2003. Preliminary interpretation of Portland cement hydration process using resistivity measurements. *ACI materials,* MAY-JUN, 100(3), pp. 253-257.

55. Maekawa, K., Ishida, T. & Kishi, T., 2008. *Multi-Scale Modeling of Structural Concrete.* First ed. s.l.:Taylor & Francis e-Library.

56. Margaret Damilola, O., 2013. Syntheses, characterization and binding strength of geopolymes: A review. *International Journal of Materials Science and Applications,* 2(6), pp. 185-193.

57. McArthur, H. & Spalding, D., 2004. *Engineering Materials Science: Properties, Uses, Degradation, Remediation.* Cambridge: Woodhead Publishing Limited.

58. McCann, 1988. *The Roman Port of Cosa.* s.l.:Scientific American.

59. Mindess, S., & Young, J.F., 1981. *Concrete.* s.l.:Englewood Cliffs, NJ: Prentice Hall.

60. Mohammed, S., Carrigan, C. & McKenna, S., 2013. Trends and developments in green cement and concrete technology. *International Journal of Sustainable Built Environment,* 2012(1), pp. 194-216.

61. Mulheron, D. M., 2012. *Concrete Technology Notes,* Guildford: University of Surrey.

62. Neville, A., 2011. *Properties of Concrete.* 5th ed. s.l.:s.n.

63. Neville, A. & Brooks, J., 1987. *Concrete Technology.* s.l.:Longman.

64. Pacheco-Torgal, F., Castro-Gomes, J. & Jalali, S., 2007. Alkali-activated binders: A review. Part 2. About materials and binders manufacture. *Construction and Building Materials,* 22(7), pp. 1315-1322.

65. Palomo, A. & Fernandez-Jimenez, A., 2011. *Alkaline activation, procedure for transforming fly ash into new materials. Psrt 1: Applications.* Denver-USA, World of Coal Ash (WOCA).

66. Parekh, D. & Modhera, C., 2011. Assessment of recycled aggregate Concrete. *Journal of Engineering Research and tudies,* II(I), pp. 1-9.

67. Popovics, S., 1982. *Fundamentals of portland cement concrete: Aquantitative approch.*. New York: NY:Wiley.

68. Provis, J., Lukey, G. & Deventer, J. S. v., 2005. Do Geopolymers Actually Contain Nanocrystalline Zeolites? A Reexamination of Existing Results. *Chemistry of Materials,* 17(12), pp. 3075-3085.

69. Provis, J. & Van Deventer, J., 2009. *Geopolymers Structure, Processing, properties and industrial applications.* Melbourne-Australia: Woodhead Publishing.

70. R. Szostak, R. F. T. S., 1989. *Molecular Sieves: Principles of Synthesis and Identification.* Second ed. London: Blackie Academic & Professional, an imprint of thomson science.

71. R.K. Dhir and M.R. Jones, 1994. *Additional materials and allowable contents in cement.* London: E & FN Spon.

72. Rangan, B., 2010. *Fly Ash-Based Geopolymer Concrete.* Mumbai-India, Allied Publishers Private Limited, pp. 68-106.

73. Siddique, R., 2007. *Waste Materials and By-Products in Concrete.* s.l.:Springer-Verlag.

74. Siddique, R. & Iqbal Khan, M., 2011. *Supplementary Cementing Materials.* s.l.:Springer-Verlag.

75. Silva, F. & Thaumaturgo, C., 2002. Fiber Reinforcement and Fracture Reponse in Geopolymeric Mortars. *Fatigue Fract Engng Mater Struct,* Volume 26, pp. 167-172.

76. Skvara, F. et al., 2005. *Concrete Based on Fly Ash Geopolymers,* Prag: Institute of Chemical Technology.

77. Song, S., Sohn, D., Jennings, H. & Mason, T., 2000. Hydartion of alkali-activated ground granulated blast furnace slag. *Materials Science,* Volume 35, pp. 249-257.

78. Song, X., 2007. *Development and Performance of Class F Fly Ash Based Geopolymer concretes against sulphuric acid attack,* Sydney: University of New South Wales.

79. Soura Kr.Das, A. K. a. A., 2014. Geo-Polymer Concrete-Green Concrete for the future. *International Journal of Civil Engineering Research,* pp. 21-28.

80. Soutsos, M., Barnett, S., Bungey, J. & Millard, S., 2005. Fast Track Construction with High-Strength Concrete Mixes Containing Ground Granulated Blast Furnace Slag. *The Seventh International Symposium on Utilization of High-Strength/High Performance Concrete,* Volume 228, pp. 255-270.

81. Steiger, R., 1995. The history of concrete. *Concrete Journal.*

82. Van Jaarsveld, J. G. S., Deventer , J. G. J. & Lorenzen, L., 1997. The Potential Use of Geopolymeric materials to immobilise toxic metals: Part . Theory and applications. *Minerals Engineering,* 10(7), pp. 659-669.

83. Wallah, S. & Rangan, B., 2006. *Low-Calcium Fly Ash-Based Geopolymer Concrete: Long-Term Properties,* Perth, Australia: Research Report GC 2, Faculty of Engineering Curtin University of Technology.

84. Wang, H., Li, H. & Yan, F., 2005. Synthesis and mechanical properties of metakaolinite-based geopolymer. *Colloids and Surfaces A: Physicochemical and Engineering Aspects,* 268(1-3), pp. 1-6.

85. Wang, K. et al., 2006. *Developing A Simple And Rapid Test For Monitoring The Heat Evolution Of Concrete Mixtures For Both Laboratory And Field Applications,* s.l.: Center for Transportation Research and Education Iowa State University .

86. Wei, X. & Li, Z., 2005. Study on hydration of Portland cement with fly ash using electrical measurement. *Material and Structure,* Issue 38, pp. 411-417.

87. Wei, X. & Li, Z., 2005. Study on hydration of Portland cement with fly ash using electrical measurment. *Materials and Structures,* Volume 38, pp. 411-417.

88. Williams, P. et al., 2002. Microanalysis of alkali-activated fly ash–CH pastes. *Cement and Concrete Research,* June, 32(6), pp. 963-972.

89. Winter, N., 2005. *Understanding Cement.* United Kingdom: Interpreting Cement Science.

90. Winter, N. B., 2012. *Understanding Cement: The Fast Star User-friendly Insight into Cement Production, Cement Hydration and Cement and Concrete Chemistry.* s.l.:WHD Microanalysis Consultants Ltd.

91. Xiao, L. & Li, Z., 2008. Early-age hydration of fresh concrete monitored by non-contact electrical resistivity measurement. *Cement and Concrete Research ,* 38(3), pp. 312-319.

92. Xie, Z. & Xi, Y., 2001. Hardening mechanisms of an alkaline-activated class F fly ash. *Cement and Concrete Research,* 31(9), pp. 1245-1249.

93. Xie, Z. & Xi, Y., 2001. Hardening mechanisms of an alkaline-activated class F fly ash. *Cement and Concrete Research ,* Volume 31, pp. 1245-1249.

94. Xu, H. & Deventer, . J. V., 2000. The geopolymerisation of alumino-silicate minerals. *International Journal of Mineral Processing,* 59(3), pp. 247-266.

95. Xu, H. & Deventer, J. v., 2002. Geopolymerisation of Multiple Minerals. *Minerals Engineering,* 15(12), pp. 1131-1139.

Appendix A

1. Mix Design:

Mix A1(100% PFA)		Mix B1(100% PFA)		Mix C1(100% PFA)	
PFA (Kg)	5	PFA (Kg)	5	PFA (Kg)	5
SAND (Kg)	13.75	SAND (Kg)	13.75	SAND (Kg)	13.75
Added water (ml)	1,100	Added water (ml)	1,400	Added water (ml)	950
NaOH (ml)	153.8	NaOH (ml)	92.8	NaOH (ml)	185.6
Water glass (ml)	725.2	Water glass (ml)	436.6	Water glass (ml)	869.5
Mix A2(50% PFA)		Mix B2(50% PFA)		Mix C2(50% PFA)	
PFA (Kg)	2.5	PFA (Kg)	2.5	PFA (Kg)	2.5
GGBS)kg)	2.5	GGBS)kg)	2.5	GGBS)kg)	2.5
SAND)Kg)	13.75	SAND)Kg)	13.75	SAND)Kg)	13.75
Added water (ml)	110	Added water (ml)	1,400	Added water (ml)	950
NaOH (ml)	153.8	NaOH (ml)	92.8	NaOH (ml)	185.6
Water glass (ml)	725.2	Water glass (ml)	436.6	Water glass (ml)	869.5
Mix A3(30%PFA)		Mix B3(30%PFA)		Mix C3(30%PFA)	
PFA (kg)	1.5	PFA (kg)	1.5	PFA (kg)	1.5
GGBS (kg)	3.5	GGBS (kg)	3.5	GGBS (kg)	3.5
SAND (Kg)	13.75	SAND (Kg)	13.75	SAND (Kg)	13.75
NaOH (ml)	153.8	NaOH (ml)	92.8	NaOH (ml)	185.6
Water glass (ml)	725.2	Water glass (ml)	436.6	Water glass (ml)	869.5
Added water (ml)	1100	Added water (ml)	1400	Added water (ml)	950
Mix A4(70%PFA)		Mix B4(70%PFA)		MixC4(70%PFA)	
PFA (kg)	3.5	PFA (kg)	3.5	PFA (kg)	3.5
GGBS (kg)	1.5	GGBS (kg)	1.5	GGBS (kg)	1.5
SAND (Kg)	13.75	SAND (Kg)	13.75	SAND (Kg)	13.75
NaOH (ml)	153.8	NaOH (ml)	92.8	NaOH (ml)	185.6
Water glass (ml)	725.2	Water glass (ml)	436.6	Water glass (ml)	869.5
Added water (ml)	1100	Added water (ml)	1400	Added water (ml)	950

Calculation:				
Average weight of each geopolymer (kg)			0.6	
Needed cubes		36		
weight of batch required (kg)		21.6		
5% extra for losses (kg)		0.9		
weight of Total batch required(kg)		22.5		
Calculation of Alkalai concentration				
Na		22.99		
Si		28.685		
O		15.999		
Molar mass of Na2SiO3	122.06324 g/mol			
SiO2		60.683	61	
Na2O		61.979	62	
SiO2: Na2O		02:01		The 2:1 ratio is a manufacturing specification for the Na2SiO3
Water Glass solution(Sodium Silicate solution)				
Na2Sio	H2O		Na2SiO3	
1180		728.1	452	

Sodium Silicate(g)					
SiO2	Na2O				
30.12	15.06				
Concentration of within Na2SiO soln	118				
Concentration	38.30%				
SiO2	25.52542373				
Na2O	12.76271186				
H2O	61.71186441				
Sodium hydroxide (g)	29				
Na2O	22.99			AD	7.61
Total Na2O	38.05			AM	1.26328021
Total H2O	838				
Con. In 1000g of H2O	45.40031023				
Molar concentration Na2O	0.732263068				
Molar concentration NaOH	1.847379641				
Calculation of Alkalai concentration B					
Na	22.99				
Si	28.685				
O	15.999				

Molar mass of Na2SiO3	122.06324 g/mol					
SiO2		60.683	61			
Na2O		61.979	62			
SiO2: Na2O		02:01		The 2:1 ratio is a manufacturing specification for the Na2SiO3		
Water Glass solution(Sodium Silicate solution)						
Na2Sio	H2O		Na2SiO3			
196		120.93	75.07			
Sodium Silicate(g)						
SiO2	Na2O					
49.98		25.088				
Concentration of within Na2SiO soln		196				
Concentration		38.30%				
SiO2		25.5				
Na2O		12.8				
H2O		61.7				
Sodium hydroxide (g)		29				
Na2O		22.475			AD	9.5126
Total Na2O		47.563			AM	0.95164066
Total H2O		231				
Con. In 1000g of H2O		205.9628459				

Molar concentration Na2O	3.321981385			
Molar concentration NaOH	8.572855188			
Calculation of Alkalai concentration c				
Na	22.99			
Si	28.685			
O	15.999			
Molar mass of Na2SiO3	122.06324 g/mol			
SiO2	60.683	61		
Na2O	61.979	62		
SiO2: Na2O	02:01		The 2:1 ratio is a manufacturing specification for the Na2SiO3	
Water Glass solution(Sodium Silicate solution)				
Na2Sio	H2O	Na2SiO3		
196	120.93	75.07		
Sodium Silicate(g)				
SiO2	Na2O			
49.98	25.088			
Concentration of within Na2SiO soln	196			
Concentration	38.30%			
SiO2	25.5			
Na2O	12.8			
H2O	61.7			

Sodium hydroxide (g)	29		
Na2O	22.475	AD	9.5126
Total Na2O	47.563	AM	0.951640656
Total H2O	182		
Con. In 1000g of H2O	261.8920452		
Molar concentration Na2O	4.224065245		
Molar concentration NaOH	10.90081353		

Appendix B

Chemical compositions (elements) of fly ash (% by weight)

Element	O	AL	SI	K	Ca
Weight %	52	15.1	24.7	3	5.2
Atomic %	66.4	11.5	17.9	1.6	2.7

Chemical compositions (elements) of GGBS (% by weight)

Element	O	Mg	Al	Si	Ca
Weight %	36.2	1.8	3.4	11	47.5
Atomic %	56	1.9	3.1	9.7	29.3

Appendix C

EDAX TEAM

28-days-3-4

Author: samira safari

Sample Name: A3-20℃

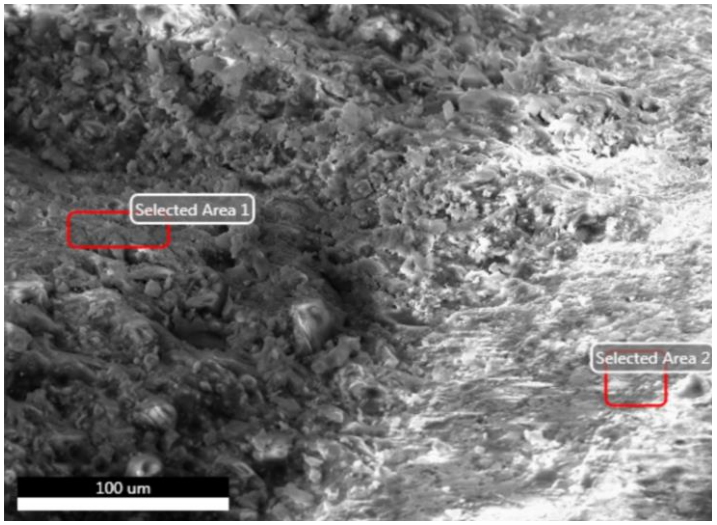

Selected Area 1

kV: 20	Mag: 1000	Takeoff: 40.1	Live Time(s): 30	Amp Time(µs): 1.92	Resolution:(eV)

Selected Area 1

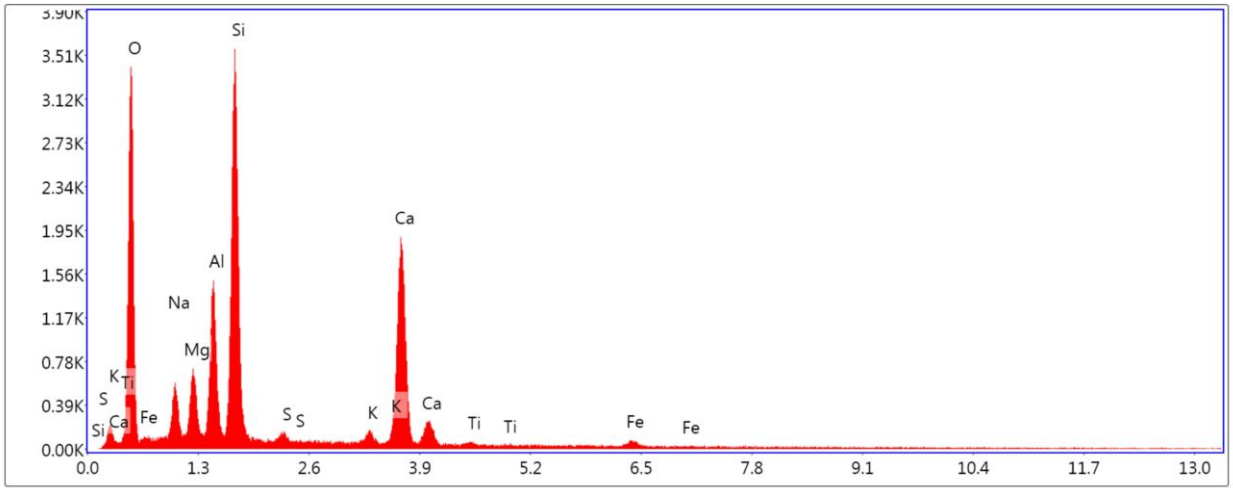

Lsec: 30.0 0 Cnts 0.000 keV Det: Octane Super Det

eZAF Smart Quant Results

Element	Weight %	Atomic %	Net Int.	Error %	Kratio	Z	R	A	F
O K	51.9	66.9	825.9	9.1	0.1373	1.0531	0.9709	0.2514	1.0000
NaK	5.6	5.0	163.2	9.5	0.0188	0.9576	0.9972	0.3492	1.0048
MgK	3.8	3.2	192.3	8.1	0.0176	0.9742	1.0048	0.4685	1.0077
AlK	6.7	5.1	408.8	6.4	0.0372	0.9383	1.0120	0.5843	1.0103
SiK	15.4	11.3	1048.2	5.1	0.0978	0.9591	1.0187	0.6581	1.0067
S K	0.4	0.3	26.3	16.8	0.0030	0.9395	1.0311	0.7472	1.0169

K K	0.6	0.3	33.6	13.5	0.0051	0.8896	1.0471	0.9278	1.0589
CaK	14.4	7.4	698.5	2.6	0.1268	0.9059	1.0518	0.9543	1.0173
TiK	0.2	0.1	8.4	54.9	0.0017	0.8212	1.0603	0.9440	1.0330
FeK	1.0	0.4	23.1	18.1	0.0083	0.8080	1.0721	0.9928	1.0798

Selected Area 2

kV: 20 Mag: 1000 Takeoff: 40.1 Live Time(s): 30 Amp Time(µs): 1.92 Resolution:(eV)

Selected Area 2

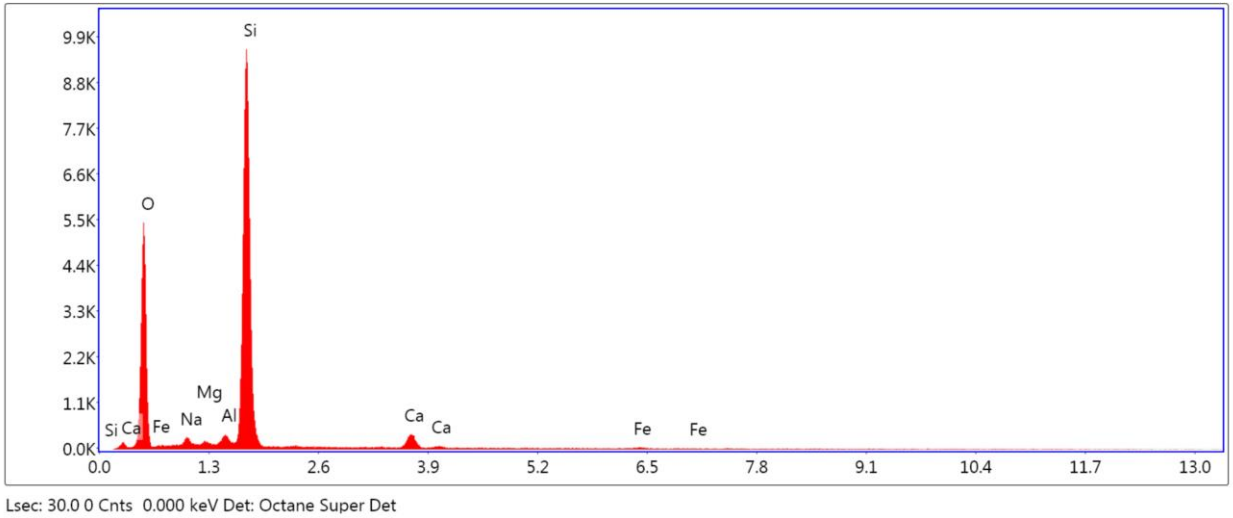

Lsec: 30.0 0 Cnts 0.000 keV Det: Octane Super Det

eZAF Smart Quant Results

Element	Weight %	Atomic %	Net Int.	Error %	Kratio	Z	R	A	F
O K	56.2	69.5	1298.3	7.8	0.2131	1.0414	0.9772	0.3639	1.0000
NaK	2.5	2.2	77.7	10.7	0.0089	0.9465	1.0030	0.3714	1.0070
MgK	0.5	0.4	29.1	17.2	0.0026	0.9628	1.0104	0.5173	1.0131
AlK	1.1	0.8	78.2	9.0	0.0070	0.9272	1.0174	0.6651	1.0234
SiK	36.4	25.6	2916.3	3.6	0.2686	0.9476	1.0239	0.7770	1.0031
CaK	2.6	1.3	125.3	6.0	0.0225	0.8947	1.0561	0.9335	1.0217
FeK	0.6	0.2	15.7	26.1	0.0056	0.7976	1.0754	1.0029	1.1051

28-days-3-4

Author: samira safari
Sample Name: A3-70℃

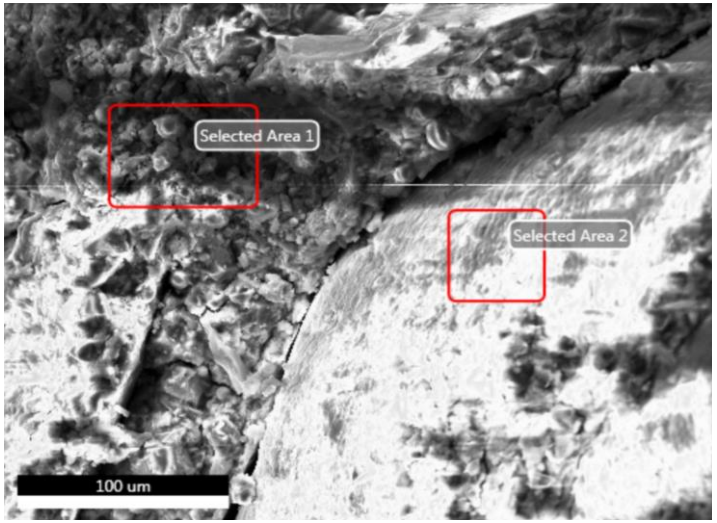

kV: 20	Mag: 1000	Takeoff: 35.5	Live Time(s): 30	Amp Time(µs): 1.92	Resolution:(eV)

Selected Area 1

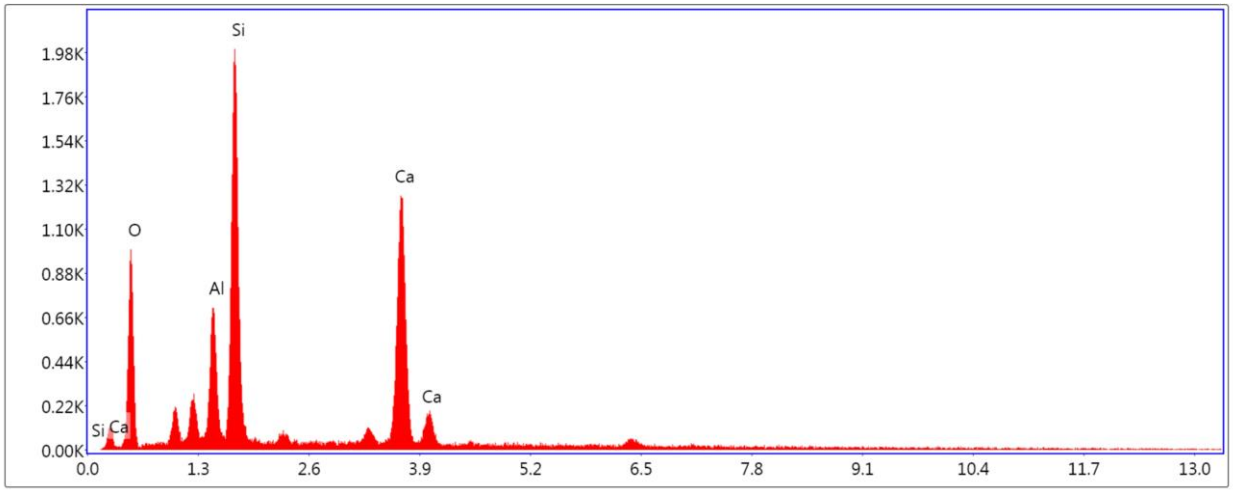

Lsec: 30.0 0 Cnts 0.000 keV Det: Octane Super Det

eZAF Smart Quant Results

Element	Weight %	Atomic %	Net Int.	Error %	Kratio	Z	R	A	F
O K	49.2	66.3	239.5	10.4	0.0967	1.0588	0.9643	0.1859	1.0000
AlK	7.0	5.6	197.0	6.5	0.0435	0.9440	1.0063	0.6490	1.0139
SiK	19.5	15.0	593.2	4.9	0.1344	0.9650	1.0132	0.7075	1.0086
CaK	24.3	13.1	488.2	2.7	0.2153	0.9120	1.0473	0.9582	1.0132

Selected Area 2

kV: 20	Mag: 1000	Takeoff: 35.5	Live Time(s): 30	Amp Time(µs): 1.92	Resolution:(eV)

Selected Area 2

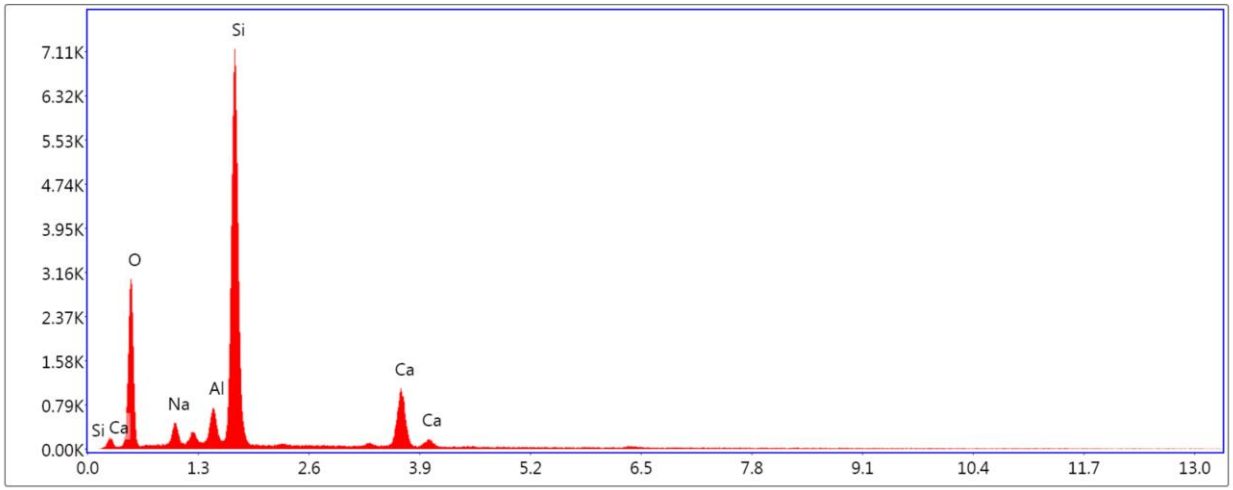

Lsec: 30.0 0 Cnts 0.000 keV Det: Octane Super Det

eZAF Smart Quant Results

Element	Weight %	Atomic %	Net Int.	Error %	Kratio	Z	R	A	F
O K	49.5	64.0	740.6	9.0	0.1416	1.0510	0.9720	0.2720	1.0000
NaK	4.9	4.4	135.0	9.4	0.0179	0.9556	0.9981	0.3786	1.0062
AlK	3.6	2.8	217.2	6.4	0.0227	0.9363	1.0129	0.6551	1.0193

SiK	32.3	23.8	2149.4	4.0	0.2306	0.9570	1.0196	0.7427	1.0045
CaK	9.6	5.0	396.7	3.2	0.0828	0.9038	1.0525	0.9360	1.0170

EDAX TEAM

28-days-3-4

Author: samira safari

Sample Name: B3-20℃

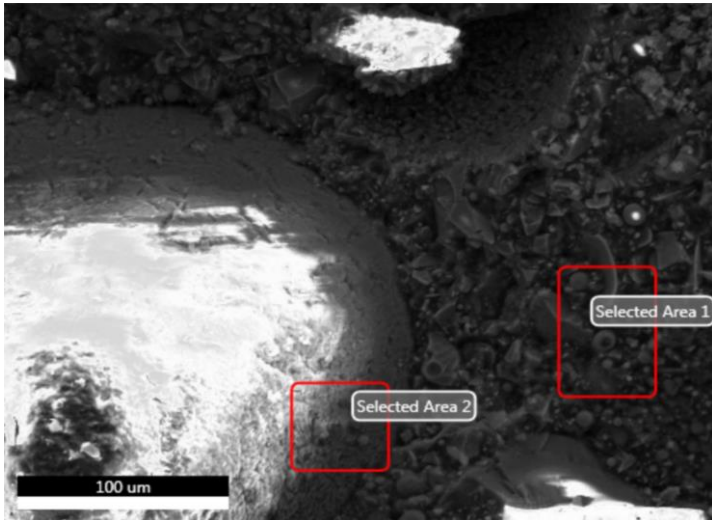

Selected Area 1

kV:	20	Mag:	1000	Takeoff:	39.3	Live Time(s):	30	Amp Time(µs):	1.92	Resolution:(eV)

Selected Area 1

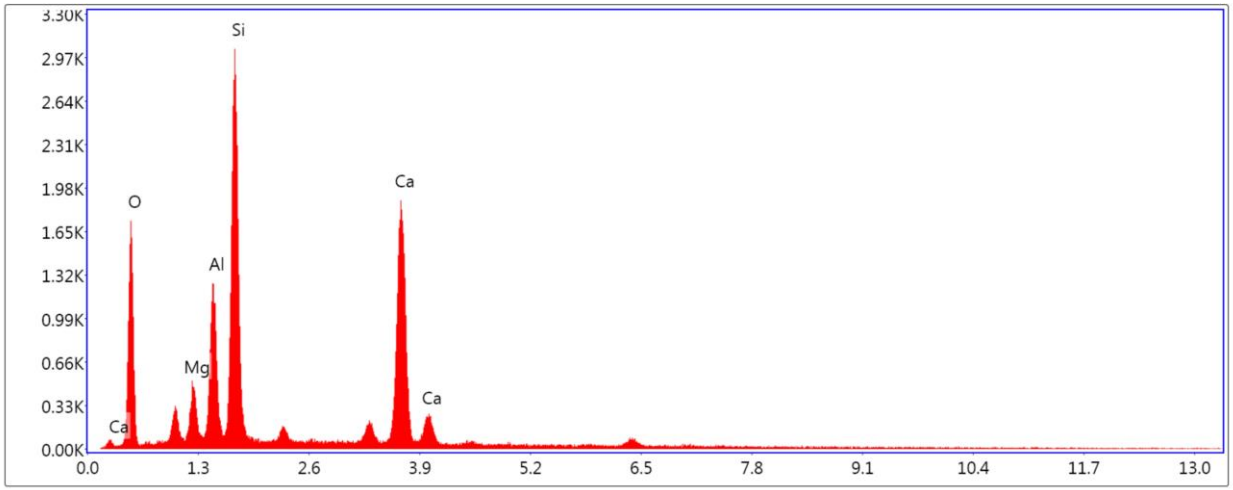

Lsec: 30.0 0 Cnts 0.000 keV Det: Octane Super Det

eZAF Smart Quant Results

Element	Weight %	Atomic %	Net Int.	Error %	Kratio	Z	R	A	F
O K	48.0	64.5	404.0	10.0	0.0995	1.0586	0.9653	0.1959	1.0000
MgK	3.4	3.0	124.4	8.7	0.0169	0.9797	0.9998	0.5078	1.0094
AlK	7.9	6.3	351.2	6.1	0.0473	0.9438	1.0071	0.6270	1.0125
SiK	18.7	14.3	896.6	4.9	0.1239	0.9647	1.0140	0.6822	1.0079
CaK	22.1	11.9	724.6	2.5	0.1949	0.9116	1.0480	0.9549	1.0137

kV: 20	Mag: 1000	Takeoff: 39.3	Live Time(s): 30	Amp Time(µs): 1.92	Resolution:(eV)

Selected Area 2

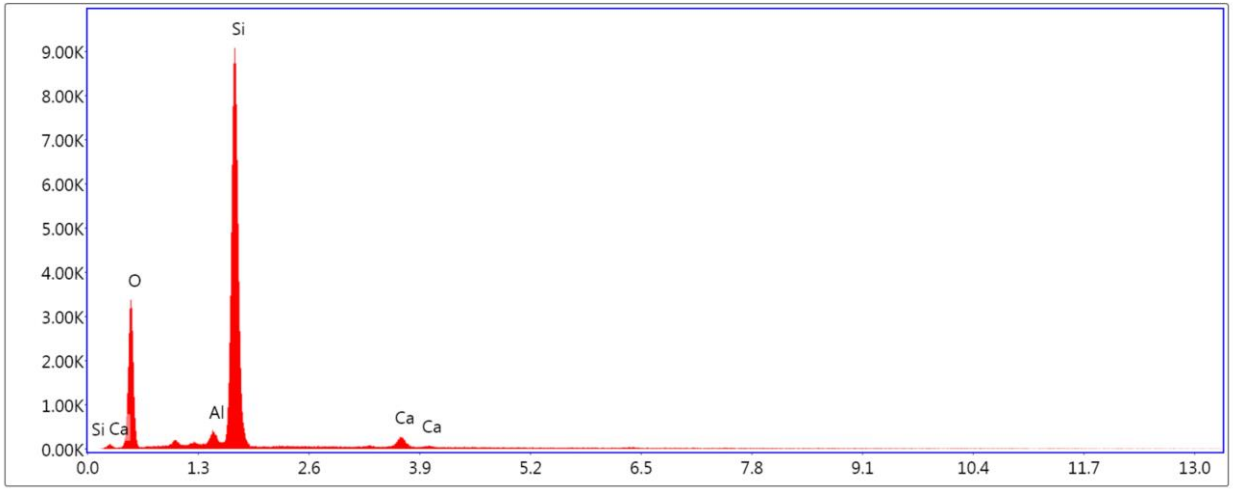

Lsec: 30.0 0 Cnts 0.000 keV Det: Octane Super Det

eZAF Smart Quant Results

Element	Weight %	Atomic %	Net Int.	Error %	Kratio	Z	R	A	F
O K	51.6	65.5	801.1	8.4	0.1764	1.0452	0.9747	0.3274	1.0000
AlK	1.8	1.4	102.6	7.2	0.0124	0.9308	1.0152	0.7135	1.0295
SiK	43.9	31.8	2745.0	3.3	0.3391	0.9513	1.0218	0.8091	1.0029
CaK	2.7	1.4	94.5	7.0	0.0227	0.8983	1.0544	0.9210	1.0196

EDAX TEAM

28-days-3-4

Author: samira safari

Sample Name: C3-20℃

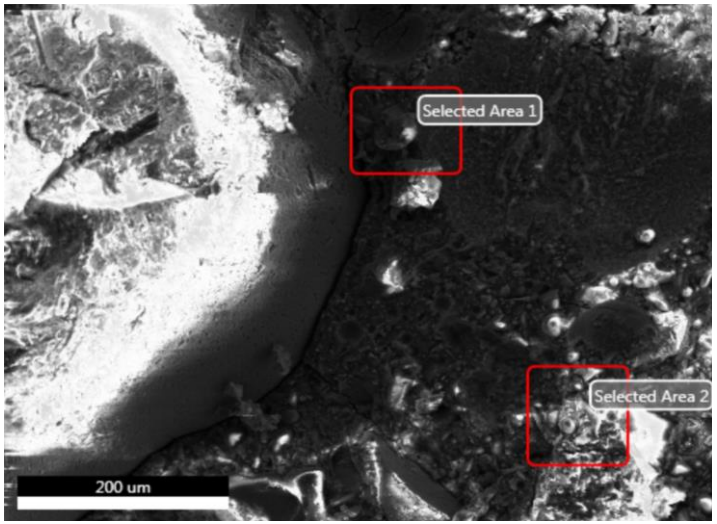

EDAX TEAM

Selected Area 1

kV:	20	Mag:	500	Takeoff:	35.4	Live Time(s):	30	Amp Time(µs):	1.92	Resolution:(eV)

Selected Area 1

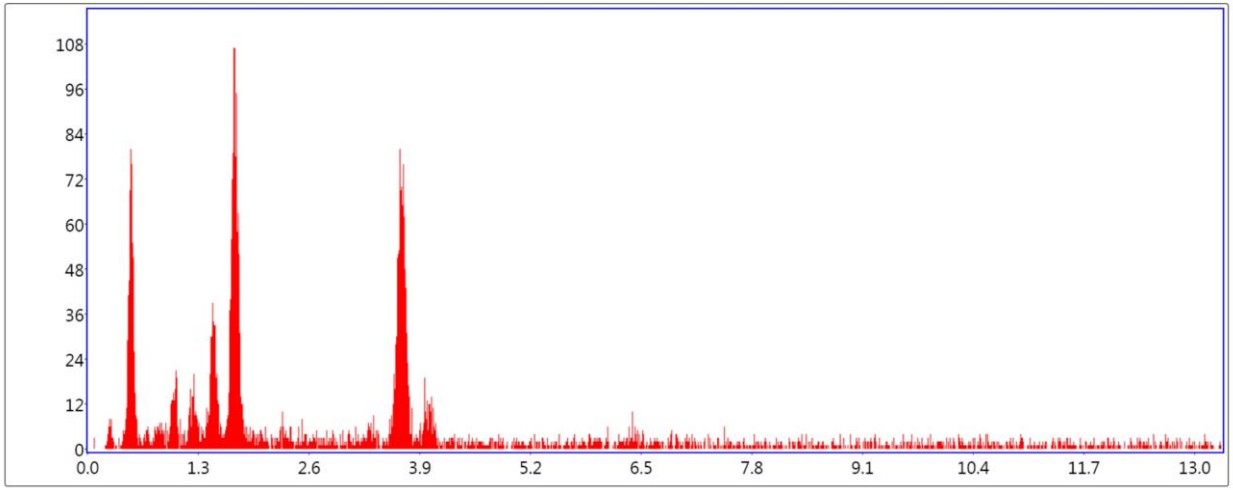

Lsec: 30.0 0 Cnts 0.000 keV Det: Octane Super Det

kV: 20	Mag: 500	Takeoff: 35.4	Live Time(s): 30	Amp Time(µs): 1.92

Selected Area 2

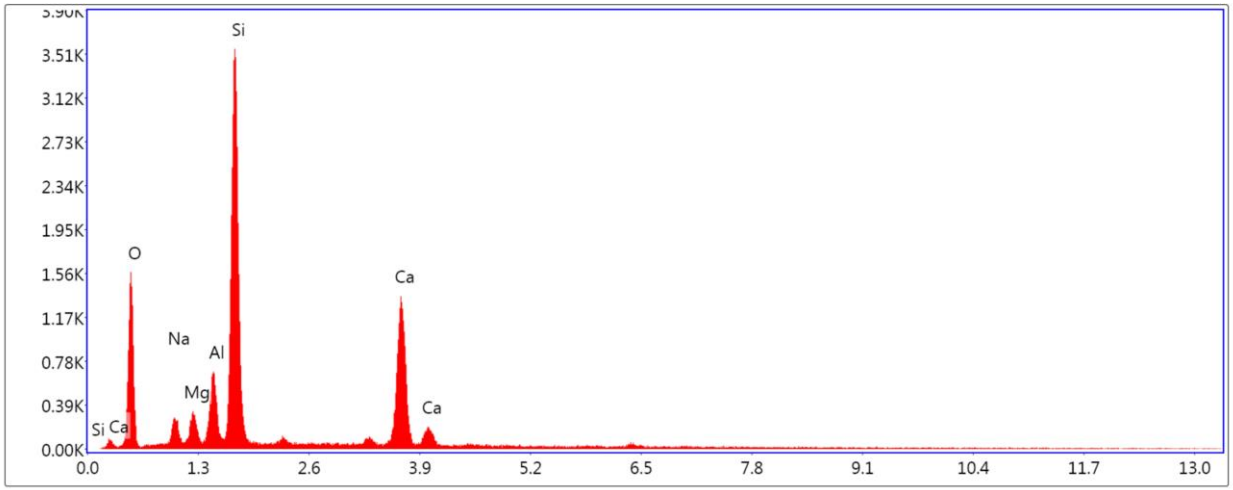

Lsec: 30.0 0 Cnts 0.000 keV Det: Octane Super Det

eZAF Smart Quant Results

Element	Weight %	Atomic %	Net Int.	Error %	Kratio	Z	R	A	F
O K	46.2	61.9	369.3	9.9	0.1042	1.0581	0.9667	0.2133	1.0000
NaK	3.7	3.4	65.8	11.0	0.0129	0.9624	0.9933	0.3637	1.0057
MgK	2.3	2.1	74.2	9.9	0.0115	0.9791	1.0010	0.4983	1.0099
AlK	4.8	3.8	186.4	6.8	0.0288	0.9431	1.0083	0.6263	1.0153
SiK	25.0	19.1	1086.5	4.6	0.1720	0.9641	1.0152	0.7083	1.0065
CaK	18.0	9.6	510.4	2.9	0.1573	0.9109	1.0489	0.9458	1.0145

28-days-3-4

Author: samira safari

Sample Name: B4

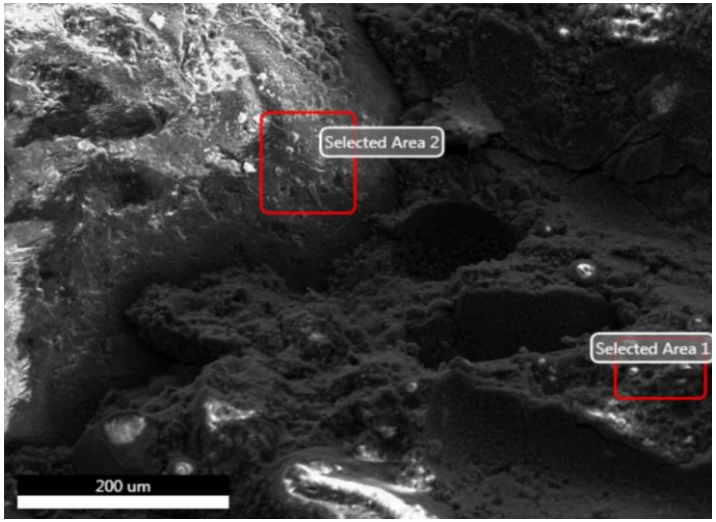

Selected Area 1

kV: 20	Mag: 500	Takeoff: 39.7	Live Time(s): 30	Amp Time(µs): 1.92	Resolution:(eV)

Selected Area 1

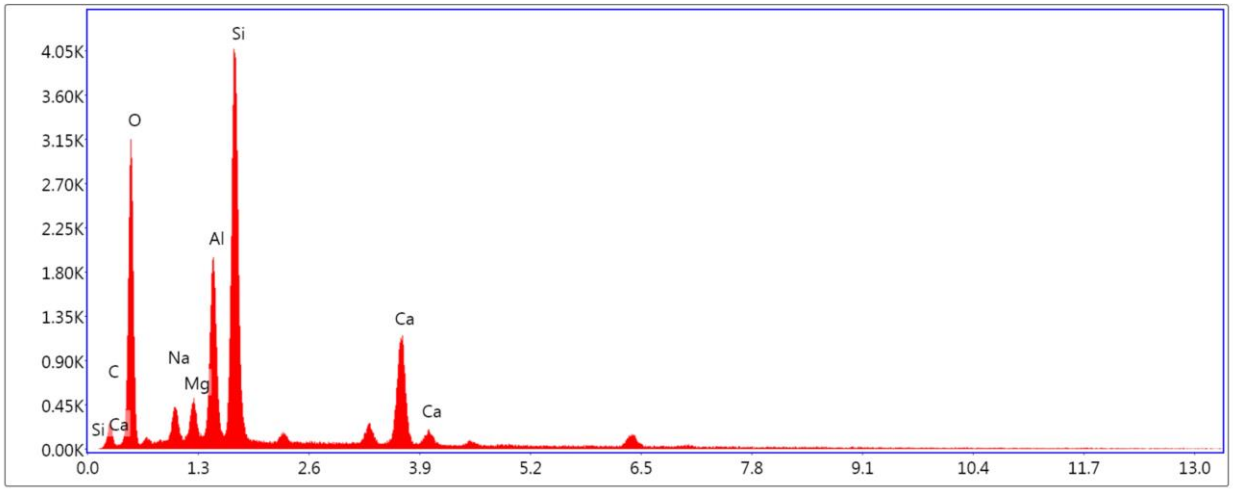

Lsec: 30.0 0 Cnts 0.000 keV Det: Octane Super Det

eZAF Smart Quant Results

Element	Weight %	Atomic %	Net Int.	Error %	Kratio	Z	R	A	F
C K	11.2	17.5	55.8	12.6	0.0216	1.0820	0.9586	0.1780	1.0000
O K	48.0	56.1	747.3	9.2	0.1223	1.0361	0.9797	0.2460	1.0000
NaK	3.7	3.0	116.5	10.2	0.0132	0.9416	1.0052	0.3770	1.0054
MgK	2.3	1.8	125.7	8.6	0.0113	0.9577	1.0126	0.5132	1.0092
AlK	8.4	5.8	561.9	5.6	0.0503	0.9224	1.0195	0.6419	1.0111
SiK	17.5	11.6	1241.3	4.7	0.1140	0.9426	1.0260	0.6886	1.0052
CaK	8.9	4.2	435.7	2.9	0.0779	0.8900	1.0577	0.9601	1.0185

Selected Area 2

kV:	Mag:	Takeoff:	Live Time(s):	Amp Time(µs):	Resolution:(eV)
20	500	39.7	30	1.92	

Selected Area 2

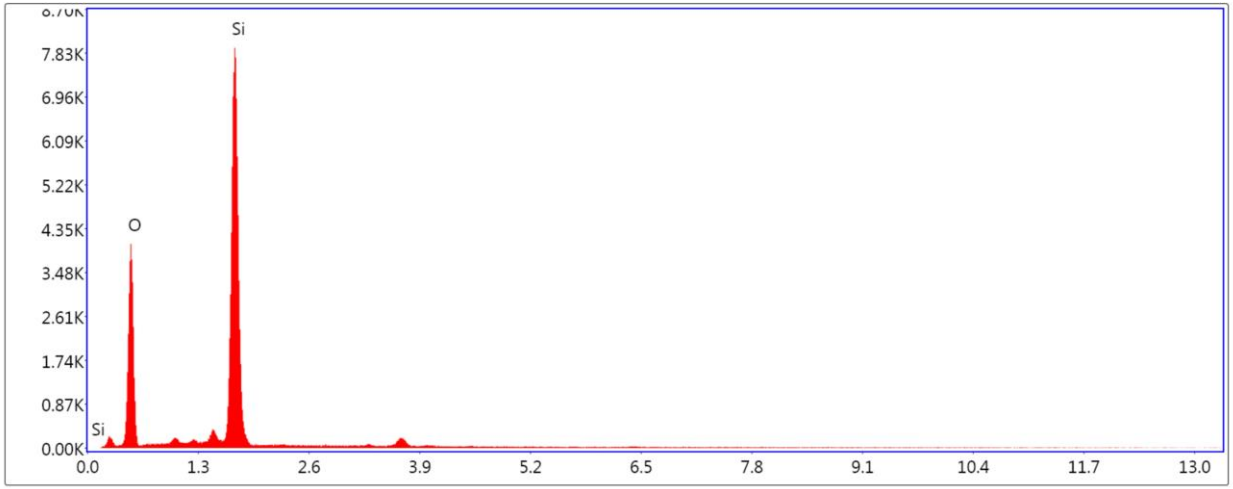

eZAF Smart Quant Results

Element	Weight %	Atomic %	Net Int.	Error %	Kratio	Z	R	A	F
O K	57.5	70.4	966.1	7.6	0.2336	1.0379	0.9788	0.3912	1.0000
SiK	42.5	29.6	2431.5	3.2	0.3298	0.9442	1.0252	0.8205	1.0024

Appendix C

Risk Assessment

Personal Protective Equipment (PPE) that will be worn at all time on workplace will improve protect people upon injury, infection and disease as much as possible, these objects are shown up in Figure A. By ensuring that all the safety issues will be used during work in the laboratory, therefore, the risk assessment will be completed.

Figure A: list of PPE (Gloves, Lab Coat, Breathing mask and safety glasses)

Civil Engineering Risk Assessment – Laboratory Based

Project title :	Early-Age Engineering Properties of Geopolymer Composites	Date : August /2013
Student name : Samira Safari		Student number : 0721531
Student email address : Samira.safari@brunel.ac.uk		
Supervisor : Dr Xiangming Zhou		
Location of work : Civil eng lab, ETC, Tower A manufacturing lab		
Level / year : *MPhil*		
Persons at Risk : Researcher		
General Hazards : Chemical		
Hazardous substances : *eg fine particulate dust, acids etc* **YES** ■ **NO** ☐	**COSHH** assessment completed and material safety data sheet supplied : **YES** ■ **NO** ☐	
Risks: Chemical, Toxic Physical : *Horbar mixer* Chemical : Sodium Silicate and Sodium Hudroxide Biological : N/A		
Current risk controls : Physical : Personal Chemical : PPE Biological : N/A		

Additional controls needed :
1. Is Respiratory Protective Equipment needed : **YES** ■ **NO** ☐ *eg face mask* **2.** Type, make and model of RPE required : *eg FFP3, Uvex silv-Air P3 valved mask 2310* Date completed on : **3.** Is Face fit testing needed : **YES** ■ Re-test date 1 year : **NO** ☐ *(For face fit testing please see your technician)*
List all other Personal Protective Equipment : Safety boots, Gloves, Lab coat, Face mask

Further developments / additions to project			
	Date :	Description :	Action necessary :
1st			
2nd			
3rd			
4th			

Method statement / Details of project and objectives:
The project will required handling chemical substances. All chemical substances will be held using all necessary PPE at all time.